



THE HONG KONG
POLYTECHNIC UNIVERSITY

香港理工大學

Pao Yue-kong Library

包玉剛圖書館

Copyright Undertaking

This thesis is protected by copyright, with all rights reserved.

By reading and using the thesis, the reader understands and agrees to the following terms:

1. The reader will abide by the rules and legal ordinances governing copyright regarding the use of the thesis.
2. The reader will use the thesis for the purpose of research or private study only and not for distribution or further reproduction or any other purpose.
3. The reader agrees to indemnify and hold the University harmless from and against any loss, damage, cost, liability or expenses arising from copyright infringement or unauthorized usage.

IMPORTANT

If you have reasons to believe that any materials in this thesis are deemed not suitable to be distributed in this form, or a copyright owner having difficulty with the material being included in our database, please contact lbsys@polyu.edu.hk providing details. The Library will look into your claim and consider taking remedial action upon receipt of the written requests.

**SMOKE TOXICITY AND THERMAL HAZARDS OF
FIRE RESISTING GLASS WITH HIGH FIRE
RESISTANCE RATING**

WU MIAO

Ph.D

The Hong Kong Polytechnic University

2014

The Hong Kong Polytechnic University

Department of Building Services Engineering

**SMOKE TOXICITY AND THERMAL HAZARDS OF
FIRE RESISTING GLASS WITH HIGH FIRE
RESISTANCE RATING**

WU MIAO

A thesis submitted in partial fulfillment of the
requirement for the Degree of Doctor of Philosophy

July 2013

CERTIFICATE OF ORIGINALITY

I hereby declare that this thesis is my own work and that, to the best of my knowledge and belief, it reproduces no material previously published or written, nor material that has been accepted for the award of any other degree or diploma, except where due acknowledgement has been made in the text.

_____ (Signed)

WU Miao _____ (Name of student)

ABSTRACT

Architectural features with glass panels have been designed in big modern construction projects. Fire resisting glass products have the ability to remain their integrity in fires. They are good replacements of standard glass products used in buildings. It has been observed that smoke is emitted when burning the protective layers of those glass products. The smoke emitted from these products can be potentially harmful during fires, causing injuries or even deaths. The objective of this thesis is firstly to carry out an in-depth study on smoke toxicity and other related fire safety aspects of fire resisting glass with higher rating. Secondly, thermal hazards upon breaking of glass in a room fire are also studied.

Common types of fire-resisting glass available, especially the ones with high fire resistance rating, were reviewed. The compositions of fire resisting glass products are not released by manufacturers, especially those from the Far East. It has been observed that smoke is emitted when burning the protective layers of glass products. Relevant fire safety standards and codes were reviewed. Key aspects such as fire resistance, impact safety and toxic potency were studied.

Smoke toxicity is an important aspect in fire safety assessment. The hazards of smoke and common smoke toxicants were reviewed. Selected methods used for quantifying

fire gas toxicity such as lethal toxic potency and fractional effective dose were outlined. Applications of bench-scale and large-scale smoke toxicity tests were also discussed according to their fire effluent generating and assessing methods.

Samples of insulating glass available in the local market were selected. Chemical compositions of the protective layers and gases discharged from the protective layers of fire resisting glasses upon heating in different atmosphere were examined. A variety of techniques, including X-ray photoelectron spectroscopy (XPS), Fourier transform infrared spectroscopy (FTIR), thermogravimetric Fourier transform infrared spectroscopy (TG-FTIR), pyrolysis-gas chromatography-mass spectrometry (Py-GC-MS) and tubular furnace coupled Fourier transform infrared spectroscopy (TF-FTIR), were employed.

Cone calorimeter has been proven to be a suitable tool for assessing the smoke toxicity of materials under well-ventilated conditions. Five samples of fire-resisting glass were tested with a cone calorimeter to study their behaviour under different fire conditions. The toxic gas yields others than their concentrations measured were used for lethal toxic potency and fractional effective dose estimations. The calculation procedures were clarified.

Destruction of window glass can introduce ventilation through the opening causing high heat release rate and even flashover. This brings concerns to the fire safety of buildings

with large window area or even glass façade. Many useful correlation equations derived for estimating the heat release rate for a post-flashover room fire were applied in performance-based design. Three correlation equations were justified by reported experimental data. Two sets of reported experimental results on post-flashover room fires with transient heat release rates measured by oxygen consumption calorimetry were used.

LIST OF PUBLICATIONS

Publications related to this thesis

Wu M. and Chow W.K. 2011. Thermal Empirical Equations for Post-flashover Compartment Fires. *Fire Safety Science*, 10, p. 1489-1497.

Wu M. and Chow W.K., 2012. A review on fire resistant glass with high rating. Presented at 18th National Symposium of Higher Education Institutes on Engineering Thermal Physics, 17-19 May 2012, Guangzhou, China.

Wu M. and Chow W.K., 2012. Experimental Justification on Thermal Empirical Equations for Post-Flashover Compartment Fires. *Journal of Fire Sciences*, 30(6), p. 511–534.

Wu M., Chow W.K. and Ni X.M., 2014. Characterization and Thermal Degradation of Protective Layers in High Rating Fire-Resistant Glass. *Fire and Materials* – Accepted to publish.

Wu M. and Chow W.K., 2013. A review on fire-resistant glass with high rating. *Journal of Applied Fire Science*, 23(1), p. 59-76.

Other publications

Wang X.S., Chow W.K. and Wu M., 2008. A review on determining water spray droplet characteristics by laser techniques. *Journal of Applied Fire Science*, 18(3), p. 211-239.

Zou G.W., Dong H., Gao Y., Chow W.K. and Wu M., 2008. Experimental study on blocking fire and smoke by water curtain. *Journal of Applied Fire Science*, 18(1), p. 1-36.

Gao Y., Liu Q.K., Chow W.K. and Wu M., 2014. Analytical and experimental study on multiple fire sources in a kitchen. *Fire Safety Journal*, 63, p. 101-112.

Gao Y., Chow W.K. and Wu M., 2013. Thermal performance of window glass panes in an enclosure fire. *Construction and Building Materials* – Accepted to publish.

ACKNOWLEDGMENTS

This work described was supported by a grant from the Research Grants Council of the Hong Kong Special Administrative Region, China for the project “Smoke Emission in Burning Fire Resisting Glass with Higher Rating” (PolyU 5145/07E) with account number B-Q05q.

I would like to express my gratitude to my supervisor, Professor W.K. Chow, for his guidance, encouragement and patience throughout the course of preparing for and conducting the research.

My sincere thanks go to Dr S.S. Han and Dr X.M. Ni for their assistance in conducting the experiments. I would also like to thank my fellow PhD classmates N. Cai and J. Liu for their help with proof reading.

Finally, I thank my parents and friends for their love, support and encouragement.

CONTENTS

Abstract		i
List of Publications		iv
Acknowledgements		vi
Contents		vii
List of Tables		xi
List of Figures		xiii
Nomenclature		xvi
Chapter 1	Introduction	
1.1	Background	1
1.2	Objectives and Methodology	2
Chapter 2	Fire Resisting Glass with High Rating	5
2.1	Introduction	5
2.2	Classifications of Fire Resisting Glass	6
2.3	Non-insulating Fire Resisting Glass	7
2.4	Insulating Fire Resisting Glass	9
2.5	Fire Resistance Testing	12
2.6	Other Related Testing	15
2.7	Summary	16

Chapter 3	Smoke Toxicity and Assessments	
3.1	Introduction	18
3.2	Asphyxiant Gases	19
3.3	Irritant Gases	21
3.4	Quantification of Toxic Potency	23
3.5	Bench-scale Tests on Smoke Toxicity	27
3.6	Large-scale Tests on Smoke Toxicity	29
3.7	Summary	30
Chapter 4	Characterization of Protective Layers in High Rating Fire Resisting Glass	
4.1	Introduction	32
4.2	Sample Selections	33
4.3	X-ray Photoelectron Spectroscopy (XPS)	34
4.4	Fourier Transform Infrared Spectroscopy (FTIR)	35
4.5	Discussions	36
4.5	Summary	37
Chapter 5	Thermal Decomposition of Protective Layers in High Rating Fire Resisting Glass	
5.1	Introduction	38
5.2	Experimental Methods	39
5.3	Thermogravimetric Fourier Transform Infrared Spectroscopy	

	(TG-FTIR)	40
5.4	Pyrolysis-Gas Chromatography-Mass Spectrometry (Py-GC-MS)	43
5.5	Tubular Furnace Coupled Fourier Transform Infrared Spectroscopy (TF-FTIR)	43
5.6	Discussions	44
5.7	Possible Chemical Reactions	46
5.8	Summary	49
Chapter 6	Smoke Toxicity Assessment of Burning Fire Resisting Glass in a Cone Calorimeter	
6.1	Introduction	51
6.2	Cone Calorimeter Testing	52
6.3	Experiments with a Cone Calorimeter	54
6.4	Hazard Assessment	57
6.5	Discussions	60
6.6	Case Study of Toxic Hazard Analysis	61
6.7	Summary	62
Chapter 7	Thermal Empirical Equations for Post-flashover Compartment Fires	
7.1	Introduction	64
7.2	The Babrauskas and Williamson (BW) Equation	66
7.3	The McCaffrey, Quintiere and Harkleroad (MQH) Equation	69

7.4	The Simplified Babrauskas (VB) Equation	72
7.5	Summary	75
Chapter 8	Experimental Justifications on Thermal Empirical Equations for Post-flashover Compartment Fires	
8.1	Introduction	76
8.2	Full-scale Burning Tests	78
8.3	Fitting with Experimental Data by Chow et al.	80
8.4	Fitting with VTT Data	88
8.5	Discussions	90
8.6	Summary	93
Chapter 9	Conclusions	94
Tables		T-1
Figures		F-1
References		R-1

LIST OF TABLES

Table 2.1	Properties of typical fire resisting products	T-1
Table 2.2	Comparisons of standard fire resistance tests in different countries	T-2
Table 3.1	Summary of important asphyxiant and irritant gases	T-3
Table 3.2	Summary of main toxicity test methods of fire smoke	T-4
Table 4.1	Characteristics of selected fire resisting samples	T-5
Table 4.2	Chemical elements with atomic percentages detected by XPS	T-6
Table 4.3	Functional groups with characteristic absorption peaks detected by FTIR	T-7
Table 5.1	Thermogravimetric characterization of samples in air and nitrogen with $20\text{ }^{\circ}\text{C}\cdot\text{min}^{-1}$ heating rate	T-8
Table 5.2	Comparisons of chemical compositions of the gases from different tests	T-9
Table 6.1	Characteristics of fire resisting samples for cone calorimeter tests	T-10
Table 6.2	Summaries of fire resisting glass samples in cone calorimeter tests	T-11
Table 8.1	Justification of BW equation using data by Chow et al. (2003)	T-12

Table 8.2	Fitting MQH and VB equations using data by Chow et al. (2003)	T-14
Table 8.3	Fitting results by Hietaniemi et al. (2004)	T-15

LIST OF FIGURES

Figure 2.1	Standard temperature-time curves	F-1
Figure 4.1	Appearance of the tested samples	F-2
Figure 4.2	XPS spectra of samples	F-3
Figure 4.3	FTIR spectra of samples at room temperature	F-4
Figure 4.4	FTIR spectra of samples from room temperature to 600 °C at 20 °C·min ⁻¹ heating rate	F-5
Figure 5.1	TG/DTG profiles of samples in air at 20 °C·min ⁻¹ heating rate	F-6
Figure 5.2	TG/DTG profiles of samples in nitrogen at 20 °C·min ⁻¹ heating rate	F-7
Figure 5.3	Comparison of TG profiles in air and nitrogen at 20 °C·min ⁻¹ heating rate	F-8
Figure 5.4	FTIR spectra of gases emitted in air at 20 °C·min ⁻¹ heating rate from TG-FTIR	F-9
Figure 5.5	GC patterns and gas compositions detected by MS from Py-GC-MS	F-10
Figure 5.6	FTIR spectra of gases emitted in argon at 10 °C·min ⁻¹ heating rate from TF-FTIR	F-11
Figure 5.7	FTIR spectra of gases emitted in air at 10 °C·min ⁻¹ heating rate from TF-FTIR	F-12

Figure 5.8	Summary of reactions for the thermal decomposition of polyacrylamide	F-13
Figure 5.9	Summary of reactions for the thermal decomposition of citric acid	F-14
Figure 5.10	Summary of reaction for the thermal decomposition of glycerol	F-15
Figure 6.1	Appearance of the tested samples before and after heating 30 Minutes in a cone calorimeter	F-16
Figure 6.2	Cone calorimeter tests	F-18
Figure 6.3	Carbon dioxide concentrations recorded	F-19
Figure 6.4	Evaluated carbon dioxide yields	F-20
Figure 6.5	Case FED analysis of fire effluents from fire resisting glass panes	F-21
Figure 8.1	The room calorimeter by Chow et al. (2003)	F-22
Figure 8.2	Opening arrangement from Chow et al. (2003)	F-23
Figure 8.3	Measured gas temperatures reported by Chow et al. (2003)	F-24
Figure 8.4	Transient heat release rates reported by Chow et al. (2003)	F-25
Figure 8.5	The long cavity by Hietaniemi et al. (2004)	F-26
Figure 8.6	Maximum heat release rate against maximum gas temperature reported by Chow et al. (2003)	F-27
Figure 8.7	Transient results on the set of data with maximum gas temperatures reported by Chow et al. (2003)	F-28
Figure 8.8	Transient heat release rate with all gas temperatures reported by	

	Chow et al. (2003)	F-29
Figure 8.9	Transient results of maximum gas temperatures data set with temperature over 600 °C by Chow et al. (2003)	F-30
Figure 8.10	Transient results of maximum gas temperatures data set after reaching 20 kW·m ⁻² by Chow et al. (2003)	F-31
Figure 8.11	Matching maximum heat release rate and temperature at above 600 °C on maximum gas temperatures data set by Chow et al. (2003)	F-32
Figure 8.12	Transient results on the set of data with maximum gas temperatures reported by Hietaniemi et al. (2004)	F-33
Figure 8.13	Transient heat release rate with all gas temperatures reported by Hietaniemi et al. (2004)	F-34

NOMENECLATURE

A_w	Total wall area of compartment (m^2)
A_v	Area of ventilation opening (m^2)
a_m	Constant related to total heat release rate in MQH equation ($kW \cdot ^\circ C^{-3/2}$)
a_f	Slope of fitted line related to MQH equation ($kW \cdot ^\circ C^{-3/2}$)
b_v	Constant related to total heat release rate in simplified VB equation (kW)
b_p	Maximum combustion efficiency
C_i	Concentration of toxic component i (ppmv)
$(Ct)_i$	Specific dose required to produce lethality of toxic component i (ppmv·min)
C_p	Specific heat capacity of gas ($kJ \cdot kg^{-1} \cdot K^{-1}$)
c_v	Constant related to total heat release rate in simplified VB equation ($^\circ C$)
c_w	Specific heat capacity of the wall material ($kJ \cdot kg^{-1} \cdot K^{-1}$)
FED	Fractional effective does
FED_c	Fractional effective dose estimated from the cone calorimeter test data
g	Gravitational acceleration ($m \cdot s^{-2}$)

h_v	Height of ventilation opening (m)
h_{vb}	Height of vent bottom above floor (m)
h_w	Effective heat transfer coefficient through ceiling and walls (kW·m ⁻² ·K ⁻¹)
$pkHRR$	peak heat release rate (kW·m ⁻²)
k_w	Thermal conductivity of wall material (kW·m ⁻¹ ·K ⁻¹)
LC_{50}	lethal toxic potency (g·m ⁻³)
m_A	Constant related to total heat release rate in BW equation (kW·°C ⁻¹)
m_{AL}	Constant related to heat lost in BW equation (kW·°C ⁻¹)
m_{AV}	Constant related to ventilation provision heat lost in BW equation (kW·°C ⁻¹)
m_f	Slope of fitted line related to BW equation (kW·°C ⁻¹)
\dot{m}_a	Air flow rate through the ventilation opening (kg·s ⁻¹)
\dot{m}_p	Fuel mass loss rate (kg·s ⁻¹)
\dot{q}	Heat release rate of fire (kW)
\dot{q}_L	Heat lost rate (kW)
\dot{q}_{max}	Maximum heat release rate measured (kW)
\dot{q}_{mf}	Minimum heat release rate for flashover (kW)
\dot{q}_s	stoichiometric heat release rate (kW)
R^2	Correlation coefficient

R_f	Heat fluxes ($\text{kW}\cdot\text{m}^{-2}$)
T_f	Fire temperature ($^{\circ}\text{C}$)
T_{fmax}	Maximum fire temperature measured ($^{\circ}\text{C}$)
T_0	Air temperature of hall ($^{\circ}\text{C}$)
T^*	Baseline temperature ($^{\circ}\text{C}$)
t	Exposure time (s)
t_B	Burning time of fuel (s)
t_R	Time for radiative heat flux to reach 20 kWm^{-2} (s)
t_p	Thermal penetration time (s)
t_T	Time for air temperature next to ceiling to reach 600°C (s)
THR	Total heat release rate ($\text{MJ}\cdot\text{m}^{-2}$)
TTI	Time to ignition (s)
V	Chamber volume for closed systems or total air volume for flow through systems (m^3)
\dot{V}_f	Ventilation factor for ventilation opening ($\text{m}^{5/2}$)
W_v	Width of ventilation opening (m)
x	Flashover propensity ($\text{kJ}\cdot\text{m}^{-2}\cdot\text{s}^{-2}$)
y	Fire risk parameter related to total heat released THR ($\text{MJ}\cdot\text{m}^{-2}$)
z	Fire risk parameter related to smoke hazard ($\text{m}^3\cdot\text{kg}^{-1}$)

α	Parameter related to the BW equation of minimum heat release rate for flashover ($\text{kW}\cdot\text{m}^{-5/2}$)
β	Factor to modify m_{AV} in BW equation
Δh_c	Effective calorific value of fuel ($\text{kJ}\cdot\text{kg}^{-1}$)
Δm	Sample mass loss (g)
δ_w	Wall surface thickness (m)
ε_f	Gas emissivity
θ_1	Burning rate stoichiometry factor in simplified VB equation
θ_2	Wall steady-state losses factor in simplified VB equation
θ_3	Wall transient losses factor in simplified VB equation
θ_4	Opening height factor in simplified VB equation
θ_5	Combustion efficiency factor in simplified VB equation
ρ_0	Density of air at ambient temperature ($\text{kg}\cdot\text{m}^{-3}$)
ρ_w	Density of wall material ($\text{kg}\cdot\text{m}^{-3}$)
σ	Stefan-Boltzmann constant ($\text{kW}\cdot\text{m}^{-2}\cdot\text{K}^{-4}$)
φ	Equivalence ratio
[X]	Concentration of gas X (ppmv)
[X] _c	Cumulative Concentration of gas X (ppmv)
$pk[X]$	Peak concentration of gas X (ppmv)

CHAPTER 1 INTRODUCTION

1.1 Background

Glass façade systems can provide better external view and have clear advantages in making use of day-lighting to save lighting energy consumption [Krarti et al., 2005; Wong et al., 2005; Ihm et al., 2009]. It has been increasingly used in tall building, especially those with green and sustainable designs, all over the world [Wong et al., 2005; Aboulnaga, 2006; Li and Tsang, 2008]. Many of these constructions are commercial buildings found in densely populated areas in the Far East including Hong Kong, Singapore and Mainland China. Fire safety concerns have been raised for glass façade systems in such buildings [Chow, 2005a; Chow et al., 2006].

During fires, conventional glass panels crack and introduce ventilation through the opening causing back-draft or flashover [Emmons, 1986; Cuzzillo and Pagni, 1998]. Fire resisting glass products with better fire performance are often installed in big openings or glass façade systems [GGF, 2011]. When heat insulation is required, fire resisting glass system with protective interlayers made up of materials such as aqueous gel or metal silicates can be used [Klein, 1993].

Some research has been done on the breakage of fire resisting glass with protective interlayer in fires [Klassen et al., 2006; Manzello et al., 2007; Babrauskas, 2011]. However, the compositions of fire resisting glass products are not released by manufacturers, especially those from the Far East. It has been observed that smoke is emitted when burning the protective layers of these glass products. The smoke emitted from these products can be potentially harmful during fires, causing injuries or even deaths. Efforts should be put in to study the smoke emitted from burning the fire resisting glass products.

1.2 Objectives and Methodology

The main objective of this thesis is to gain more understandings of the fire behaviours and gas emissions of fire resisting glass products and thereby apply these findings for much needed safety protection measures when installing fire resisting glass in largely glazed buildings.

Common types of fire resisting glass available, especially the ones with high fire resistance rating, need to be reviewed. The possible chemical compositions of the protective layers used in the fire resisting products are to be surveyed as well as relevant fire safety standards and codes. Key aspects such as fire resistance and impact safety are to be considered.

Smoke toxicity is an important aspect in fire safety assessment. The hazards of smoke and common smoke toxicants are to be reviewed. Both bench-scale and large-scale methods used for quantifying fire gas toxicity such as lethal toxic potency and fractional effective dose are concerned.

The first stage is to understand the possible chemical compositions of the protective layers. Product samples available in the local market are to be selected. Compositions of the protective layers of these glass samples are to be measured by X-ray photoelectron spectroscopy (XPS) and Fourier transform infrared spectroscopy (FTIR).

Chemical compositions of the protective layers and gases discharged from the protective layers of fire resisting glasses upon heating in different atmosphere are to be examined. A variety of techniques, including X-ray photoelectron spectroscopy (XPS), Fourier transform infrared spectroscopy (FTIR), thermogravimetric Fourier transform infrared spectroscopy (TG-FTIR), pyrolysis-gas chromatography-mass spectrometry (Py-GC-MS) and tubular furnace coupled Fourier transform infrared spectroscopy (TF-FTIR), were employed.

Samples of fire resisting glass will be tested with a cone calorimeter to study their behaviour under different fire conditions. The toxic gas yields with their concentrations measured will be used for lethal toxic potency and fractional effective dose estimations. The calculation procedures will be clarified.

Destruction of window glass can introduce ventilation through the opening causing high heat release rate and even flashover. Many useful correlation equations derived for estimating the heat release rate for a post-flashover room fire are applied in performance-based designs. Three correlation equations will be justified by reported experimental data. Two sets of reported experimental results on post-flashover room fires with transient heat release rates measured by oxygen consumption calorimetry are to be used.

CHAPTER 2 FIRE RESISTING GLASS WITH HIGH RATING

2.1 Introduction

Architectural features with glass panels are commonly featured in large-scale construction projects. Many of these constructions are symbolic buildings found in the Far East including Hong Kong, Singapore, Mainland China, Japan, Korea and Malaysia. Some are supertall buildings of height over 300 m [Chow, 2009]. Designs such as glass façade are commonly employed in these buildings comprising of framework, glass panes and other accessories, such as acoustic insulation and wind pressure relief. Such glass systems are mainly used as vertical walls with special features such as double-skin façades. The trend of using glass systems as floor and ceiling for vision extension has also started [Chow, 2005b]. In case of fire, the spread of flame and smoke from a closed compartment with adequate fire resistance rating to the neighbouring areas is often caused by the destruction of glass panes. Openings are then found after breaking the glass. Further, the entire glass system of the panes may not be fixed properly by following the standard. The propagation of fire through glazed opening is a great concern [Klein, 1993].

A wide range of glass materials has been used by the building industry, and these glass materials are classified in standards such as BS 952-1 [1995]. Most glass products will

crack quickly upon heating because of the temperature difference between the surfaces and edges [Vondrasek, 2003; Chow and Gao, 2008; Chow et al., 2010]. The discharge of cold water of the fire suppression systems, which might break the heated glass panels [Sato et al., 2006] into pieces, is another concern. Because conventional glass materials are weak spots in a building, fire resisting glass has been developed.

Common types of fire resisting glass, especially the ones with high ratings, are to be reviewed. Tests and standards used to assess these products are also to be examined.

2.2 Classifications of Fire Resisting Glass

Fire resisting glass can be defined [BS EN 13501-2, 2008] as a glass system consisting of one or more transparent or translucent panes with appropriate mounting, e.g. frames, seals and fixing materials. The system can also satisfy appropriate fire resistance criteria. Performance criteria and standard tests for fire resisting constructions in different countries were reviewed and compared [Hadjisophocleous and Benichou, 1999; Hung and Chow, 2002]. The most relevant performance criteria of fire resisting glass are integrity with assigned symbol E and insulation with assigned symbol I as indicated in BS EN 13501-2 [2008]. A supplementary criterion of radiation with assigned symbol W is also specified in some standards such as BS EN 13501-2 [2008] and GB 15763.1 [2009].

Common glass products which provide some resistance to fire and are given fire ratings are reviewed briefly [Klein, 1993; Amstock, 1997; Rutledge, 2006; Razwick, 2006; Lyons, 2007; Wood, 2007]. Glass and Glass Federation (GGF) [2011] provides a detailed guideline on the specification and use of fire resisting glass products available in the UK market. The types of glasses and the performances of fire resisting glass products available in the US are also reviewed [Curkeet, 2003; Q'Keeffe, 2007]. Fire resisting glass can be classified into three types: those satisfy integrity criterion only; those satisfy both integrity and radiation criterion; and those satisfy both integrity and insulation criterion. Some literature refers integrity or radiation as non-insulating [Lyons, 2007; GGF, 2011]. Hence, fire resisting glass can be divided into two categories: non-insulating and insulating.

2.3 Non-Insulating Fire Resisting Glass

Various types of glass products are available for different building and construction purposes [Amstock, 2007]. Some of these glass products are regarded as non-insulating fire resisting, which provide integrity against fire. Integrity can be defined as the ability of a material to withstand fire exposure on one side without the transmission of fire as a result of the passage of flames or hot gases [BS EN 13501-2, 2008].

Wired glass has been the only glass offering some fire resistance for decades, and it has been accepted as a generic product [Amstock, 1997; Vondrasek, 2003, Lyons, 2007]. Wired glass is made by embedding a wire mesh throughout the glass pane [Curkeet, 2003; Q'Keeffe, 2007; GGF, 2011]. In a fire, the glass usually breaks quickly, but it is still held together by the integral wire mesh at the same spot. The integrity limit is reached when the glass softens and is pulled out of the glazing pocket.

With the development of glass technologies, other non-insulating glass products, such as toughened soda lime-silicate glass, toughened borosilicate glass, glass ceramics etc., have been developed. These products are toughened physically or chemically to increase resistance to thermal stress [Amstock, 1997; Lyons, 2007]. They can better withstand the impact of thermal shock and block the passage of flame and smoke, but they cannot stop heat transmission by radiation and conduction. When building occupants evacuate, intense radiation is a threat if the glass areas are adjacent to escape routes. Hence, products with the ability to reduce radiant energy are developed.

Reflective coated glass is made by applying thin layer of oxides or other compounds of tin, aluminium, titanium and alloys such as stainless steel on the glass pane surface [Collins et al., 1997]. The metal coating is visually transparent and can reduce the heat transferred to the glass by reflecting radiant energy in a fire. Most of the energy reduced is in the infrared portion of the spectrum where the glass is opaque and a good absorber. The effect of a metallic coating on fire resisting glass was reported by Fawcett [1996].

Resin laminated glass is the other type that can reduce heat transmission. It is made by bonding layers of glass with polymer layers. During a fire, the polymer interlayer carbonizes to give an opaque layer, which holds the glass panes together and reduces heat radiation [GGF, 2011]. These are also wired, tempered borosilicate and ceramic glasses. It is suggested that several polymers, such as the ones from fluorocarbon family, can be used in the layers of this glass [Sakamoto et al., 1993; Friedman et al., 1999]. However, polyvinyl butyral (PVB) with fire resisting additives is the most commonly used material [Gomez, 1987; Curkeet, 2003]. As the adhesive polymer layer prevents the dispersal of glass fragments during an impact, resin laminated fire resisting glass is also used as safety glasses.

Both reflective coated and resin laminated glasses have the ability to reduce heat transmission in fires. However, they cannot provide insulation in standard fire resistance test, and they are not usually considered as insulating glass.

Fire resisting properties of these products are summarized in Table 2.1.

2.4 Insulating Fire Resisting Glass

Insulation is the ability of a material to withstand fire exposure on one side without the transmission of fire to the unexposed side by limit heat transfer due to conduction,

convection and radiation (in addition to integrity) [GGF, 2011]. Insulating fire resisting glass can block significant amount of heat transfer; it is manufactured by laminating glass pane with fire resisting layers. There are two main types of insulating fire resisting glasses: intumescent and gel laminated glass.

Gel insulated glass is produced by sealing aqueous gel layers in the inter-space between toughened silicate glass panes [Curkeet, 2003]. During a fire, the gel releases water and absorbs considerable amount of energy. Water evaporates and the fire side glass breaks. Evaporation of the water results in the formation of an insulating crust, which prevents the penetration of heat. This product is made to the required size as it cannot be cut. Performance range of this type of products is made possible by the varying thickness of the gel [GGF, 2011].

The main components of the aqueous gel interlayer are water, water soluble salt and polymer which act as a gelling agent [Ortmans and Hassiepen, 1989; Holzer and Gelderie, 1993; Frommelt et al., 2002]. Derivatives of acrylic acid, such as acrylamide, are commonly used to form polymer. The polymerization is achieved by adding a catalyst and a cross link agent, for example diethylaminopropionitrile (DEAPN) and N, N'-methylenebisacrylamide (MBA). Due to the toxicities of acrylic acids, the use of other non-toxic components such as polyvinyl alcohol have also been proposed [Holzer and Gelderie, 1991; Holzer and Gelderie, 1993]. The water soluble salt is generally a salt of alkali metal or ammonium such as chlorides of sodium and calcium and it should

be compatible with the rest of the chemical system. The salt often has strongly corrosive effects on the metal frame of the glass system; anticorrosive chemicals, such as an alkali phosphate, can also be added to the aqueous gel [Ortmans and Hassiepen, 1989]. The aqueous gel layers are sealed within layers of toughened glass panes using conventional sealing system, and a primer can also be used to generate adhesion between aqueous gel and silicate glass panes [Schueller et al., 1997].

Intumescent laminated glass incorporates special interlayers which turn opaque and foam to form a thick solid layer upon exposure to heat. This intumescent interlayer inhibits the passage of conductive and radiant heat and becomes resistant to fire. The glass layers adjacent to the fire crack retain integrity owing to adhesion with the interlayers. They are generally made with annealed glass and can be cut. Depending on the thickness of the glass, the number of interlayers and interlayer combination, fire resistance (integrity and insulation) of up to 2 hours can be achieved, if appropriate glass and frame sizes are used [De Boel, 1984; Vanderstukken, 1993].

The intumescent laminated glass is made by drying hydrated alkali metal silicates mixture on glass panes, and the production process has been described in a number of patents [De Boel, 1981; Nolte, 1984; Goelff, 2009]. The main component hydrated alkali metal silicates were reported to have a weight ratio $\text{SiO}_2:\text{M}_2\text{O}$ in the range of 2.5:1 to 5.0:1 and a water content of 10 to 40 percent. Sodium silicate is used as intumescent material, and the commercial product with weight ratio $\text{SiO}_2:\text{Na}_2\text{O}$ of 3.4:1 is considered

suitable for this use. It is suggested that additives can improve fire resistance of the intumescent interlayer. The effects of organic compounds on the fire resistance of interlayer were reviewed, and some examples of organic compounds include glycerol and citric acid [De Boel and Baudin, 1980; Nolte et al., 1998; Holland et al., 2005]. When exposed to fire, the fire side glass sheet is likely to shatter into pieces and falls off. A primer layer is then applied between the fire side glass pane and the intumescent layer; the layer contains silanes such as fluorosilanes can be used as protective layer [Gelderie et al. 2000]. The adhesion between the primer layer and the intumescent layer decreases at high temperature, and this causes the fire side glass to separate completely from the intumescent material which remains intact.

Fire resisting properties of these insulating products are also summarised in Table 2.1.

2.5 Fire Resistance Testing

The degrees of fire protection required for different areas of a building vary according to building codes [Hung and Chow, 2002; Q'Keeffe, 2007]. The glass assemblies in these locations must carry the same or higher fire resistance rating. Fire glass products providing only integrity are commonly used on windows and doors; while the fire glass products regarded as providing integrity and insulation can be used on high-rated fire walls.

There are currently a large number of different standard tests in fire resistance testing, and these tests include comparable fire endurance testing procedures and requirements [Hung and Chow, 2002; Q'Keeffe, 2007; GGF, 2011]. The glass product must be tested as a part of a complete fire resisting glass system in a furnace test. The glass system is installed in the open face of a vertical fire test furnace in which the fire severity follows a prescribed time-varying temperature curve, known as the standard temperature-time curve. The standard temperature-time curves used in different countries are identical [Davis, 2003], and Figure 2.1 shows typical standard temperature-time curves [BS476-20, 1987; GB/T 12513, 2006; ASTM E 119, 2011; BS EN 1365-1, 2012]. The most relevant acceptance criteria for fire glass are integrity and insulation. The criterion load-bearing capacity is applied to glass system used in structural loading applications such as load-bearing walls and floors. The criterion radiation specified in some standards such as BS EN 1365-1 [2012] and GB/T 12513 [2006] is only required by a limited number of countries. Although the actual time in the standard tests is recorded to the near-integral minute, fire resistance ratings are given at standard intervals, e.g. 30, 60, 90, or 120 minutes. Comparisons of typical standard fire resistance tests BS476-20 [1987], BS EN 1365-1 [2012], ASTM E 119 [2011] and GB/T 12513 [2006] are shown in Table 2.2.

The British standard BS 476-20 [1987] and BS 476-22 [1987] are long established fire resistance test used in the UK relevant for glass systems. Under UK building regulations [ADB, 2006a; 2006b], the adapted European standards, such as BS EN 1363-1 [2012],

BS EN 1363-2 [1999], BS EN 1364-1 [1999], BS EN 1365-1 [2012], BS EN 1365-2 [2000] and BS EN1634-1 [2008], can also be used to classify glass products.

In United States and Canada, many different standard tests were employed for fire resistance testing of glass products [Curkeet, 2003; Q'Keeffe, 2007]. Fire glass which only provides integrity is tested as windows and doors by standard tests such as NFPA 252 [2012], NFPA 257 [2012], UL 9 [2009], UL 10B [2008] and UL 10C [2009]. Fire glass products can be used on high-rated (more than one hour) walls where insulation is usually required, these products are usually tested by standard tests such as ASTM E 119 [2011], NFPA 251 [2006] and UL 263 [2011]. These fire tests are conducted in two parts. The first part is the furnace test which includes the essential procedures aforementioned. After the furnace test, the glass assembly is subjected to a hose stream test immediately. During the procedure, water is pumped through a fire hose onto the entire exposed area of the glass assembly. At the same time, it has to remain intact with minimum amount of breakage that is allowed by the test standards. There are debates about the use of hose stream tests for fire resisting glass products. Some believe that hose stream tests can demonstrate the ability of fire resisting glass to withstand thermal shock [Berhinig, 2003; Razwick, 2006; Hemingway, 2009]; others think that hose stream tests are not designed for testing thermal shock, thus they are inadequate for fire resisting glass testing [Q'Keeffe, 2007; Griffiths, 2008; SAFTI *FIRST*, 2010]. Currently, hose stream tests are not used in any other countries except United States and Canada.

According to GB 15763.1 [2009], fire resisting glass products should be tested by the standard of GB/T 12513 [2006] in China. In Hong Kong, glass products are mainly tested in accordance with BS 476-22 [1987] and certificated as being capable of resisting the action of fire for the specified periods according to the old version FRC Code [1996] and the new FS Code [2011].

Standard fire resistance test is intended for product classification against pass or fail criteria with controlled fire conditions and allows the expected performances of test elements to be compared over a common basis [Wood, 2007]. However, there is no direct correlation between the fire test results and the duration of resistance in a real fire [Knecht, 2008]. Conditions such as fire exposure in a real fire are much more complicated than the ones specified in standard tests. The ratings and classifications of fire resisting glass products obtained from these standard fire tests are indications of performance, but they do not represent the behaviour of these products in a real building fire.

2.6 Other Related Testing

Common glass products break into long sharp shards under impact. In order to reduce the possibility of severe cutting and piercing injuries, safety testing is needed for glass products if they are to be placed in locations where accidental impact may occur. The

safety glass products are required not to break or break safely during standard safety tests. Impact safety rating are given by standard tests, including standards BS6262-4 [2005], BS EN 12600 [2002], ANSI Z97.1 [2009] and CPSC 16CFR1201 [2008].

2.7 Summary

Nearly 30 years ago, it was recognized that most victims of fires die from smoke or toxic gases and not from burns, and smoke is the main threat to life in a building fire [Gann et al., 1994; Purser, 2008; Stec and Hull, 2011]. However, smoke toxicity standards have not yet even been established in building codes and regulations of fire safety provisions in Hong Kong and many countries in the Far East [Chow et al., 2004; Chow C.L. and Chow W.K., 2011]. One of the main reasons is that it is difficult to study the toxicity of smoke. The release of toxic gas depends not only on the burning materials, but also on the manner how the materials are burnt [Purser, 2008].

Fire resisting glass products have the ability to remain their integrity in fires. They are good replacements of standard glass products used in building. Fire resisting glass can be divided into two categories: non-insulating and insulating. When heat insulation is required, glass systems with protective layers such as toughened glass can be used. There are two main types of insulating fire resisting glasses namely intumescent and gel laminated glass. The main components of gel interlayer are water, water soluble salt and

gelling agents such as polyacrylamide and polyvinyl alcohol. The intumescent laminated interlayer is made of hydrated alkali metal silicates mixed with organic components such as citric acid and glycerol.

The compositions of fire resisting glass products are not released by manufacturers, especially those from the Far East. It has been observed that smoke is emitted when burning the protective layers of glass products. This raises a safety question concerning smoke emissions, especially for buildings with large glazing area. Efforts should be put in to study the smoke emitted from burning the fire resisting glass products.

CHAPTER 3 SMOKE TOXICITY AND ASESSEMENTS

3.1 Introduction

Fires can cause a great loss of life and property. Building fires pose a big threat to life in the densely populated areas such as big cities all over the world, particularly in the Far East including Seoul, Shanghai, Beijing, Singapore and Hong Kong [Chow, 2005a]. The use of new architectural features [Chow, 2005a] and new building and furnishing materials [Purser, 2008; Stec and Hull, 2011] has increased this threat. The main hazards of fire are from the heat and smoke produced from burning combustibles [Hall, 2002]. For occupants escaping from a fire, the hazards can be separated into the effects of heat, visual obscuration by smoke, irritant and asphyxiant gases [ISO 13571, 2007].

The burning of combustible materials and the heat produced from it in a building fire can affect the structural integrity and even cause the building to collapse [Hall and Twomey, 2008]. Heat exposure can cause hyperthermia and thermal burns of the skin and respiratory tract [Gann and Bryner, 2008]. The threats to occupants from smoke were reviewed briefly by Gann [2001] and Hartzell [2001]. Smoke obscuration can cause impaired vision, while irritant gases can cause sensory and respiratory tract irritation. They can both affect mobility and the ability to negotiate escape routes. And

asphyxiant gases can affect the central nervous system, which can lead to impaired judgement, disorientation, incapacitation and death.

A large number of gas species present in fire effluents are considered as hazardous and toxic. Analysis of fire statistics shows that inhalation of toxic fire gases is the leading cause of fire-related death and injuries [Gann et al., 1994; Stec and Hull, 2011]. The most important fire gases are listed and given in standards such as ISO 13344 [2004] and ISO 13571 [2012]. The toxic fire gases are divided into asphyxiant or irritant gases. Toxicity of the fire gases has been recognized as a serious problem since 1970s [Hull and Stec, 2010; Purser, 2008], since then large amount of researches have been undertaken in the area of fire gas toxicity and its assessment.

Smoke toxicity is an important aspect in fire safety assessment. The hazards of smoke and common smoke toxicants are to be reviewed. Both bench-scale and large-scale methods used for quantifying fire gas toxicity such as lethal toxic potency and fractional effective dose are concerned.

3.2 Asphyxiant Gases

Asphyxiant gases such as carbon monoxide (CO), hydrogen cyanide (HCN), Oxygen (O₂) and Carbon dioxide (CO₂) were reviewed in detail by Purser [2010a]. Asphyxiant

gases can cause insufficient oxygen supply to the brain and body tissues resulting in tissue hypoxia. These gases are also referred as narcotic gases as they affect central nervous system resulting in incapacitation and even death. The severity of the effects depends on the accumulated dose and increases with increasing dose. It was pointed out by Purser [2008] that exposure to asphyxiant gases is the main cause of death in fires.

Major asphyxiant gases are recognised as CO and HCN. CO affects body tissues by compete with O₂ to bind with haemoglobin in red cells and reduce the O₂ levels in blood [Purser, 2010a]. The affinity of haemoglobin for CO to form caboxyhaemoglobin (COHb) is 200 times greater than that for O₂ to form oxyhaemoglobin (O₂Hb) [Hull and Stec, 2010]. The presence of COHb inhibits the release of O₂ from O₂Hb and further reduces O₂ availability. Exposure to CO at level of 1000 ppmv for 30 minutes can cause an adult to loss consciousness, and exposure at 2000 ppmv can results in death [Purser, 2010a]. HCN is much more toxic than CO [Hartzell, 2003]. Hydrolysis of HCN in blood produces cyanide ion (CN⁻) which is distributed into body fluids in tissues and organs. It is reviewed by Purser [2010a] that CN⁻ has no direct effect on oxygen level in the blood, but inhibits the utilization of oxygen in cells causing loss of cellular functions and then cell deaths particularly in the heart and brain. It was also pointed out that exposure to HCN at level of 100 ppmv for 30 minutes can be fatal for humans. HCN is rarely the primary cause in fire fatalities, and it is generally agreed to be addictive in its effect to CO [Gann and Bryner, 2008]. The immediately dangerous to health or life (IDLH) values for CO and HCN are 1200 and 50 ppmv respectively [NIOSH, 1994].

O₂ depleted atmospheres can also be important, especially during later stages of exposure. At a low O₂ level, approximately 6 to 10 % [Hartzell, 2003], it also causes direct narcotic effects which can lead to loss of consciousness and deaths. It is reviewed by Hull and Stec [2010] that inhalation of CO₂ can stimulate respiration causing more intakes of oxygen and other toxic gases, and the toxicity of CO₂ was considered to be moderate and causing loss of consciousness at 70000 ppmv in a few minutes. The IDLH value for CO₂ is considered to be 40000 ppmv [NIOSH, 1994].

Summary of the important asphyxiant gases are shown in Table 3.1.

3.3 Irritant Gases

Irritant gases can cause sensory and even pulmonary irritations [Purser, 2010b]. The symptoms include discomfort and pain in the eyes, nose, throat and upper respiratory tract resulting in breath-holding, coughing and excessive secretion of mucus. These symptoms can reduce a person's mobility and ability to negotiate escape routes. At high concentration, irritant gases can penetrate into lungs causing irritation and tissue damage which may result in post-exposure respiratory distress and death. These irritants include hydrogen halides, nitrogen oxides and organic and inorganic irritants.

The most important hydrogen halide is hydrogen chloride (HCl) [Hull and Stec, 2010]. It is likely to be present in fire gases burning polyvinyl chloride (PVC) or with presence of fire retardants containing chlorine. HCl is both irritating to the sensory and pulmonary systems, and it is intolerable irritating to humans at a low concentration of 100 ppmv but only causes death at very high concentrations. Hydrogen bromide (HBr) and hydrogen fluoride (HF) produced from burning polymer or fire retardants show irritant effects at comparable concentrations to those of HCl [Gann and Bryner, 2008]. ISO 13571 [2012] suggests that the incapacitation concentrations of HCl, HBr and HF are 1000, 1000 and 500 ppmv respectively, and NIOSH [1994] sets the IDLH values for HCl, HBr and HF at 50, 30 and 30 ppmv respectively.

Nitrogen oxides mixture, which can be represented as NO_x , contains nitric oxide (NO) and nitrogen dioxide (NO_2) with NO_2 being the main toxicant [Gann and Bryner, 2008]. Both NO and NO_2 can cause pulmonary irritations and may cause post-exposure respiratory distress and death. The incapacitation concentration of NO_2 is suggested to be 250 ppmv [ISO 13571, 2012], and the IDLH values for NO and NO_2 are 100 and 20 ppmv respectively [NIOSH, 1994].

There are a number of organic substances can be considered as organic irritants such as acrolein, formaldehyde, benzene, phenol and toluene [Hull and Stec, 2010]. Acrolein and formaldehyde are recognized as the most important organic irritants by ISO 13571 [2012], which suggests that the incapacitation concentrations of acrolein and

formaldehyde are 30 and 250 ppmv respectively. NIOSH [1994] suggests the IDLH values for acrolein and formaldehyde to be 2 and 20 ppmv respectively.

The most investigated inorganic irritant is the sulphur dioxide (SO₂) [Gann and Bryner, 2008]. Its toxic effect is considered to be additive to the other irritants mentioned above. The incapacitation concentration of SO₂ is suggested to be 150 ppmv by ISO 13571 [2012], and the IDLH values for SO₂ is 100 ppmv [NIOSH, 1994].

Summary of the important irritant gases are also included in Table 3.1.

3.4 Quantification of Toxic Potency

The toxicity of fire gas is determined by the product concentration in the target body and the time for which the toxicant is maintained [Purser, 2008]. It is not practical to measure the amount of the toxicants accumulated in affected body, hence secondary measurements are often used. It was recognised by Haber [1924] that toxicity depends upon the dose accumulated, toxic potency is expressed as the product of time and concentration.

LC₅₀ is a standard value used in combustion toxicology to measure the toxic potency of individual fire gases or of smoke. It is defined as the lethal concentration of a toxic gas

or fire effluent statistically calculated from concentration-response data that causes death in 50% of test animals for a specified exposure and post-exposure time [ISO13344, 2004; ASTM 1678, 2010].

Existing LC_{50} data for fire gases and many materials can be used to calculate fire effluent toxicity from analytic data without the use of test animals. This approach is referred as the fractional effective dose (FED) methodology [Hartzell and Emmons, 1988]. FED is defined as the ratio of the exposure dose for an asphyxiant toxicant to that exposure dose of the asphyxiant expected to produce a specified effect on an exposed subject of average susceptibility [ISO 13344, 2004]. An FED equal to 1 indicate that the concentration of an individual fire gas or of smoke will be lethal to 50% of test animals for over 30 minutes of exposure. Mathematically FED by Hartzell and Emmons, 1998] can be expressed as:

$$FED = \sum_{i=1}^n \sum_{t_1}^{t_2} \frac{C_i}{(Ct)_i} \Delta t \quad (3.1)$$

where, C_i (in ppmv) is the concentration of toxic component i ; $(Ct)_i$ (in ppmv·min) is the specific dose required to produce lethality; and t (in min) is the time increment.

The N-Gas Model developed by the National Institute of Standards and Technology (NIST) suggests that toxic potency of a product can be estimated from a small number of

combustion gases [Levin et al., 1985; Babrauskas et al., 1998]. Two equations using rat lethality data are described in ISO 13344 [2004]. The first equation of *FED* developed [Levin et al., 1988; Babrauskas et al., 1991b] can be expressed as:

$$FED = \frac{m[CO]}{[CO_2] - b} + \frac{21 - [O_2]}{21 - LC_{50,O_2}} + \frac{[HCN]}{LC_{50,HCN}} + \frac{[HCl]}{LC_{50,HCl}} + \frac{[HBr]}{LC_{50,HBr}} \quad (3.2)$$

which reduces to

$$FED = \frac{m[CO]}{[CO_2] - b} + \frac{21 - [O_2]}{21 - 5.4} + \frac{[HCN]}{150} + \frac{[HCl]}{3700} + \frac{[HBr]}{3000}$$

where, $[CO_2]$, $[O_2]$ are the volume fraction of CO_2 and O_2 ; $[CO]$, $[HCN]$, $[HCl]$ and $[HBr]$ are the concentration (in ppmv) of the gas CO , HCN , HCl and HBr respectively; and $LC_{50,HCN}$, $LC_{50,HCl}$ and $LC_{50,HBr}$ are the LC_{50} values (in ppmv) for HCN , HCl and HBr respectively. The constants m and b are the slope and intercept of the interactive curve of CO and CO_2 . The values of m and b are -18 and 122000 if $[CO_2]$ is 5% or less and 23 and -38600 when the $[CO_2]$ is above 5%.

The other equation developed by Purser [2000a] is expressed as:

$$FED = \left(\frac{[\text{CO}]}{LC_{50,\text{CO}}} + \frac{[\text{HCN}]}{LC_{50,\text{HCN}}} + \frac{[X]}{LC_{50,X}} + \frac{[Y]}{LC_{50,Y}} \right) \times V_{\text{CO}_2} + Z_A + \frac{21 - [\text{O}_2]}{21 - 5.4} \quad (3.3)$$

where, $V_{\text{CO}_2} = 1 + \frac{e^{0.14[\text{CO}_2]} - 1}{2}$ and $Z_A = 0.05[\text{CO}_2]$. $[X]$ and $[Y]$ are concentration (in ppmv) of the each acid gas and organic irritant. $LC_{50,X}$ and $LC_{50,Y}$ are the LC_{50} values (in ppmv) for X and Y .

The LC_{50} values for each gas based on rats exposed for 30 minutes in equation (3.3) by the standard ISO 13344 [2004] are also given in Table 3.1.

Once the FED value of the test sample is determined by the N-gas model from some toxicity tests, the fire toxicity of it can be calculated. The toxicity of the test sample can be expressed as an LC_{50} ($\text{g}\cdot\text{m}^{-3}$) which is related to the mass loss Δm (g) and chamber volume (for closed systems) or total air volume (for flow through systems) V (m^3) as:

$$LC_{50} = \frac{\Delta m}{FED \times V} \quad (3.4)$$

3.5 Bench-scale Tests on Smoke Toxicity

The yields of toxic products in building fires depend on the combustible materials present. It is also highly dependent on the fire scenarios and thermal decomposition conditions that the combustible materials are in [Purser, 2008]. Fire scenarios and building structure determine the growth and spread of the fire and the rate of product evolution. Thermal decomposition conditions include the temperature and oxygen supply and whether it is flaming or non-flaming. Three basic thermal decomposition conditions have been classified as fire stages in ISO 19706 [2011] as non-flaming, well-ventilated flaming, under-ventilated flaming.

Bench-scale toxicity tests have been introduced to model evolution of toxic products under different thermal decomposition conditions. There has been extensive research in bench-scale smoke toxicity tests since 1970s [Gann and Bryner, 2008]. Eight different bench-scale test methods have been first introduced in ISO TR 9122-4 [1993]. The ideal characteristics and evaluation criteria of fire effluent toxicity test method have been described in the standard ISO 16312-1 [2010]. The technical report ISO TR 16312-2 [2007] has been produced to provide guidance for evaluation criteria applications in 12 commonly used test methods. A wide range of bench-scale smoke toxicity tests was reviewed recently [Hull and Paul, 2007; Hull, 2010]. Typically, the bench-scale toxicity tests can be divided into closed chamber or flow-through methods.

In closed chamber tests, the specimen of the test material is thermally decomposed and the resulting effluent accumulates within the cabinet [Hull and Paul, 2007]. The effluent is produced through the fire stages from well-ventilated to under-ventilated, but without giving any indication of how the yield varies with fire condition. NBS (National Bureau of Standards, now the National Institute of Standards and Technology) cup test [Levin et al., 1982], which was used in 80 and 90s [Levin et al., 1985; Babrauskas et al., 1991a] is an example of closed chamber tests. It was later adopted into radiant furnace test method, which was standardized into ASTM E 1678 [2010] and employed in studies by Gann [2004] and Gann et al. [2007]. Closed cabinet tests used in ISO 5659-2 [2012] and NFPA 270 [2013] and the British defence standard DEF STAN 02-713 [2012] are also included in this category.

For flow through tests, the specimen is thermally decomposed in a furnace with control of ventilation, which drives the effluent to the gas sampling systems or measurement device [Hull, 2010]. The simple tube furnace flow through test NF X 70-100 [2006] was designed for the French rail system. It is a small-scale test with fixed air flow rate and have been used in studies of various materials [Hull et al., 2007, 2008]. Steady state tube furnace test DIN 53436 [1981-2003] was designed to allow the possibility of controlling the fire conditions during burning [Babrauskas, 2000; Hertzberg et al., 2003; Gann, 2004]. And this method was later adapted into the Purser furnace method, specified in BS 7990 [2003], ISO/TS 19700 [2007] and IEC TS 60695-7-50 [2002], which have been used in studies by Hull et al. [2002, 2009] and Stec et al. [2008, 2009].

Other flow-through methods also include University of Pittsburgh (UPITT) test [Barrow et al., 1976] and the cone calorimeter test [ISO 5660-1, 2002; ISO 5660-2, 2002]. Cone calorimeter was originally developed to determine the heat release rate and effective heat of combustion for building materials. It was later modified to assess parameters, such as ignitability, smoke evolution, and toxicity, simultaneously. Problems in using the gas concentration measured in the exhaust duct of the cone calorimeter following ISO 13344 [2004] have been studied [Han and Chow, 2004, 2005].

Bench scale tests enable detailed studies of pathological mechanisms and lethality for individual toxic gases and fire effluent mixtures. The LC_{50} is a good model for evaluation of the lethal concentration of fire effluent. These tests also allow evaluation of toxic effects of fire effluent mixtures from measured concentrations of key known toxic species. Data obtained can be used by the *FED* model to calculate the time at which the summed effective doses reach unity, at which point impair escape capability or incapacitation is predicted to occur. Summary of main bench-scale toxicity test methods of fire smoke are given in Table-3.2.

3.6 Large-scale Tests on Smoke Toxicity

Large-scale measurements of combustion product toxicity enable both fire scenarios and thermal decomposition conditions to be monitored [Blomqvist and Simonson-McNamee,

2010]. Large-scale fire tests, such as room corner test ISO 9750 [1993], open calorimeter ISO 24473 [2008], single burning item (SBI) test EN 13823 [2010] and cable tests BS EN 60332-3-10 [2010], have been developed. These fire tests have been adapted to include toxic gas measurements providing data in many studies [Purser 2000b; Blomqvist and Lönnemark, 2001; Gann et al., 2003, 2010]. Due to the high cost of large-scale tests, they are much less popular than bench-scale tests for research and actual evaluation of products [Stec et al. 2009; Babrauskas, 2000].

Efforts have been put in to validate bench-scale fire toxicity methods against large-scale room fires in many studies [Babrauskas et al., 1991a; Babrauskas, 1997, 2000; Gann et al., 2007; Hull et al., 2008; Stec et al., 2009]. The accuracy of various bench-scale fire toxicity methods for obtaining smoke toxic potency data was assessed. The aims of these studies were to validate bench-scale data for use in engineering hazard calculations, and provide useful information for control of the hazard due to combustion products.

3.7 Summary

In building fires, combustibles materials burn and give out heat and toxic effluent. Both asphyxiant and irritant fire gases produced from burning the combustibles materials are hazardous to the occupants. Irritant gases can cause sensory irritations which reduce the occupants' mobility and the ability to negotiate escape routes during evacuation. At

high concentration, irritant gases can cause irritation and tissue damage which may result in post-exposure respiratory distress and death. These irritants include hydrogen halides, nitrogen oxides, organic and inorganic irritants. Asphyxiant gases can affect the central nervous system and cause impaired judgement, disorientation, incapacitation and death.

Standard values are used in combustion toxicology to measure the toxic potency of individual fire gases or of smoke. Toxic potency is often expressed as the product of time and concentration. Smoke toxicity testing methods are available for toxic hazards evaluation of building products and materials. Bench-scale toxicity tests have been developed to model toxicants evolution of commercial products under different thermal decomposition conditions. Bench-scale tests are more commonly used for research and actual evaluation of products, as large-scale tests are very expensive to be carried out.

CHAPTER 4 CHARACTERIZATION OF PROTECTIVE LAYERS IN HIGH RATING FIRE RESISTING GLASS

4.1 Introduction

Fire resisting glass products have been developed to provide better performance against fire [Klein, 1993; Amstock, 1997; Rutledge, 2006; Razwick, 2006; Lyons, 2007; Wood, 2007]. These fire resisting glass products with different fire performance have been reviewed [Curkeet, 2003; Q'Keeffe, 2007; GGF, 2011]. As discussed in Chapter 2, fire resisting glass can be divided into two categories: non-insulating and insulating. When heat insulation is required, appropriate glass systems are available in the local market. These systems are equipped with protective layers between glass panes, using materials such as aqueous gel that contains water, water soluble salt and polymer, or intumescent interlayers of metal silicate mixtures.

It was observed that smoke emitted from protective layers during fire resistance tests. The smoke can be toxic and harmful, causing injuries or even deaths. Preliminary test [Wu and Chow, 2012] in which insulating glass were burnt showed that carbon monoxide (CO) was emitted. The chemical compositions of some fire resisting glasses, especially those from China, are not known. Calcium silicate and sodium silicate in

semi-solid or solid form act as a suitable bond, and a fire barrier might be formed. Such materials are used, but it is also possible that other products are added to stabilize them. Investigational work is necessary to assess both the smoke concentration and toxicity of the gases emitted from the protective layers during burning. The first stage is to understand the possible chemical compositions of the protective layers.

Six glass samples available in the local market are selected. Compositions of the protective layers of these glass samples were measured by X-ray photoelectron spectroscopy (XPS) and Fourier transform infrared spectroscopy (FTIR).

4.2 Sample Selections

Six glass samples available in the local market have been selected. The six selected glass samples have multi-layer structures and are transparent with protective layers filled in between glass panes. The samples are labelled as sample 1 to 6. Sample 1 to 4 are produced by sealing gel-like protective layer in the inter-space of glass boxes. Sample 5 and 6 are produced by laminating protective interlayer in between the glass panes without sealing.

Sample 1, 5 and 6 have the same area of 10 cm by 10 cm, and have the same thickness of 2.5 cm. Sample 2 and 3 are of 15 cm by 10 cm rectangular shapes; they are 2.0 cm

and 1.7 cm thick respectively. Sample 4 is of a 23 cm by 16.4 cm right angle triangular shape and has a thickness of 2.6 cm. The appearance of the glass samples and the protective layers scraped off from the samples are shown in Figure 4.1. All six samples are insulating fire glass with claimed fire resistance in the range of 25 to 60 min. The characteristics of the selected sample are summarised in Table 4.1. The possible gases emitted from the protective layers and the compositions of the protective layers are concerned. Therefore, only the protective layers were tested.

4.3 X-ray Photoelectron Spectroscopy (XPS)

XPS was employed to identify the chemical elements of the protective layers. XPS measurements were conducted on a Thermo Scientific ESCALAB 250 spectrometer with a monochromatic Al K α X-ray source. The spectrometer energy scale was calibrated to the C 1s core level line at 284.8 to 285.8 eV, and the spectra were recorded in the range of 0 to 1350 eV.

The XPS spectra of protective layer samples are shown in Figure 4.2. The detected chemical elements with their corresponding peak binding energies and atomic percentages for each sample are also shown in Figure 4.2. The chemical elements and their relative composition percentage for the six samples are summarised in Table 4.2. The six samples can be divided into two types according to the elements contained as

seen from Table 4.2. Sample 1 to 4 have similar chemical compositions and they mainly contain elements carbon (C), oxygen (O), nitrogen (N), chlorine (Cl), sodium (Na), potassium (K) and magnesium (Mg). Sample 4 also contains a small atomic percentage (about 1.3 at. %) of sulphur (S). Sample 5 and 6 have similar chemical compositions, and they mainly contain C, O, Cl, Na and silicone (Si). It should also be noted that hydrogen (H) and helium (He) could not be detected by XPS.

4.4 Fourier Transform Infrared Spectroscopy (FTIR)

Fourier transform infrared spectroscopy (FTIR) was employed to find possible functional groups in the protective layers. FTIR spectra were recorded on a Thermo Scientific Nicolet 8700 spectrometer in the range of 400 to 4000 cm^{-1} at room temperature.

FTIR spectra of protective layer samples at room temperature are shown in Figure 4.3. Functional groups with characteristic absorption peaks detected by FTIR are summarized in Table 4.3. As shown in Figure 4.3 and Table 4.3, sample 1 to 4 have similar functional groups with possible compositions containing water, amides and alcohols. It is also shown that sample 5 and 6 have similar functional groups with possible compositions containing water, silicates, alcohols and carboxylates. Figure 4.3

also shows that the water contents of sample 5 and 6 are much lower than that of sample 1 to 4.

FTIR spectra of protective layer samples from room temperature up to 600 °C are shown in Figure 4.4. For sample 1 to 4, most of the water content is lost before 300 °C is reached, while the amides break significantly above 250 °C. For sample 5 and 6, the water content is much less than that of sample 1 to 4 and is lost below 200 °C, and the carboxylate also breaks down at low temperatures below 300 °C.

As shown in Figure 4.3 to 4.4 and Table 4.3, the samples are again divided into two groups, and this classification accords with the XPS observations.

4.5 Discussions

From the XPS and FTIR observations, it can be suggested that the gel-like sample 1 to 4 contain mainly water, water soluble salts and amides with possible presence of alcohols. The polymers present in sample 1 to 4 are likely to be mainly polyacrylamide with possible presence of polyvinyl alcohol. It is also suggested that the intumescent sample 5 and 6 contain water metal silicates with possible presence organic components of carboxylates and alcohols. The organic components could be a mixture of citric acid

and glycerol. These suggestions cohere with the findings from the literatures [Amstock, 1997; GGF, 2011; Wu and Chow, 2012].

Chemical compositions of the protective layers which are derived from FTIR and XPS spectra might not be so accurate. These tests on chemical compositions give us a basic knowledge of these fire resisting glass samples. More tests are needed for accurate composition information.

4.5 Summary

According to the XPS and FTIR results, there are two types of protective layers of the fire resisting glass. One consists of water, water soluble salt and amides with possible presence of alcohols, and the other consists of water metal silicates with possible presence of carboxylate and alcohols. FTIR characterizations also indicated that sample 5 and 6 contain much little moisture than the other samples.

CHAPTER 5 THERMAL DECOMPOSITION OF PROTECTIVE LAYERS IN HIGH RATING FIRE RESISTING GLASS

5.1 Introduction

Smoke emitted from heating the protective layers of fire resisting glass can be hazardous [Wu and Chow, 2012]. Because there are no emission controls on smoke, especially its toxicity during burning, investigational work is necessary. Chemical compositions of the gases discharged upon heating may vary in different testing conditions. There has been no other test report or journal that has reported on the compositions of the gases emitted from heating fire resisting glass. These measurements are useful for understanding the possible behaviours of fire resisting glasses.

Emission of smoke and toxic gases is highly dependent on the burning conditions, which are complex in real room fires [Purser, 2008]. The yields of different gases vary greatly in different ventilation and thermal conditions. For example, high concentration of carbon monoxide would be generated if the combustion is incomplete due to inadequate air supply or cooling of the burning objects. It is important to study the chemical compositions of the gases discharged from the protective layers of fire resisting glasses upon heating in different temperature ranges and atmospheres.

Six glass samples available in the local market are selected. Thermal behaviours of the protective layers of these glass samples were monitored by thermogravimetric Fourier transform infrared spectroscopy (TG-FTIR), pyrolysis-gas chromatography-mass spectrometry (Py-GC-MS) and tubular furnace coupled Fourier transform infrared spectroscopy (TF-FTIR). It is difficult to heat up the glass inside the instrument. Therefore, the protective layer was taken out from the glass for these small-scale experiments. Results on the liberated chemicals in these tests are to be reported.

5.2 Experimental Methods

The six selected glass samples mentioned in Chapter 4 have multi-layer structures and are transparent with protective layers filled in between glass panes. The samples are labelled as Sample 1 to 6. Sample 1 to 4 are produced by sealing the gel-like protective layer in the inter-space of a glass boxes. Sample 5 and 6 are produced by laminating the protective interlayer in between the glass layers without sealing. The appearance of the glass samples and the protective layers scraped off from the samples are shown in Chapter 4 Figure 4.1. Because of the difficulties in heating up the glass samples in the instruments, the protective layer was taken out from the glass for these small-scale experiments as done in Chapter 4.

TG-FTIR analysis was conducted on a Netzsch TG209 which was connected to a Bruker Vector TM-22. For the TG analysis, 30 mg of each sample was heated at a heating rate of 20 °C·min⁻¹ from ambient to 900 °C in both nitrogen and air with 40 ml·min⁻¹ gas flow rate. FTIR spectra were also recorded for the gas emitted in the TG tests.

Py-GC-MS analysis was conducted on a HP 6890 connected to a Waters Micromass GCT. For the Py-GC analysis, each sample was heated at a heating rate of 80 °C·min⁻¹ from ambient to 600 °C in vacuum. The samples were heated to 600 °C in 8 minutes and held at 600 °C for a further 18 minutes. Chromatograms of the pyrolysates were recorded and the MS spectra of the interested peaks were analyzed.

TF-FTIR analysis was conducted with a Thermo Scientific Nicolet 8700 spectrometer. About 4 g of each sample was heated at a heating rate of 10 °C·min⁻¹ from ambient to 800 °C in both argon and air with 100 ml·min⁻¹ gas flow rate. Gas emitted from the tubular furnace at different temperature range was collected into a gasbag and then tested with FTIR.

5.3 Thermogravimetric Fourier Transform Infrared Spectroscopy (TG-FTIR)

Weight loss profiles for each sample in air and nitrogen at 10 °C·min⁻¹ heating rate (labelled as the TG curves) are plotted in Figures 5.1 and 5.2 respectively. The

derivative weight losses calculated (labelled as the DTG curves) are plotted in Figures 5.1 and 5.2. As shown in Figure 5.1 and 5.2, weight losses start once the samples are heated in air or nitrogen. For sample 1 to 4, the main devolatilization occurs with maximum rate around 130 °C, and it is followed by slower further weight loss with weight losses peaks appearing at 200 to 700 °C. For sample 5 and 6, the main devolatilization occurs around 150 °C, and it is followed by further weight loss with weight losses peaks appearing at 250 to 500 °C.

Total weight loss, maximum weight loss rate and temperature at maximum weight loss rate of six samples are summarized and compared in air and nitrogen in Table 5.1. As shown in Table 5.1, the differences between the total weight loss of each sample in air or nitrogen are very small. It can be seen that total weight losses for sample 5 and 6 are much lower than that of sample 1 to 4. It is also shown that maximum weight loss rates of each sample are affected very little by the presence of air or nitrogen. The temperature at maximum weight loss rate of sample 1 to 4 in air or nitrogen varies less than that of sample 5 and 6.

TG profiles of the six samples in air and nitrogen are compared separately in Figure 5.3 (a) and (b). Figure 5.3 shows that the shapes of the TG profiles of each sample in air or nitrogen are very similar, indicating that the atmosphere has very little influence on the thermal decomposition behaviour. TG profiles of sample 1 to 4 are identical, and sample 5 and 6 has very similar TG profiles.

Gas emitted from heating each sample in air during the TG test is analyzed by FTIR, and the FTIR spectra of the gases with identified compositions are shown in Figure 5.4. As shown in Figure 5.4, the main compositions of the gases emitted from sample 1 to 4 are similar; the gases also contain carbon dioxide (CO₂), water (H₂O) and a small amount of hydrogen chloride (HCl) and Ammonia (NH₃). The compositions of the gases emitted from sample 5 and 6 are similar, as the gases contain H₂O, CO₂ and a small amount of HCl.

Combine the observations from both Figures 5.1 (a) to (d) and 5.4 (a) to (d), it is shown that the weight loss peaks of sample 1 to 4 around 130 °C are mainly induced by water evaporation, whereas those appearing at 200 to 300 °C are possibly attributed to decomposition of amides releasing H₂O, NH₃ and CO₂. The decomposition of amides can be identified mainly at 300 to 600 °C, where the weight loss peaks around 350 °C are associated with releasing of H₂O, CO₂ and NH₃, and those around 500 °C are associated with releasing H₂O, CO₂ and HCl. From Figures 5.1 (e) and (f) and 5.4 (e) and (f), it can be seen that the weight loss peaks of sample 5 and 6 around 150 °C is mainly induced by water, whereas those appearing above 200 °C are attributed to decomposition of carboxylates releasing H₂O, CO₂ and HCl. It is also seen that the signals of HCl are stronger for sample 1 to 4 than those for sample 5 and 6.

The chemical compositions of the gases detected by TG-FTIR in air are summarized in Table 5.2.

5.4 Pyrolysis-Gas Chromatography-Mass Spectrometry (Py-GC-MS)

Chromatograms of the pyrolysates are recorded from the Py-GC-MS tests, and the data is listed in Figure 5.5. The MS spectra of the interested peaks are analyzed, and the main compositions are shown in Figure 5.5. As shown in Figure 5.5, the main compositions of the gases identified from sample 1 to 4 are similar; the gases also contain CO₂, H₂O and a small amount of HCl. Small amounts of NH₃ are also detected in pyrolysates from sample 3 and 4. The compositions of the gases emitted from sample 5 and 6 contain H₂O, CO₂, HCl and alkenes and aldehydes. Carbon monoxide (CO) was also found in the pyrolysates from sample 6.

The chemical compositions of the gases detected by Py-GC-MS in vacuum are also summarized in Table 5.2.

5.5 Tubular Furnace Coupled Fourier Transform Infrared Spectroscopy (TF-FTIR)

Gas emitted from heating each sample in argon and air during the TF test was analyzed by FTIR and the FTIR spectra of the gases, and identified compositions are shown in Figures 5.6 and 5.7 respectively. As shown in Figures 5.6 and 5.7, the products from heating each sample in argon or air are very similar. The main compositions of the

gases emitted from sample 1 to 4 contain CO₂, H₂O and a small amount of CO, HCl and NH₃. For sample 5 and 6, the main compositions of the gases emitted contain H₂O, CO₂ and a small amount of CO and HCl. It is also shown that the signals of HCl are stronger for sample 1 to 4 than those for sample 5 and 6. The signals of CO₂ are much stronger at temperature above 200 °C when heating in air for sample 1 to 5, and this increase in CO₂ is not obvious for sample 6. The decomposition of sample 1 to 4 in air is mainly identified in the temperature range of 300 to 600 °C and possibly attributed to decomposition of the amides. The decomposition of carboxylates in air starts above 200 °C for sample 5 and 6.

The chemical compositions of the gases detected by TF-FTIR in both argon and air are summarized in Table 5.2.

5.6 Discussions

The chemical compositions of the gases detected by TG-FTIR in air, Py-GC-MS in vacuum and TF-FTIR in both argon and air are summarized in Table 5.2. As shown in Table 5.2, the three tests gave similar results, as H₂O, CO₂ and HCl are the main components of the gasses emitted from the protective layers upon heating. In some samples, NH₃ is also found. Some species of alkyl (-C-H), carbonyl (-C=O) were

reflected in the FTIR spectra, but the molecules could not be deduced from the limited experimental data.

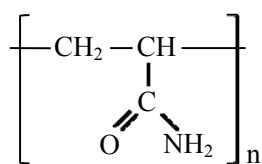
Among the three techniques, Py-GC-MS is most sensitive, whose detection limit is much lower than others. Also, it has real-time detection. But pyrolysis can only be conducted in vacuum, and the highest temperature is 600 °C. Under the present conditions, Py-GC-MS tests in other atmosphere and higher temperatures cannot be conducted. Furthermore, it is difficult to distinguish whether some species in mass spectrometry come from pyrolysis or ionization. TF-FTIR is more intuitionistic and the process of gases emitting can be observed directly. The temperature range is wider and up to 800 °C and the atmosphere can be controlled. But real-time characterizations on the gases cannot be conducted. The gases were collected into the gasbags over certain temperature ranges and then taken out for FTIR tests. FTIR spectra can only reflect the changes of emitted gases over different temperature ranges. During this process, some gases such as H₂O might be condensed and gases such as HCl and NH₃ might be dissolved into condensed water and cannot be detected in FTIR tests. Meanwhile, some gases with low concentration cannot be identified, either. TG-FTIR has the widest temperature range up to 900 °C, and it can be used to derive real time characterization of the gases emitted from the samples during heating. 3-dimensional FTIR spectra can reflect the changes of different gases over time.

Gases emitted from the protective layers heated in air and in argon and in vacuum are similar. H₂O, CO₂ and HCl are the main components, and NH₃ is also found from sample 1 to 4. The decomposition of amides in sample 1 to 4 in air is mainly identified in the temperature range of 250 to 600 °C. The decomposition of carboxylates in air is found to start above 200 °C for sample 5 and 6. Sample 5 and 6 produce less HCl than other samples upon heating. This finding also coheres with observations from the TF-FTIR tests that less smoke and irritating gas were produced from sample 5 and 6.

Carbon monoxide detected by Py-GC-MS and TF-FTIR indicates that oxygen might not be sufficient for combustion. Other species were found in different test results, but this may be due to different conditions such as temperature, flow rate, amount of raw materials, and instrumental errors. The chemical reactions occurred during the heating process are complex and affected by many factors.

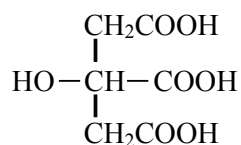
5.7 Possible Chemical Reactions

As discussed in Chapter 4, it has been suggested that the gel-like sample 1 to 4 contain mainly water, water soluble salts and amides with possible presence of alcohols and main polymers present in sample 1 to 4 are likely to be polyacrylamide. Polyacrylamide is a polymer formed from acrylamide subunits:



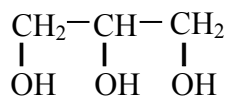
It has been suggested that thermal decomposition of polyacrylamides is influenced by many factors and can be divided into several temperature regions [Leung et al., 1987; Van Dyke and Kasperski, 1993; Caulfield et al., 2002]. Below temperatures of about 220 °C, polyacrylamides are generally thermally stable and the weight loss of the gel is attributed to loss of bound water. Above approximately 220 °C, polyacrylamides begin to undergo irreversible chemical changes. In the temperature range 220 to 340 °C, NH₃ and H₂O are released as by-products of imidization and dehydration. Above temperature of 340 °C, breakdown of the main polymeric backbone dominates the reactions giving off more CO₂. Reactions for the thermal decomposition of polyacrylamide summarized by Leung and colleagues [1987] are shown in Figure 5.8. As seen in Figure 5.1 and 5.4, weight loss of the gel samples is caused by loss of water content below 250 °C; NH₃ is detected at 250 to 350 °C; release of CO₂ is mainly observed after 300 °C and peaked around 450 °C. These observations coherer with the proposed reaction scheme for thermal decomposition of polyacrylamide.

It is suggested in Chapter 4 that the intumescent sample 5 and 6 contain water metal silicates with possible presence of carboxylates and alcohols. The organic components are suggested to be a mixture of citric acid and glycerol. The structural formula of citric acid is:



Thermal decomposition of citric acid has been studied by Barbooti and Al-Sammerrai [1986]. Citric acid melts around 150 °C and dehydrates to give aconitic acid on heating at 175 °C. Further heating forms methyl maleic anhydride. Reactions for the thermal decomposition of citric acid [Barbooti and Al-Sammerrai, 1986] are summarized in Figure 5.9.

The structural formula of glycerol is:



Thermal decomposition of glycerol has been reported [Stein et al., 1982]. Acrolein is the principal product of glycerol decomposition below 350 °C, and acetaldehyde is also formed above 450 °C. Above 600 °C, acetaldehyde and acrolein will further decompose by radical mechanisms. Reactions for the thermal decomposition of glycerol [Stein et al., 1982] are summarized in Figure 5.10. As seen in Figure 5.1 and 5.4, the first weight loss peak of the intumescent samples is observed around 160 °C; two more weight loss peaks are observed in temperature range 300 to 450 °C with first peak CO₂ release around 450 °C; the second peak release of CO₂ is observed above 600 °C. These

observations coherer with the proposed reaction scheme for thermal decomposition of citric acid and glycerol.

5.8 Summary

Experimental studies on the gases emitted from fire resisting glass upon heating were conducted. Techniques of TG-FTIR, Py-GC-MS, TF-FTIR were employed to examine the chemical compositions of the gases discharged from the protective layers when heated in different atmosphere. The three methods of TG-FTIR, Py-GC-MS, TF-FTIR gave similar results. Water vapour, carbon dioxide and hydrogen chloride gases were emitted upon heating. Gases emitted from the protective layers heated in air, in argon and in vacuum are similar in that water vapour, carbon dioxide and hydrogen chloride are the main components. Sample 5 and 6 produce less hydrogen chloride than the other samples upon heating. Carbon monoxide was produced in the Py-GC-MS and TF/FTIR results, and this could be ascribed to inadequate oxygen for combustion. Possible chemical reactions of the sample contents upon heating were also proposed.

It is difficult to carry out tests with the whole pieces of glass samples inside the heating apparatus. Therefore, the protective layers were taken out for testing. These bench-scale measurements give important information for understanding the possible behaviors of fire resisting glasses in real fires. However, these measurements are just qualitative

under some standard testing conditions. More detailed tests are needed to quantify the amount of gases emitted from burning glass in real fires for estimating toxicity parameters.

CHAPTER 6 SMOKE TOXICITY ASSESSMENT OF BURNING FIRE RESISTING GLASS

6.1 Introduction

Designs employing large amount of glass panels such as glass façades are widely used in contemporary buildings in the Far East [Chow C.L. and Chow W.K., 2010]. Fire resisting glass products are good replacements of conventional products. Fire resisting glass system consists of one or more transparent or translucent panes with appropriate mounting, e.g. frames, seals and fixing materials [BS EN 13501-2, 2008]. The system should also satisfy appropriate fire resistance criteria. Standard tests in different countries used for fire resistance assessment of the glass products were reviewed and compared [Hung and Chow, 2002; Wu and Chow, 2012]. Common performance criteria relevant to fire resisting glass in these standard tests are integrity and insulation. A supplementary criterion of radiation is also specified in some standards such as BS EN 1365-1 [2012] and GB/T 12513 [2006]. A brief review of fire resisting glass was presented by Wu and Chow [2012].

Some glass systems available in the local market [Wu and Chow, 2012] are provided with protective layers such as aqueous gel in between panels such as toughened glass; or intumescent interlayers of metal silicates between annealed glass panes. The chemical

compositions of the interlayers depend on the method of making and the fire resistance they are required. Smoke is emitted while heating up the protective layers of those glass products [Wu and Chow, 2012; 2013]. The smoke emitted from these glass products would have potential health and safety effects to people trapped inside and firemen going into the fire site. Therefore, both smoke concentration and toxicity should be assessed. Smoke toxicity should also be recommended in assessing the fire responses of glass products.

Five samples of insulating fire glass available from the local market are selected. The thermal behaviours of the samples are to be tested in a cone calorimeter exposed to 50 kW·m⁻² and 70 kW·m⁻² heat fluxes.

6.2 Cone Calorimeter Testing

The building fire safety code [FS Code, 2011] was released in September 2011 in Hong Kong. However, the approach of study, adaption of methodology, level of investigation and effort paid on fundamental research in the entire study should be watched. For example, effect of smoke toxicity on tenability limits was not yet specified clearly. Only temperature of smoke layer, visibility and carbon monoxide concentration were mentioned on specifying smoke effect on tenability limits. The importance of specifying smoke toxicity was pointed out recently [Chow C.L. and Chow W.K., 2011] with

reference to published experimental data on studying smoke toxicity of burning video compact discs (VCD) with a cone calorimeter [Chow et al., 2002; Chow and Han, 2004; Han and Chow, 2005].

Cone calorimeter is now the most powerful bench-scale test for fire hazard assessment [Babrauskas, 1992b]. There is a conical heater which can give radiative heat flux of up to $100 \text{ kW}\cdot\text{m}^{-2}$. The heat release rate is measured based on the principle of oxygen consumption. The maximum size of the sample to be tested is $10 \text{ cm} \times 10 \text{ cm}$ and up to 5 cm thick. The method for assessing heat release rate and effective heat has been standardized into ISO 5660-1 [2002]. It can also be used to assess ignitability as specified in BS 476-13 [1987] and ISO-5657 [1997] or smoke generation as specified in ISO 5660-2 [2002]. It was reviewed as a bench-scale apparatus for toxicity assessment and compared with other bench-scale apparatus by Gann [2004]. When used for toxicity testing, the apparatus is considered as well ventilated and best-suited for consider the toxicity of materials in the well-ventilated fire stages [Hull, 2010]. The carbon monoxide yields of cable materials in the cone calorimeter have been found to correlate with an equivalent ratio of 0.7 [Hull et al., 2005].

Cone calorimeter method was employed as one of the bench-scale methods by Babrauskas et al. [1991a] to assess the toxicity of Douglas fir, rigid polyurethane foam and PVC, and the results were compared with data obtained from real-scale toxicity assessment methods. Further studies by Babrauskas [1997, 2000] have used cone

calorimeter method for toxicity assessment of building materials such as sandwich panels and wall insulations. It was pointed out by Babrauskas [1997] that cone calorimeter gives more realistic CO yields than the DIN 53 436 tube furnace based on ISO 9705 test. More studies on fire effluents from burning common building and furnishing materials using cone calorimeter method have also been reported [Hertzberg et al., 2003; Blomqvist et al., 2003; Chow et al., 2004; Han and Chow, 2004, 2005].

6.3 Experiments with a Cone Calorimeter

Samples of insulating fire glass available from the local market were selected and shown in Figure 4.1 and 6.1. As shown in Figure 4.1, sample 4 is of triangular shape and could be tested in the cone calorimeter; hence only samples 1 to 3, 5 and 6 were tested. Characteristic of samples were summarized in Table 6.1. Sample 1 to 3 produced by sealing the gel-like protective layer in the inter-space of a glass boxes. Sample 5 and 6 were produced by laminating the protective interlayer in between the glass layers without sealing. Sample 1, 5 and 6 have the same area of 10 cm by 10 cm and the same thickness of 2.5 cm. Sample 2 and 3 are of 15 cm by 10 cm rectangular shapes; they are 2.0 cm and 1.7 cm thick respectively. In order to test sample 2 and 3 in the cone calorimeter, the samples were protected on both sides by aluminium foil leaving the centre area of 10 cm by 10 cm exposed.

Samples of fire resisting glass were tested with a cone calorimeter [ISO 5660-1, 2002] under different heat fluxes R_f of $50 \text{ kW}\cdot\text{m}^{-2}$ and $70 \text{ kW}\cdot\text{m}^{-2}$ as shown in Figure 6.2. The samples were tested under horizontal orientation with pilot ignition using the electric spark for 30 minutes for each test. The appearance of the glass samples after heating is also shown in Figure 6.1. The heat release rate Q_t (in $\text{kW}\cdot\text{m}^{-2}$), concentrations of oxygen [O_2], carbon monoxide [CO] and carbon dioxide [CO_2] and sample mass (in g) under the two incident heat fluxes were measured as a function of time.

Four key parameters [Petrella, 1994; Chow, 2002; Han and Chow, 2004, 2005] were deduced for fire hazard assessment:

- (i) Time to ignition, TTI (in s) is defined as the duration from the sample exposed under the heat flux to the ignition of the sample (taken as the time when a self-sustaining flame was observed).
- (ii) Peak heat release rate, $pkHRR$ (in $\text{kW}\cdot\text{m}^{-2}$).
- (iii) Total heat release rate, THR (in $\text{MJ}\cdot\text{m}^{-2}$)
- (iii) Peak carbon monoxide concentration, $pk[\text{CO}]$ (in ppmv).

LC_{50} is the lethal toxic potency used and defined as lethal concentration of a toxic gas or fire effluent causes death in 50% of test animals for a 30 minutes exposure [ISO13344, 2004; ASTM 1678, 2010]. As only CO and CO_2 were measured in this cone calorimeter,

and toxic potency LC_{50} for CO_2 is much greater than that for CO (i.e. 5000 ppmv) [Babrauskas, 1997]. The fractional effective dose (FED) can be deduced by the CO concentration [Chow et al., 2004; Han and Chow, 2004, 2005]. An FED equal to 1 indicate that the concentration of an individual fire gas or of smoke will be lethal to 50% of test animals for over 30 minutes of exposure. The toxic potency LC_{50} for CO denoted by $LC_{50,CO}$ is taken to be 5000 ppmv, and the fractional effective dose estimated from the cone calorimeter test data is expressed as:

$$FED_c = \frac{[CO]_c}{5000} \quad (6.1)$$

where $[CO]_c$ is the cumulative concentration of CO in the volume V of 0.01 m^3 can be estimated using the volumetric flow rate of exhaust gas in the cone calorimeter \dot{V}_{cone} as:

$$[CO]_c = \frac{\int_0^t [CO] \dot{V}_{cone} dt}{0.01} \quad (6.2)$$

The predicted LC_{50} (in $\text{g}\cdot\text{m}^{-3}$) for a testing sample is calculated from the sample mass loss Δm , FED_c and the volume V (0.01 m^3) for cone test using equation (3.4):

$$LC_{50} = \frac{\Delta m}{0.01 FED_c} \quad (6.3)$$

Results for the above key parameters are summarized in Table 6.2.

As seen from the experiments the fire glass samples cannot be ignited easily. The insulating layers will burn more vigorously under higher heat fluxes, $pk[CO]$ and FED_c will increase significantly. Note that in a flashover room fire, radiation heat fluxes are $20 \text{ kW}\cdot\text{m}^{-2}$ at the floor, $35 \text{ kW}\cdot\text{m}^{-2}$ on the wall, and $50 \text{ kW}\cdot\text{m}^{-2}$ at the ceiling. The burning environment of the samples is difficult to estimate. Hence, the samples were tested under higher heat fluxes of at least $50 \text{ kW}\cdot\text{m}^{-2}$ in the cone calorimeter.

During the experiments, it was observed that heat release rates were very low. $pkHRR$ and THR values for the samples were zero. Carbon dioxide emission was too low to be detected for the tests. CO was emitted while testing under high heat fluxes. Higher content of carbon monoxide was liberated from burning the samples at high heat fluxes. Only the $[CO]$ was recorded and presented in Figure 6.3.

6.4 Hazard Assessment

As discussed by Petrella [1994] and expanded later by Chow [2002], two parameters x and y are estimated to study the thermal effect and one parameter z is used to quantify the smoke hazard.

The first parameter is the flashover propensity x (in $\text{kJ}\cdot\text{m}^{-2}\cdot\text{s}^{-2}$) given by:

$$x = \frac{pkHRR}{TTI} \quad (6.3)$$

Based on the experimental results, materials can be rated in an arbitrary scale of x as:

Low risk to flashover LRF : 0.0 to 1.0

Intermediate risk to flashover IRF : 1.0 to 10

High risk to flashover HRF : 10 to 100

Very high risk to flashover VHRF : > 100

The second parameter is y on the THR (in $\text{MJ}\cdot\text{m}^{-2}$), i.e.

$$y = THR \quad (6.4)$$

Similarly, materials are rated as:

Very low risk of heat generation VLRH : 0.0 to 1.0

Low risk of heat generation LRH : 1.0 to 10

Intermediate risk of heat generation IRH : 10 to 100

High risk of heat generation HRH : > 100

The third parameter [Han and Chow, 2004] is z (in $\text{m}^3 \cdot \text{kg}^{-1}$), taken as reciprocal of LC_{50} as:

$$z = \frac{1000}{LC_{50}} \quad (6.5)$$

Similarly, materials are rated as:

Low risk of toxic hazard LRTH	: 0 to 1.0
Intermediate risk of toxic hazard IRTH	: 1.0 to 10
High risk of toxic hazard HRTH	: 10 to 100
Very high risk of toxic hazard VHRTH	: > 100

These three parameters x , y , z are calculated for the insulating fire glass samples to quantify their fire risks. Values of x , y and z calculated for the selected samples are shown also in Table 6.2. The selected fire resisting glass sample have low risk to flashover and very low risk to heat generation. They have low to intermediate risk to toxic hazard.

6.5 Discussions

As seen from the cone calorimeter results, sample 1 to 3 have smaller CO yield than that from sample 5 and 6 under heating. This is possibly the result of high water content of the gel laminates in sample 1 to 3. The LC_{50} values of the five samples selected are in the range of 12325 to 291 $\text{g}\cdot\text{m}^{-3}$. The five samples have low risk to flashover and very low risk to heat generation. They have low to intermediate risk to toxic hazard and the parameter is in the range of 0.1 to 4.

Toxic effect of real products can be calculated from real-scale mass loss rate and real-scale LC_{50} on burning. It was found from a developed database that LC_{50} in actual fires would not be deviated much from LC_{50} determined by bench-scale tests. However, the mass loss rates in a real fire and in a bench-scale test varied significantly. Babrauskas [2000] suggests that the burning rate should be reduced, rather than making the effluent less toxic. The key concern is how the materials are burnt, as incomplete combustion of polymer will give higher levels of carbon monoxide. The large-scale tests are needed for validation of bench-scale data for use in engineering hazard calculations. Smoke toxicity effects due to other toxic gases for common building materials in real-scale fires can then be estimated by deriving correlation expressions through cone calorimeter tests under high heat fluxes encountered in post-flashover fires. This will provide useful information for control of the hazard due to combustion products.

6.6 Case Study of Toxic Hazard Analysis

The toxic hazard of fire resisting glass structures can be analysed using the fractional effective dose methodology. A room of length 5 m, width 4 m and height 3 m is assumed to have one wall of length 4 m and height 4 m which is built using fire resisting glass panes. During fire, the fire resisting glass panes are assumed to release CO as the main fire gas. The CO yields of different types of fire resisting glass panes under heating can be evaluated from data shown in Figure 6.2, and the results are presented in Figure 6.3. The emitted CO is assumed to be dispersed into the room of length 5 m, width 4 m and height 3 m. The fractional effective dose shown in equation (3.1) is defined as the sum of exposure dose to the predicted incapacitation exposure dose ratios for toxicants. Hence, the fractional effective dose for fire effluent containing only CO can be expressed as [ISO13571, 2012]:

$$FED = \frac{[CO] \times \text{time}}{35000} \quad (7.20)$$

where, [CO] can be calculated by yield of CO over the room size and the value of 35000 ppmv·min is taken as the incapacitation dose. The incapacitation is predicted when *FED* exceed 1.

FED of the fire effluent from each fire resisting glass pane was calculated at each time for the period of 30 minutes and the results are presented in Figure 6.4. As shown in Figure 6.4, sample 1 and 2 are relatively less hazardous than the other products. It is shown that tenability limit is reached due to the incapacitation effect of the CO gas generated by glass panes of sample 3, 5 and 6 under heating. For sample 6, the tenability limit is reached around 7 and 13 minutes under heat flux of 50 and 70 kW·m⁻² respectively. For sample 5, the tenability limit is reached around 14 and 17 minutes under heat flux of 50 and 70 kW·m⁻² respectively. The tenability limit is reached around 30 minutes under heat flux of 70 kW·m⁻² for sample 3.

6.7 Summary

The fire behaviour of five insulating fire resisting glass samples available in the market was assessed by a cone calorimeter. Tests under different incident heat fluxes of 50 kW·m⁻² and 70 kW·m⁻² were carried out. The heat release rate was very low. Carbon dioxide emission was too low to be detected. Carbon monoxide was emitted while testing under high heat fluxes. Higher content of carbon monoxide was liberated from burning the samples at high heat fluxes.

Parameters x , y and z with an arbitrary scale for assessing the propensity to flashover, total heat released and smoke toxicity are proposed to test combustible building materials with quantitative data.

The LC_{50} values of the five samples selected were in the range of 12325 to 291 $\text{g}\cdot\text{m}^{-3}$. The five samples were found to have low risk to flashover and very low risk to heat generation. They were also found to have low to intermediate risk to toxic hazard and the toxic hazard parameter was in the range of 0.1 to 4.

The toxic potency values of LC_{50} and FED have been recognised as very useful parameters in assessing materials while setting up design guides or regulations on selecting materials, and implementing engineering performance-based fire codes. Both FED and LC_{50} in real-scale fires can be worked out together with fire models for studying the consequences of fire scenarios on burning different combustibles. It was proposed that FED can be estimated by measuring carbon dioxide and carbon monoxide in a cone calorimeter. A database on fire behaviour for local materials should be developed from those full-scale burning tests.

CHAPTER 7 THERMAL EMPIRICAL EQUATIONS FOR POST-FLASHOVER COMPARTMENT FIRES

7.1 Introduction

In a compartment fire, the destruction of window glass can introduce ventilation through the opening causing back-draft or flashover [Cuzzillo and Pagni, 1998]. Conventional glass panels cracked quickly because of thermal stress caused by the temperature difference between the surfaces and edges [Emmons, 1986]. Fire resisting glass products with better fire performance are often used in big openings or glass façade system. During fires, the integrity limits of fire resisting glass products are reached by cracking or even pulling out of the glazing pocket. The resultant openings bring air supplies providing oxygen to burn up all stored combustibles to give a big fire [Chow, 1997; Chow and Han 2006; Chow C.L. and Chow W.K., 2010]. This is particularly obvious for buildings with high window-to-wall area ratio. This brings concerns to the fire safety of buildings with large window area or even glass façade.

Works on flashover phenomenon reported in the literature were mainly based on estimating air flow rate across opening in the room fire. These included pioneer works by Kawagoe [1958] on hydrostatic models to give a relation on ventilation factor. It was followed by many other works [Quintiere, 1976; Rockett, 1976; Babrauskas and

Williamson, 1978; Babrauskas, 1980; Quintiere and McCaffrey, 1980; Thomas et al., 1980; McCaffrey et al., 1981; Thomas, 1981; Walton and Thomas, 1988; Morgan, 1989] with experimental data reported in the literature on deriving, assessing or verifying such useful design empirical equations. Although there had been many studies on flashover fire, the understanding is still limited to thermal aspects. This is because firstly there are thousands of intermediate combustion chemical reactions while burning the fuel. Secondly, turbulent flow in air mixing is difficult to model. Thirdly, thermal radiation heat fluxes cannot be calculated accurately without measuring empirical parameters. In those works, heat release rate used to be assessed by the fuel mass loss rate. Flashover was commonly determined by observing whether flame came out of the doors. Results might be different if the heat release rates are measured by oxygen consumption calorimetry [Babrauskas, 1992a].

Empirical equations relating room fire temperature and heat release rate for post-flashover fires are commonly used in PBD projects. One was derived by Babrauskas and Williamson [Babrauskas and Williamson, 1978; Babrauskas, 1980] denoted as the BW equation. The equation derived by McCaffrey et al. [1981] is denoted as the MQH equation. Another approximate simplified method proposed by Babrauskas in 1981 to determine fire temperature was also suggested and denoted as the VB equation.

7.2 The Babrauskas and Williamson (BW) Equation

A thermal balance equation in a room fire was set up by Babrauskas with Williamson in 1978 [Babrauskas and Williamson, 1978; Babrauskas, 1980]. The heat release rate \dot{q} (in kW) is related to the air flow rate \dot{m}_a (in $\text{kg}\cdot\text{s}^{-1}$), fire temperature T_f (in $^{\circ}\text{C}$), ambient air temperature T_0 (in $^{\circ}\text{C}$), heat lost \dot{q}_L (in kW) and specific heat capacity C_p (in $\text{kJ}\cdot\text{kg}^{-1}\cdot^{\circ}\text{C}^{-1}$) of air by:

$$\dot{q} = \dot{m}_a C_p (T_f - T_0) + \dot{q}_L \quad (7.1)$$

The heat generation term \dot{q} can be expressed in terms of fuel mass loss rate \dot{m}_p (in $\text{kg}\cdot\text{s}^{-1}$) and effective calorific value Δh_c (in $\text{kJ}\cdot\text{kg}^{-1}$) as:

$$\dot{q} = \dot{m}_p \Delta h_c \quad (7.2)$$

The air flow rate \dot{m}_a through an opening of area A_v (in m^2) and height h_v (in m) is:

$$\dot{m}_a = 0.5 A_v (h_v)^{0.5}$$

Note that $A_v(h_v)^{0.5}$ is the ventilation factor V_f (in $\text{m}^{5/2}$) relating to \dot{q} as justified before [Chow et al.]:

$$\dot{m}_a = 0.5V_f \quad (7.3)$$

The heat loss rate \dot{q}_L can be expressed in terms of wall area A_w (in m^2), gas emissivity ε_f of 0.5 and Stefan-Boltzmann constant σ of $5.67 \times 10^{-11} \text{ kW}\cdot\text{m}^{-2}\cdot\text{C}^{-4}$.

$$\dot{q}_L = \varepsilon_f \sigma (T_f^4 - T_0^4) (0.4A_w) \quad (7.4)$$

For normal room shapes, A_w and $A_v(h_v)^{0.5}$ are correlated (perhaps satisfying building regulations to become common design practice) with $A_w / A_v(h_v)^{0.5}$ of about $50 \text{ m}^{-1/2}$, C_p is about $1 \text{ kJ}\cdot\text{kg}^{-1}\cdot\text{C}^{-1}$. Putting in numerical values to all these parameters, and \dot{q} is simplified to:

$$\dot{q} = 600V_f \quad (7.5)$$

Using equation (7.3) for \dot{m}_a of $0.5V_f$, the minimum amount of fuel burnt at this rate under stoichiometric mixing would give 3000 kJ per kg of air consumed. Therefore, the stoichiometric heat release rate \dot{q}_s (in kW) is $3000 \dot{m}_a$, or

$$\dot{q} = 1500V_f \quad (7.6)$$

The desired minimum heat release rate for flashover \dot{q}_{mf} (in kW) is 40% of \dot{q}_s ,

$$\dot{q}_{mf} = 600V_f \quad (7.7)$$

Based on experimental data with heat release rate curve by mass loss rate of fuel [Babrauskas and Williamson, 1978; Babrauskas, 1980], \dot{q}_{mf} is 50% of \dot{q}_s , varying between $0.3\dot{q}_s$ to $0.7\dot{q}_s$. Note that the air intake rate would be lying within the range from 30% to 70% of air intake rate required for stoichiometric combustion. This gives a parameter α to the BW equation of \dot{q}_{mf} as:

$$\dot{q}_{mf} = \alpha V_f \quad (7.8)$$

Value of α is $750 \text{ kWm}^{-5/2}$, but lying between $450 \text{ kWm}^{-5/2}$ (for $0.3\dot{q}_s$) to $1050 \text{ kWm}^{-5/2}$ (for $0.7\dot{q}_s$).

Equation (7.1) was labelled as BW equation and simplified to:

$$\dot{q} = m_A (T_f - T_o) \quad (7.9)$$

This is a straight line with the slope m_A (in kW·°C⁻¹) having two parts m_{AV} and m_{AL} :

$$m_A = m_{AV} + m_{AL} \quad (7.10)$$

The first part m_{AV} (in kW·°C⁻¹) is related to ventilation provision given by equations (7.1) and (7.3).

$$m_{AV} = 0.5V_f C_p \quad (7.11)$$

The second part m_{AL} (in kW·°C⁻¹) is related to heat lost given by equation (7.4).

$$m_{AL} = \varepsilon_f \sigma (0.4A_w) (T_f + T_o) (T_f^2 + T_o^2) \quad (7.12)$$

7.3 The McCaffrey, Quintiere and Harkleroad (MQH) Equation

Another correlation expression relating \dot{q} to T_f labelled as MQH equation in this paper was reported by McCaffrey, Quintiere and Harkleroad [1981]. A thermal balance

equation similar to equation (7.1) was also considered with \dot{q}_L (in kW) expressed in terms of an effective heat transfer coefficient through ceiling and walls h_w ($\text{kW}\cdot\text{m}^{-2}\cdot\text{°C}^{-1}$) as:

$$\dot{q}_L = h_w A_w (T_f - T_0) \quad (7.13)$$

The room fire temperature ($T_f - T_0$) is fitted by two parameters related to \dot{q}/V_f and $h_w A_w/V_f$. The following MQH equation was fitted by 8 sets of data from 112 experiments:

$$\dot{q} = \left\{ \sqrt{g} C_p \rho_0 T_0^2 \left(\frac{T_f - T_0}{480} \right)^3 \right\}^{0.5} \{ h_w A_w V_f \}^{0.5} \quad (7.14)$$

Variables in the above equation are gravitational acceleration g (in $\text{m}\cdot\text{s}^{-2}$), specific heat capacity C_p of air, density of air at ambient temperature ρ_0 (in $\text{kg}\cdot\text{m}^{-3}$), ambient air temperature T_0 , wall area A_w , area of opening A_v and height h_v as in the BW equation.

The MQH equation can be rewritten through a constant a_m as:

$$\dot{q} = a_m (T_f - T_0)^{1.5} \quad (7.15)$$

where a_m is given by:

$$a_m = \frac{(\sqrt{g} C_p r_0 T_0^2 h_w A_w V_f)^{0.5}}{480^{1.5}} \quad (7.16)$$

Thermal penetration time t_p (in s) is defined in terms of density ρ_w (in $\text{kg}\cdot\text{m}^{-3}$), specific heat c_w (in $\text{kJ}\cdot\text{kg}^{-1}\cdot^\circ\text{C}^{-1}$), thermal conductivity k_w (in $\text{kW}\cdot\text{m}^{-1}\cdot^\circ\text{C}^{-1}$), and thickness δ_w (in m) of the wall surface material:

$$t_p = \left(\frac{\rho_w c_w}{k_w} \right) \left(\frac{\delta_w}{2} \right)^2 \quad (7.17)$$

The effective heat transfer coefficient through ceiling and walls h_w is related to the exposure time t (in s) when the time of exposure is less than the penetration time as:

$$h_w = \left(\frac{\rho_w c_w k_w}{t} \right)^{0.5} \quad (7.18)$$

The variables are density ρ_w , specific heat c_w and thermal conductivity k_w of the wall surface material as before.

7.4 The Simplified Babrauskas (VB) Equation

The heat lost term \dot{q}_L in the BW equation given by equation (7.1) might not be constant. Another approximate simplified method proposed to determine fire temperature T_f was suggested by Babrauskas [1981]. T_f is related to a baseline temperature T^* (in °C), T_o and five factors on burning rate stoichiometry factor θ_1 , equivalence ratio φ , wall steady-state loss factor θ_2 , wall transient loss factor θ_3 , opening height effect factor θ_4 and combustion efficiency factor θ_5 by:

$$T_f = T_o + (T^* - T_o)\theta_1\theta_2\theta_3\theta_4\theta_5 \quad (7.19)$$

The burning rate stoichiometry factor θ_1 can be expressed as an equivalence ratio φ , and for $\varphi < 1$:

$$\theta_1 = 1 + 0.51(\ln\varphi) \quad (7.20)$$

φ is a function of \dot{q} and V_f :

$$\varphi = \frac{\dot{q}}{1500V_f} \quad (7.21)$$

The wall steady-state loss factor θ_2 is expressed in terms of V_f , A_w , k_w and δ_w of the wall as:

$$\theta_2 = 1 - 0.94 \exp \left\{ -54 \left(\frac{V_f}{A_w} \right)^{2/3} \left(\frac{\delta_w}{k_w} \right)^{1/3} \right\} \quad (7.22)$$

The wall transient loss factor θ_3 is expressed in terms of V_f , A_w , exposure time t , ρ_w , c_w and k_w of the wall material:

$$\theta_3 = 1 - 0.92 \exp \left\{ -150 \left(\frac{V_f}{A_w} \right)^{0.6} \left(\frac{t}{k_w \rho_w c_w} \right)^{0.4} \right\} \quad (7.23)$$

At steady state, the wall transient losses factor θ_3 is taken to be 1.

The opening height effect factor θ_4 is related to h_v :

$$\theta_4 = 1 - 0.25(h_v)^{-0.3} \quad (7.24)$$

The combustion efficiency factor θ_5 is related to maximum combustion efficiency b_p :

$$\theta_5 = 1 + 0.5 \ln b_p \quad (7.25)$$

From equations (7.19) to (7.25),

$$\dot{q} = 211V_f \exp\left\{\frac{T_f - T_o}{0.51(T^* - T_o) \theta_2 \theta_3 \theta_4 \theta_5}\right\} \quad (7.26)$$

The equation can be rewritten as:

$$\dot{q} = b_v \exp\left((T_f - T_o)/c\right) \quad (7.27)$$

where b_v (in kW) is given by:

$$b_v = 211V_f \quad (7.28)$$

and c_v (in °C) is given by:

$$c_v = 0.51(T^* - T_o) \theta_2 \theta_3 \theta_4 \theta_5 \quad (7.29)$$

7.5 Summary

Field surveys indicated that large amount of combustibles are stored in dense cities. Many post-flashover big fires had been resulted by burning up such combustibles as observed. Taking Hong Kong [Chow, 2010] as an example, most of the factories moved to China since the early 1980s. Very few big post-flashover fires in factories were reported in the past 20 years. Small design fires were then accepted by some PBD projects. But there are more fire incidents in old factory buildings built 40 years ago. Possible reason might be that some factories in light plastics industry are starting to move back to Hong Kong. Secondly, such industrial buildings are now functioning as mini-warehouses. These old buildings used as storage areas will have much more combustibles, but not yet classified as warehouses. Appropriate fire protection systems are then not provided. Three big post-flashover fires occurred had already killed four firemen in the past few years. Training in fighting against post-flashover fires should be enhanced. Fire safety provisions in these industrial buildings must be upgraded. Flashover should be studied properly in PBD projects. Systematic full-scale burning tests should be carried out for better understanding the fire response of new architectural features and modern materials. The heat release rate for flashover fires should be high while using as a design parameter.

CHAPTER 8 EXPERIMENTAL JUSTIFICATIONS ON THERMAL EMPIRICAL EQUATIONS FOR POST- FLASHOVER COMPARTMENT FIRES

8.1 Introduction

Fire hazard assessment is a key element in performance-based design (PBD) [CIBSE Guide E, 2010] for providing appropriate fire safety in buildings. In applying performance-based design to determine the fire safety provisions, heat release rate of the design fire is the first parameter to decide. The possible heat release rate was commonly estimated by correlation equations to determine the Available Safe Egress Time (ASET). Fire engineers used to show that the heat release rate in a normal room fire is low, say lower than 2.5 MW in many projects, except on sizing areas in natural venting systems. There are many PBD projects with ASET estimated from such small design fire computed from the empirical expressions. Fire safety provisions are then determined and submitted for approval [Chow, 2010]. However, several big post-flashover building fires were observed in big cities in the Far East including one in Hong Kong in March, 2010, one in Shanghai in summer, 2010 and one in Shenyang in February, 2011. Very high fire load density was observed in small residential units and offices in tall buildings. Consequently, there are concerns that the fire safety provisions are not adequate as experienced in fighting against such big fires.

Many useful correlation equations derived for estimating the heat release rate are believed to be adequate in fire engineering application. However, heat release rates in deriving those equations were mainly based on estimating mass loss rate of fuel. Flashover was commonly determined by observing whether flame came out of the doors. Results might be different if the heat release rates are measured by oxygen consumption calorimetry [Babrauskas and Grayson, 1992]. The authority is starting to challenge the use of such correlation equations as fire engineering design tools. Additional justification of the results with experiments in fire hazard assessment is now required.

Two empirical equations relating room fire temperature and heat release rate for post-flashover fires are commonly used in PBD projects. One was derived by Babrauskas and Williamson [Babrauskas and Williamson, 1978, Babrauskas, 1980] denoted as the BW equation in this paper. The other one was by McCaffrey, Quintiere and Harkleroad [McCaffrey et al., 1981], denoted as the MQH equation. Another approximate simplified method proposed to determine fire temperature was also suggested by Babrauskas in 1981, denoted as the VB equation. All three equations will be justified in this paper using experimental results reported for post-flashover fires.

The first set of full-scale burning tests was on flashover in compartment fires with heat release rate measured by oxygen consumption calorimetry reported by Chow et al. [Chow et al., 2003]. Correlation equations on the minimum heat release rates for flashover with the ventilation factor [Babrauskas and Williamson, 1978; Thomas et al.,

1980; Babrauskas, 1980; Thomas, 1981; McCaffrey et al., 1981; Quintiere, 1976; Walton W.D. and Thomas P.H., 1988; Morgan, 1989] had been justified by this set of full-scale burning tests. The second set of reported experimental data [Hietaniemi et al., 2004] was on studying cable fires in a long cavity. Transient gas temperatures measured at different locations of the room in these two sets of tests will be used to estimate the transient heat release rate. Results are then compared with the heat release rates measured in the post-flashover room fire.

8.2 Full-scale Burning Tests

Experiments on post-flashover fires were reported [Chow et al., 2003]. A room calorimeter of length 3.6 m, width 2.4 m and height 2.4 m as shown in Figure 8.1 was constructed. Ventilation factor V_f was adjusted by a door with fixed width W_v (in m) of 0.8 m but height h_v varying from 0.9 m to 1.95 m. The height of vent bottom above floor h_{vb} (in m) varies from 0 to 0.525 m. Six sets of tests, labelled A1 to A6 were carried out with different opening arrangements as shown in Figure 8.2. The values of V_f were from $0.68 \text{ m}^{5/2}$ to $2.18 \text{ m}^{5/2}$ as shown in Table 8.1.

A pool fire of 1 m diameter and 1.5 litres gasoline was placed at the room centre. The burning time of fuel t_b (in s) varied from 422 s to 621 s for the six tests. Air temperature T_o of the experimental hall varied from 15 °C to 16 °C.

Transient gas temperatures T_f were measured by 7 thermocouples at positions T1 to T4 as shown in Figure 8.1. There were 1 thermocouple each at T1, T2 and T3, and 4 thermocouples labelled T4a to T4d at T4. Measured gas temperature profiles T_f at the 7 thermocouples are shown in Figure 8.3. Transient heat release rates \dot{q} in the room fire were measured by the oxygen consumption method with results shown in Figure 8.4.

Flashover was determined by gas temperature next to ceiling reaching 600°C and radiative heat flux reaching 20 kW·m⁻² at floor. It was confirmed by watching whether there were any flames coming out of the opening. The times t_T (in s) for gas temperature next to ceiling reaching 600 °C and t_R (in s) for the radiative heat flux reaching 20 kW·m⁻² were recorded. From the transient curve on \dot{q} , the minimum heat release rates for flashover \dot{q}_{mf} were then taken out from the values of \dot{q} at t_T and t_R . Results are shown in Table 8.1.

Two tests on burning cables with plastic polyethylene (PE) sheathing in a long cavity at Technical Research Centre of Finland (VTT) were reported [Hietaniemi et al., 2004]. The cavity was of length 6 m, width 1.2 m and height 0.6 m, as shown in Figure 8.5.

The cables had diameter of 28 mm and length of 6 m. These two tests were labelled V1 on 6 PE-sheathed cables and V2 on 10 PE-sheathed cables respectively in this paper. Transient gas temperatures T_f were measured by 5 thermocouples at positions G2 to G5 as shown in Figure 8.5. A burner was positioned under the cables 50 cm from one end of the cavity. The smoke generated in the burning was collected at the other end of the cavity by a steel pipe.

The cables were ignited by the burner operating to give out thermal power of 50 kW. After ignition, the burner was turned off and removed from the cavity. Transient heat release rates measured by oxygen consumption and gas temperatures recorded are processed in a way similar to above. These two tests have different values of A_v , h_v , A_w , T_f and T_0 as shown in Table 8.2. For both tests V1 and V2, V_f was $0.39 \text{ m}^{5/2}$ as shown in Table 8.3. Values of m_{AV} , m_{AL} and m_A were estimated.

8.3 Fitting with Experimental Data by Chow et al. (2003)

Transient experimental data on heat release rate \dot{q} and the gas temperature rise $(T_f - T_0)$ at the 7 points T1 to T4 in the fire compartment reported by Chow et al. [2003] were analyzed to compare results of different stages of the fire:

- (i) Values of maximum heat release rate \dot{q}_{max} (in kW) were plotted against the maximum temperature rise, as shown in Figure 8.6.
- (ii) Transient values of \dot{q} and $(T_f - T_0)$ were analyzed only at the thermocouple points with the maximum gas temperature T_{fmax} (in °C) recorded, as shown in Figure 8.7.
- (iii) Transient values of all data on \dot{q} and $(T_f - T_0)$ were studied to investigate the range of measured values of $(T_f - T_0)$ recorded, as shown in Figure 8.8.

And then, transient values only at the thermocouple points with the maximum gas temperature T_{fmax} (in °C) recorded shown in Figure 8.7 were further analyzed:

- (iv) Only those gas temperatures T_f above 600 °C upon flashover were used, as shown in Figure 8.9.
- (v) Gas temperatures T_f when the heat flux above 20 kW·m⁻² were used, as shown in Figure 8.10.
- (vi) Time to the maximum heat release rate and time to maximum gas temperature were matched, and only gas temperature T_f over 600 °C were used, as shown in Figure 8.11.

Transient experimental data by Chow et al. [2003] were analyzed in total six ways. And the results of all six analyses were used to justify both the BW, MQH and simplified VB equations.

The BW equation was justified by putting numerical values to equation (7.10) to (7.12) for each test. The six sets of tests have different values of V_f , A_w , T_f and T_0 to give different values of m_{AV} , m_{AL} and m_A . For example, V_f is $2.18 \text{ m}^{5/2}$ for test A1a with C_p of $1.05 \text{ kJ}\cdot\text{kg}^{-1}\cdot\text{°C}^{-1}$ into equation (7.11), and then m_{AV} is calculated to be $1.145 \text{ kW}\cdot\text{°C}^{-1}$. Putting A_w of 44.52 m^2 , σ of $5.67 \times 10^{-11} \text{ kW}\cdot\text{m}^{-2}\cdot\text{°C}^{-4}$, ε_f of 0.5, T_f of 1079 K and T_0 of 288 K for test A1a into equation (7.12) gives m_{AL} of $0.86 \text{ kW}\cdot\text{°C}^{-1}$. Substituting m_{AV} and m_{AL} into equation (7.10) gives m_A of $2.00 \text{ kW}\cdot\text{°C}^{-1}$. Results of m_{AV} , m_{AL} and m_A for the six sets of tests are estimated as shown in Table 8.1.

On the fitting (i), values of maximum heat release rate \dot{q}_{max} (in kW) for the tests are plotted against the measured maximum gas temperature rise ($T_{fmax} - T_0$) among all 7 points at T1 to T4. The value of T_{fmax} (in °C) was determined from the maximum value of all gas temperatures measured by the 7 thermocouples. Maximum values T_{fmax} were found at T4b for test A1a to A5a, and at T4a for test A5b and A6 as reported before by Wu and Chow [2011] justifying only the BW equation. A straight line of correlation coefficient R^2 of 0.649 was fitted by the method of least square.

$$\dot{q}_{max} = 2.97(T_{fmax} - T_0) \quad (7.30)$$

Experimental data on \dot{q}_{max} and $(T_{fmax} - T_0)$ and the above line are shown in Figure 8.6. The value of m_A estimated by thermal balance equation (7.10) varies from 0.84 kW·°C⁻¹ for test A6 with 30% stoichiometric burning to 2.49 kW·°C⁻¹ for test A1b with 70% stoichiometric burning. Analytical results given by equation (7.10) with m_A of 0.84 kW·°C⁻¹ and 2.49 kW·°C⁻¹ are also plotted in Figure 8.6 for comparison. It is clearly observed that experimental heat release rates measured by the oxygen consumption method are much higher than the estimated values.

For fitting (ii), the transient values of \dot{q} are plotted against the corresponding transient $(T_f - T_0)$ on the set of curves with T_{fmax} for all six sets of tests and shown in Figure 8.7. The following line fitted by the method of least square for the transient data of each test with slope m_f (in kW·°C⁻¹) is found:

$$\dot{q} = m_f(T_f - T_0) \quad (7.31)$$

Values of m_f and the corresponding correlation coefficient R^2 for the six sets of tests are shown in Table 8.1. Values of m_f are from $1.65 \text{ kW}\cdot\text{°C}^{-1}$ for test A6 to $3.09 \text{ kW}\cdot\text{°C}^{-1}$ for test A1a.

For fitting (iii), \dot{q} are also plotted against all gas temperatures measured at all 7 thermocouples and shown in Figure 8.8. Values of m_f for all data are also estimated with R^2 shown in Table 8.1. It is observed that values of m_f are lying from $1.48 \text{ kW}\cdot\text{°C}^{-1}$ for test A6 to $2.98 \text{ kW}\cdot\text{°C}^{-1}$ for test A1a.

For fitting (iv), only the results with gas temperature over 600 °C are plotted in Figure 8.9. The values of $(T_f - T_0)$ with resultant heat release rate measured at flashover over $20 \text{ kW}\cdot\text{m}^{-2}$ in fitting (v) are plotted in Figure 8.10. Maximum \dot{q} and maximum $(T_f - T_0)$ with gas temperature over 600 °C in fitting (vi) are plotted in Figure 8.11. Values of m_f and the corresponding correlation coefficient R^2 for the six sets of tests in fitting (iv) to (vi) are also shown in Table 8.1.

The analytical results given by equation (7.9) and fitted lines given by equation (7.31) from BW equation are plotted for each test from Figure 8.7 to 8.11.

On justifying the MQH equation by the tests reported by Chow et al. (2003), the wall of the test room was made of brick with thickness δ_w about 0.1 m. Values of ρ_w , c_w and k_w are $2000 \text{ kg}\cdot\text{m}^{-3}$, $0.84 \text{ kJ}\cdot\text{kg}^{-1}\cdot\text{°C}^{-1}$ and $1.32 \times 10^{-3} \text{ kW}\cdot\text{m}^{-1}\cdot\text{°C}^{-1}$ respectively, and t_p is estimated to be 3182 s. The burning time in these tests is ranging from 422 to 621 s and much shorter than the penetration time. The exposure time is taken as 300 s, and h_w is estimated to be $0.086 \text{ kW}\cdot\text{m}^{-2}\cdot\text{°C}^{-1}$.

Putting numerical values of g of $9.8 \text{ m}\cdot\text{s}^{-2}$, C_p of $1.05 \text{ kJ}\cdot\text{kg}^{-1}\cdot\text{K}^{-1}$, ρ_0 of $1.2 \text{ kg}\cdot\text{m}^{-3}$, h_w of $0.086 \text{ kW}\cdot\text{m}^{-2}\cdot\text{°C}^{-1}$, T_0 about 15°C , A_w of 44.52 m^2 and V_f of $2.18 \text{ m}^{5/2}$ for test A1a into equation (7.16), and a_m is estimated to be $0.16 \text{ kW}\cdot\text{°C}^{-3/2}$. The following curve relating \dot{q} with $(T_f - T_0)$ for test A1a is found:

$$\dot{q} = 0.16(T_f - T_0)^{1.5} \quad (7.32)$$

Different values of a_m given by equation (7.16) for the six sets of tests were estimated and shown in Table 8.2.

As shown in Table 8.2, the values of a_m varied from $0.16 \text{ kW}\cdot\text{°C}^{-1}$ for test A1a and A1b to $0.09 \text{ kW}\cdot\text{°C}^{-1}$ for test A6. Analytical results with a_m of $0.16 \text{ kW}\cdot\text{°C}^{-1}$ and 0.09

$\text{kW}\cdot\text{°C}^{-1}$ are also plotted in Figure 8.6 for comparison. Analytical results given by equation (7.15) from MQH equation are plotted for each test from Figure 8.6 to 8.11.

The following line fitted by the method of least square for each test with slope a_f (in $\text{kW}\cdot\text{°C}^{-2/3}$) is given as:

$$\dot{q} = a_f (T_f - T_o)^{1.5} \quad (7.33)$$

Values of a_f and the corresponding correlation coefficient R^2 by fitting data in Figure 8.7 and 8.8 are shown in Table 8.2.

As shown in Table 8.2, the estimated heat release rate at different gas temperature was higher than the experimental value in using MQH equation.

On justifying the simplified VB equation by the tests reported by Chow et al. (2003), values of δ_w , k_w , ρ_w and c_w of the wall material are 0.1 m, $1.32 \times 10^{-3} \text{ kW}\cdot\text{m}^{-1}\cdot\text{°C}^{-1}$, $2000 \text{ kg}\cdot\text{m}^{-3}$ and $0.84 \text{ kJ}\cdot\text{kg}^{-1}\cdot\text{°C}^{-1}$ respectively. For test A1a, putting numerical values of V_f of $2.18 \text{ m}^{5/2}$ and A_w of 44.52 m^2 into equation (7.22), θ_2 is estimated to be 0.96.

Burning time is less than 650 s, hence $\frac{t}{k_w \rho_w c_w}$ is not in the range of 500 to 20000 $\text{m}^4\cdot\text{°C}^2\cdot\text{kW}^{-2}$, and the value of 0.63 is found to be a reasonable estimation for θ_3 . Putting

numerical values of h_v of 1.95 m and into equation (7.24), θ_4 is estimated to be 0.83. For equation (7.25), b_p is taken to be 0.9, and θ_5 is estimated to be 0.95. Putting numerical V_f of $2.18 \text{ m}^{5/2}$ into equation (7.28), and b_v is estimated to be 460 kW. Substituting the values of θ_2 , θ_3 , θ_4 and θ_5 into equation (7.29) gives c_v of 414 °C.

Results of b_v and c_v estimated by thermal balance equation (7.28) and (7.29) for the six sets of tests are estimated and shown in Table 8.2.

As shown in Table 8.2, the values of b_v and c_v varied from 460 kW and 414 °C for test A1a and A1b to 144 kW and 314 °C for test A6. Analytical results given by equation (7.27) with b_v and c_v of 460 kW and 414 °C as well as 144 kW and 314 °C are plotted in Figure 8.6 for comparison.

Analytical results given by equation (7.27) from simplified VB equation are plotted for each test from Figure 8.6 to 8.11. As shown in Figure 8.6 to 8.11, the estimated heat release rate at different gas temperature was higher than the experimental value in using MQH equation.

8.4 Fitting with VTT Data

Transient values of \dot{q} reported by Hietaniemi et al. (2004) are plotted against $(T_f - T_0)$ on the set of curves with T_{fmax} for test V1 and V2 and shown in Figure 8.12. As shown in Figure 8.13, transient values of \dot{q} are also plotted against $(T_f - T_0)$ for all gas temperatures measured at the 5 thermocouples for test V1 and V2.

The BW equation was justified by putting numerical values to equation (7.10) to (7.12) for each test. Test V1 and V2 have different values of V_f , A_w , T_f and T_0 to give different values of m_{AV} , m_{AL} and m_A . For example, V_f is $0.56 \text{ m}^{5/2}$ for test V1 with C_p of $1.05 \text{ kJ}\cdot\text{kg}^{-1}\cdot\text{°C}^{-1}$ into equation (7.11), and then m_{AV} is calculated to be $0.29 \text{ kW}\cdot\text{°C}^{-1}$. Putting A_w of 21.6 m^2 , σ of $5.67 \times 10^{-11} \text{ kW}\cdot\text{m}^{-2}\cdot\text{°C}^{-4}$, ε_f of 0.5, T_f of 1079 K and T_0 of 293 K for test A1a into equation (7.12) gives m_{AL} of $0.87 \text{ kW}\cdot\text{°C}^{-1}$. Substituting m_{AV} and m_{AL} into equation (7.10) gives m_A of $1.16 \text{ kW}\cdot\text{°C}^{-1}$. Results of m_{AV} , m_{AL} and m_A for test V1 and V2 are estimated as shown in Table 8.3.

The values of m_f and the corresponding correlation coefficient R^2 from fitting the experimental results shown in Figure 8.12 and 8.13 for both test V1 and V2 are also included in Table 8.3. The analytical results given by equation for each test (7.9) and

fitted lines given by equation (7.31) from BW equation are plotted together in Figure 8.12 and 8.13.

On justifying MQH equation by the tests reported by Hietaniemi et al. (2004), wall surface made of non-combustible board of thickness δ_w is about 0.012 m. The value of

$\frac{k_w}{\rho_w c_w}$ known as the thermal diffusivity of the wall surface is $0.5 \times 10^{-7} \text{ m}^2 \cdot \text{s}^{-1}$. t_p is

estimated by equation (7.17) to be 720 s.

The value of $\frac{k_w}{\rho_w c_w}$ and k_w are $0.5 \times 10^{-7} \text{ m}^2 \cdot \text{s}^{-1}$ and $0.5 \times 10^{-3} \text{ kW} \cdot \text{m}^{-1} \cdot \text{K}^{-1}$ respectively,

and h_w at 600 s is estimated by equation (7.18) to be $0.091 \text{ kW} \cdot \text{m}^{-2} \cdot \text{K}^{-1}$.

Putting numerical values of g of 9.8 ms^{-2} , C_p of $1.05 \text{ kJ} \cdot \text{kg}^{-1} \cdot \text{K}^{-1}$, ρ_0 of $1.2 \text{ kg} \cdot \text{m}^{-3}$, h_w of $0.091 \text{ kW} \cdot \text{m}^{-2} \cdot \text{K}^{-1}$, T_0 about 20°C , A_w of 21.6 m^2 and V_f of $0.6 \text{ m}^{5/2}$ for test V1 into equation (7.16), a_m is $0.058 \text{ kW} \cdot ^\circ\text{C}^{-3/2}$. The following curve relating \dot{q} with $(T_f - T_0)$ for test V1 is found:

$$\dot{q} = 0.058 (T_f - T_0)^{1.5} \quad (7.34)$$

Different values of a_m in the MQH equation given by equation (7.16) for test V1 and V2 were estimated and shown in Table 8.3. Analytical results given by equation (7.15) from MQH equation are plotted for each test from Figure 8.6 to 8.11.

Values of a_f and the corresponding correlation coefficient R^2 for fitting data in Figure 8.12 and 8.13 are also shown in Table 8.3. As shown in Table 8.3, the estimated heat release rate at different gas temperature was lower than the experimental value in using MQH equation.

8.5 Discussions

Heat release rate measured by oxygen consumption calorimetry was related to the gas temperature by a thermal balance equation [Babrauskas and Williamson, 1978; Babrauskas, 1980; McCaffrey et al., 1981]. Experimental results for both sets of tests are higher than the values estimated by the BW equation. It appears that the ventilation term on estimating heat release rate $m_{AV}(T_f - T_0)$ should be higher. The value of m_A estimated by taking 70% of those required for stoichiometric reaction \dot{q}_s would agree better with measurement.

A factor β is proposed to modify m_{AV} for estimating heat release rate at post-flashover fire by the BW equation given by equations (7.9) and (7.10):

$$\dot{q} = (\beta m_{AV} + m_{AL})(T_f - T_o) \quad (7.35)$$

The following straight line can be fitted by experimental data as in equation (7.31),

$$\dot{q} = m_f(T_f - T_o)$$

Therefore,

$$\beta m_{AV} + m_{AL} = m_f$$

or

$$\beta = \frac{m_f - m_{AL}}{m_{AV}} \quad (7.36)$$

β is 1 when m_f is same as the analytical value ($m_{AV} + m_{AL}$). For test A1a, β is $(2.98 - 0.86) / 1.14$ or 1.85 for the line fitting all data points on the 7 thermocouples T1 to T4.

Values of β for the test A1 to A6 are shown in Table 8.1. These values suggested that the burning rate due to ventilation across opening would be almost double the value of that computed by equation (7.3).

Values of β for the tests V1 and V2 are shown in Table 8.3. The values suggested that the burning rate due to ventilation across opening would be tripled the value of that computed by equation (7.3).

As reported [Babrauskas and Williamson, 1978; Babrauskas, 1980], value of \dot{q}_{mf} is 50% of \dot{q}_s , but lying between 30% to 70% of \dot{q}_s . Using this argument, the term m_{AV} due to ventilation provision would be varying from $(0.3 / 0.5)$ to $(0.7 / 0.5)$ of the value given by equation (7.11). The value of m_A equals $(m_{AV} + m_{AL})$ for $0.5\dot{q}_s$ and varies between $(0.6m_{AV} + m_{AL})$ for $0.3\dot{q}_s$ and $(1.4m_{AV} + m_{AL})$ for $0.7\dot{q}_s$. Values of m_A for test A1a is between 1.55 and $2.46 \text{ kW}^\circ\text{C}^{-1}$. The range of validity for m_A given by equation (7.10) lying between $(0.6m_{AV} + m_{AL})$ and $(1.4m_{AV} + m_{AL})$ is estimated and shown in Tables 8.1 and 8.3, and plotted in Figure 8.7 to 8.13.

8.6 Summary

The correlation BW [Babrauskas and Williamson, 1978; Babrauskas, 1980] and MQH [McCaffrey et al., 1981] equations on relating the heat release rates to gas temperature at post-flashover fires were justified by full-scale burning tests at different ventilation factors. Heat release rates for flashover fires were studied experimentally with oxygen consumption calorimetry, rather than by the mass loss rate [Utiskul and Quintiere, 2008].

It is observed that the heat release rates estimated by the BW equation [Babrauskas and Williamson, 1978; Babrauskas, 1980] were lower than the two sets of experimental measurement reported [Chow et al., 2003; Babrauskas, 1981]. Heat release rate estimated by the MQH equation [McCaffrey et al., 1981] agreed better with experiments. This equation was derived by fitting experimental data under different conditions.

The BW equation derived from thermal balance should be physically correct. However, air intake rate might be higher to give more oxygen for combustion. Comparing with the experimental data reported earlier, burning rate due to ventilation across opening would be about double the value computed by equation (7.3). Air pumping action [Harmathy, 1993; Chow and Chow, 2012] of fire plume should be considered in applying empirical correlation for estimating heat release rate. Further analysis is needed with more experiments but it is beyond the scope of this thesis.

CHAPTER 9 CONCLUSIONS

Conventional glass materials are weak spots in building fires, and fire resisting glass has been developed and installed. Understandings of the fire behaviours and gas emissions of fire resisting glass products are much needed for safety protection measure design when applying fire resisting glass in largely glazed buildings.

Apart from assessing fire resistance of glass panels by standard tests, there are no universal or state standards in fire resisting glass specifications. A glass façade system is comprised of framework, glass and other accessories. In standard fire resistance tests, the most relevant performance criteria of fire resisting glass are integrity, insulation and radiation. But in literatures, fire resisting glass can be divided into two categories: non-insulating and insulating. An overview of the common types of fire resisting glass, especially the ones with high ratings, the tests and standards used to assess these products was provided.

Fire resisting glass products are good replacements of standard glass products used in building. The chemical compositions of the glass products, which depend on the manufacturing method and the required fire resistance rating, are not listed in architectural specifications. This is common for products manufactured in the Far East. Smoke was emitted when burning the protective layers of glass products. This raises a

safety question concerning smoke emissions, especially for buildings with large glazing area.

Smoke toxicity is an important aspect in fire safety assessment. Both asphyxiant and irritant fire gases produced from burning the combustibles materials are hazardous to the occupants. The hazards of smoke and common smoke toxicants were reviewed. Toxic potency is often expressed as the product of time and concentration and used in combustion toxicology to measure the toxic potency of individual fire gases or of smoke. Smoke toxicity testing methods are available for toxic hazards evaluation of building products and materials. Bench-scale and large-scale methods used for quantifying fire gas toxicity such as lethal toxic potency and fractional effective dose were reviewed. Bench-scale tests such as cone calorimeter test are more commonly used for research and actual evaluation of products, as large-scale tests are very expensive to be carried out.

There were two types of protective layers of the fire resisting glass according to XPS and FTIR test results. Experimental studies on the gases emitted from fire resisting glass upon heating were conducted. Techniques of TG-FTIR, Py-GC-MS, TF-FTIR were employed to examine the chemical compositions of the gases discharged from the protective layers when heated in different atmosphere. The three methods of TG-FTIR, Py-GC-MS, TF-FTIR gave similar results. Water vapour, carbon dioxide and hydrogen chloride gases were emitted upon heating. Gases emitted from the protective layers

heated in air, in argon and in vacuum are similar in that water vapour, carbon dioxide and hydrogen chloride are the main components.

More detailed tests by cone calorimeter were carried out to quantify the amount of gases emitted from fire resisting glass upon heating. The fire behaviour of five insulating fire resisting glass samples available in the market was assessed. Tests under different incident heat fluxes of 50 kWm^{-2} and 70 kWm^{-2} were carried out. The heat release rate was very low. Carbon dioxide emission was too low to be detected. Carbon monoxide was emitted while testing under high heat fluxes. Higher content of carbon monoxide was liberated from burning the samples at high heat fluxes. The toxic potency values of LC_{50} and FED were calculated for selected product samples. The LC_{50} values of the five samples selected were found to be in the range of 12325 to $291 \text{ g}\cdot\text{m}^{-3}$. The five samples have low risk to flashover and very low risk to heat generation. They were found to have low to intermediate risk to toxic hazard and the toxic hazard parameter was in the range of 0.1 to 4.

Glass façade designs in buildings can be hazardous during fires. Failure of the glass system can result in large openings which introduce ventilation causing high heat release rate and even flashover. Many useful correlation equations derived for estimating the heat release rate for a post-flashover room fire were applied in performance-based designs. Three empirical correlation equations were justified by reported experimental data. Two sets of reported experimental results on post-flashover room fires with

transient heat release rates measured by oxygen consumption calorimetry were used. Estimated burning rate by correlation equations can be much lower than reported experimental data. Air pumping action of fire plume should be considered in applying empirical correlation for estimating heat release rate.

TABLES

Table 2.1: Properties of typical fire resistant products

Type	Glass product	Method of providing fire-resistance
Non-insulating	Wired glass	Glass breaks early on in the fire but is held together and in place by the embedded wire mesh [GGF, 2009]
	Toughened soda lime silicate glass	They are toughened physically or chemically to increase resistance to thermal stress. They can better withstand the impact of thermal shock and block the passage of flame and smoke [Curkeet, 2003; Lyon, 2007; GGF, 2009]
	Borosilicate	
	Glass ceramics	
	Reflective coated glazing	The metal coating is visually transparent and reduces the heat transferred to the glass by reflecting radiant energy (mostly infrared) from a fire [Curkeet, 2003]
	Resin laminated glazing	The resin-based interlayer is formulated to have resistance against fire and flaming. When exposed to a fire, the interlayer carbonizes to give an opaque layer, which holds the glass together and reduces heat radiation [Curkeet, 2003]
Insulating	Gel laminated glass	The gel interlayer absorbs heat by the evaporation of water and produces an insulating crust in the event of fire, which prevents the penetration of flame and smoke [Lyon, 2007; Amstock, 1997]
	Intumescent laminated glass	Intumescent interlayer turns opaque and foams to form a thick solid layer on exposure to heat inhibiting the passage of conductive and radiant heat [Lyon, 2007; Amstock, 1997]

Table 2.2: Comparisons of standard fire resistance tests used in different countries

Standards	Temperature / time condition (shown in Figure 2.1)	Performance criteria (conditions of failure)				
		Load-bearing	Integrity	Insulation	Radiation	Hose stream test
BS476 (1987)	$T = 345 \log_{10}(8t + 1) + 20$ (in °C)	Deflection or collapse	Cotton pad ignition or gap gauge penetration	Mean temperature rise more than 140 °C or maximum temperature rise more than 180 °C on unexposed face	N/A	N/A
BS EN 1365-1 (2012)	$T = 345 \log_{10}(8t + 1) + 20$ (in °C)	Deflection or collapse	Cotton pad ignition, gap gauge penetration or sustained flaming	Mean temperature rise more than 140 K or maximum temperature rise more than 180 K on unexposed face	Report the time for radiation to exceed 5, 10, 15, 20, 25 kW·m ⁻²	N/A
ASTM E 119 (2011)	538°C at 5 min; 704°C at 10 min; 843°C at 30 min; 927°C at 1 hr; 1010°C at 2 hrs; 1093°C at 4 hrs; 1260°C at 8 hrs or over.	Collapse	Cotton pad ignition or sustained flaming	Temperature rise more than 140 °C on unexposed face	N/A	Water pressure and duration of application specified in ASTM E 2226 (2011)
GB 12513 (2006)	$T = 345 \log_{10}(8t + 1) + T_0$; T ₀ is in the range of 5 to 40°C.	N/A	Cotton pad ignition, gap gauge penetration or sustained flaming	Mean temperature rise more than 140 °C or maximum temperature rise more than 180 °C on unexposed face	Report the time for radiation to exceed 5, 10, 15, 20, 25 kW·m ⁻²	N/A

Table 3.1: Summary of important asphyxiant and irritant gases

Important toxicants		Mechanism of effects	IDLH* (ppmv) [NIOSH, 1994]	<i>LC</i> ₅₀ (ppmv) [ISO 13344, 2004]
Asphyxiant gases	Carbon monoxide (CO)	Cause tissue hypoxia by displacing and reducing oxygen level in the blood and inhibiting oxygen release [Purser, 2010a].	1200	5700
	Hydrogen cyanide (HCN)	No direct effect on oxygen level in the blood, but prevents consumption of oxygen in the tissues [Purser, 2010a].	50	165
	Oxygen (O ₂) depletion	Cause insufficient oxygen supply to brain and part of the body [Hartzell, 2003]	N/A	N/A
	Carbon dioxide (CO ₂)	Stimulate respiration causing more intakes of oxygen and other toxic gases [Hull and Stec, 2010]	40000	N/A
Irritant gases	Hydrogen chloride (HCl)	Cause sensory irritations with symptoms include discomfort and pain, breath-holding, coughing and excessive secretion of mucus; at high concentration, irritant gases can penetrate into lungs causing irritation and tissue damage which may result in post-exposure respiratory distress and death [Purser, 2010b].	50	3800
	Hydrogen bromide (HBr)		30	3800
	Hydrogen fluoride (HF)		30	2900
	Nitric oxide (NO)		100	N/A
	Nitrogen dioxide (NO ₂)		20	170
	Acrolein		2	150
	Formaldehyde		20	750
	Sulphur dioxide (SO ₂)		100	1400

*The immediately dangerous to health or life (IDLH)

Table 3.2: Summary of main bench- scale toxicity test methods of fire smoke

Test method	Test code	ISO stage [ISO 19706, 2011]	Heat source	Ventilation in decomposition zone	Hazard assessment
Radiant furnace test methods	ASTM E 1678 [2010]	Well ventilated flaming or possibly ventilated flaming	Radiant panel	Natural ventilation	Animal exposure or chemical analysis
Tube furnace	NF X 70-100 [2006]	Non-flaming or under ventilated flaming	Tube furnace	Forced ventilation	Chemical analysis
Steady state tube furnace (DIN type)	DIN 53436 [1981-2003]	Non-flaming or under ventilated flaming	Tube furnace	Forced ventilation	Animal exposure or chemical analysis
Steady state tube furnace (Purser)	BS 7990 [2003], ISO/TS 19700 [2007] and IEC TS 60695-7-50 [2002]	Non-flaming, well or under ventilated flaming	Tube furnace	Forced ventilation	Chemical analysis
UPITT	N/A	Non-flaming, well or under ventilated flaming	Crucible	Forced ventilation	Animal exposure or chemical analysis
Cone calorimeter	ISO 5660-1 [2002] and ISO 5660-2 [2002]	Non-flaming, well or under ventilated flaming	Radiant panel	Natural convection	Heat and smoke with possible chemical analysis

Table 4.1: Characteristics of selected fire resisting samples

Sample number	Shape	Dimensions (cm)			Production method	Claimed fire resistance	
		Length	Width	Thickness		Integrity	Insulation
1	Square	10	10	2.5	Sealing gel protective layer in the inter-space of glass boxes	30	30
2	Rectangular	15	10	2.0		30	30
3	Rectangular	15	10	1.7		30	30
4	Right angle triangular	23	16.4	2.6		30	30
5	Square	10	10	2.5	Laminating protective interlayer in between the glass sheets	60	25
6	Square	10	10	2.5		60	30

Table 4.2: Chemical elements with atomic percentages detected by XPS

Sample number	Elements* (at. %)								
	C	O	N	Cl	S	Si	Na	K	Mg
1	40.01	21.95	4.77	17.16	--	--	1.22	0.44	14.46
2	38.96	20.46	4.24	19.15	--	--	1.25	0.64	15.30
3	38.51	22.70	3.96	18.50	--	--	0.56	0.15	15.62
4	35.79	25.54	4.90	17.61	1.27	--	1.49	0.11	13.29
5	26.95	41.73	0.13	2.41	--	7.69	21.09	--	--
6	36.02	40.98	--	1.83	--	7.17	14.0	--	--

*Noting that hydrogen (H) and helium (He) could not be detected by XPS

Table 4.3: Functional groups with characteristic absorption peaks detected by FTIR

Sample number	Peaks position (cm ⁻¹)								Possible chemical compositions
	H ₂ O	C=O	N-H	C-H	C-OH	C-Cl	C-O	Si-O	
1	3400	1677	1634	1452	1119	604	--	--	water, amide, alcohol
2	3400	1677	1634	1452	1119	604	--	--	water, amide, alcohol
3	3400	1677	1634	1452	1119	604	--	--	water, amide, alcohol
4	3400	1667	1634	1462	1119	604	--	--	water, amide, alcohol,
5	3400	1645	--	1462	1119	604	1032	775 581 450	water, silicates, alcohol, carboxylate
6	3400	1645	--	1462	1119	604	1032	450	water, silicates, alcohol, carboxylate

Table 5.1: Thermogravimetric characterization of samples in air and nitrogen with 20 °C·min⁻¹ heating rate

Sample number	Weight loss (%)		Maximum weight loss rate (%·min ⁻¹)		Temperature at weight loss rate (°C)	
	Air	Nitrogen	Air	Nitrogen	Air	Nitrogen
Sample 1	94.5%	96.5%	16.1	14.3	130	139
Sample 2	94.1%	90.1%	11.1	12.4	133	131
Sample 3	93.3%	92.1%	15.3	12.8	128	124
Sample 4	91.1%	91.6%	14.8	13.6	127	135
Sample 5	37.3%	32.9%	3.4	5.6	160	88
Sample 6	56.1%	50.9%	7.7	6.2	363	134

Table 5.2: Comparisons of chemical compositions of the gases from different tests

Sample number	Chemical Composition of the Gases			
	TG-FTIR	Py-GC-MS	TF-FTIR	
	Air	Vacuum	Argon	Air
1	H ₂ O, CO ₂ , HCl, NH ₃	H ₂ O, CO ₂ , HCl	H ₂ O, HCl, CO ₂ , -C-H (alkyl)	H ₂ O, CO ₂ , CO, HCl, NH ₃ , -C-H (alkyl)
2	H ₂ O, CO ₂ , HCl, NH ₃	H ₂ O, CO ₂ , HCl	H ₂ O, CO ₂ , HCl, CO, -C-H (alkyl)	H ₂ O, CO ₂ , CO, HCl, NH ₃ , -C-H (alkyl)
3	H ₂ O, CO ₂ , HCl, NH ₃	H ₂ O, CO ₂ , HCl, NH ₃	H ₂ O, CO ₂ , HCl, CO -C-H (alkyl)	H ₂ O, CO ₂ , CO, HCl
4	H ₂ O, CO ₂ , HCl, NH ₃	H ₂ O, CO ₂ , HCl, NH ₃	H ₂ O, HCl, CO ₂ , CO -C-H (alkyl)	H ₂ O, CO ₂ , CO, HCl
5	H ₂ O, CO ₂ , HCl	H ₂ O, CO ₂ , HCl, alkenes, aldehydes	H ₂ O, CO ₂ , HCl, CO, -C=O(carbonyl), -C-H (alkyl)	H ₂ O, CO ₂ , CO, HCl, - C=O(carbonyl)
6	H ₂ O, CO ₂ , HCl	H ₂ O, CO ₂ , CO HCl, alkenes, aldehydes	H ₂ O, HCl, CO ₂ , CO, -C=O(carbonyl)	H ₂ O, CO ₂ , CO, HCl -C=O(carbonyl)

Table 6.1: Characteristics of fire resisting samples for cone calorimeter tests

Sample number	Shape	Dimensions (cm)			Production method	Claimed fire resistance	
		Length	Width	Thickness		Integrity	Insulation
1	Square	10	10	2.5	Sealing gel protective layer in the inter-space of glass boxes	30	30
2	Rectangular	15	10	2.0		30	30
3	Rectangular	15	10	1.7		30	30
5	Square	10	10	2.5	Laminating protective interlayer in between the glass sheets	60	25
6	Square	10	10	2.5		60	30

Table 6.2: Summaries of fire resisting glass samples in cone calorimeter tests

Parameters	Sample 1		Sample 2	Sample 3	Sample 5		Sample 6	
	Heat flux (kW·m ⁻²)	50	70	70	70	50	70	50
Mass (g)	470	470	586	500	616	629	576	565
Thickness (cm)	2.5	2.5	2.0	1.7	2.5	2.5	2.5	2.5
Mass loss Δm (g)	90.6	85.4	78.7	72.3	27.4	32.7	38.4	25.9
Increase of Thickness (%)	0	0	0	0	70	92	44	63
$pk[CO]$ (ppmv)	6.0	8.3	9.0	16.0	12.0	18.0	18.9	44.6
CO yield (kg·kg ⁻¹)	0.0005	0.0005	0.0009	0.002	0.006	0.007	0.01	0.02
FED_c	0.74	0.79	0.74	1.17	3.00	3.77	8.03	8.91
LC_{50} (g·m ⁻³)	12325	10798	10609	6170	913	867	478	291
x (kJ·m ⁻² ·s ⁻²)	0	0	0	0	0	0	0	0
	LRF	LRF	LRF	LRF	LRF	LRF	LRF	LRF
y (MJ·m ⁻²)	0	0	0	0	0	0	0	0
	VLRH	VLRH	VLRH	VLRH	VLRH	VLRH	VLRH	VLRH
z (m ³ ·kg ⁻¹)	0.1	0.1	0.1	0.2	2	2	3	4
	LRTH	LRTH	LRTH	LRTH	IRTH	IRTH	IRTH	IRTH

Table 8.1: Justification of BW equation using data by Chow et al. (2003)

Number Parameters		Test											
		A1a	A1b	A2a	A2b	A3a	A3b	A4a	A4b	A5a	A5b	A6	
Ventilation height h_v (m)		1.95		1.8		1.6		1.45		1.2		0.9	
Height of vent bottom h_{vb} (m)		0		0		0		0.25		0.375		0.525	
Ventilation factor V_f (m ^{5/2})		2.18		1.93		1.62		1.4		1.05		0.68	
Ambient temperature T_o (°C)		15	15	15	15	16	16	15	15	16	16	16	
Burning time t_B (s)		621	488	472	556	547	524	566	531	452	422	608	
Maximum heat release rate measured \dot{q}_{max} (kW)		2642	2632	2496	2460	2112	2354	1996	1776	1335	1306	934	
Maximum temperature T_{fmax} (°C)		806	818	791	799	760	809	798	750	751	710	675	
m_A (kW·°C ⁻¹)	0.3 \dot{q}_s	m_{AV}	0.69	0.69	0.61	0.61	0.51	0.51	0.44	0.44	0.33	0.33	0.21
		m_A	1.55	1.57	1.44	1.46	1.28	1.38	1.29	1.20	1.09	1.01	0.84
	0.5 \dot{q}_s	m_{AV}	1.14	1.14	1.01	1.01	0.85	0.85	0.74	0.74	0.55	0.55	0.36
		m_{AL}	0.86	0.89	0.83	0.85	0.77	0.87	0.85	0.76	0.76	0.68	0.62
		m_A	2.00	2.03	1.84	1.86	1.62	1.72	1.59	1.49	1.31	1.23	0.98
	0.7 \dot{q}_s	m_{AV}	1.60	1.60	1.42	1.42	1.19	1.19	1.03	1.03	0.77	0.77	0.50
		m_A	2.46	2.49	2.25	2.27	1.96	2.06	1.88	1.78	1.53	1.45	1.12

Table 8.1: (Continued) Justification of BW equation using data by Chow et al. (2003)

Number Parameters \ Test		A1a	A1b	A2a	A2b	A3a	A3b	A4a	A4b	A5a	A5b	A6
		Fitting (ii)	m_f (kW·°C ⁻¹)	3.09	3.09	2.65	2.85	2.50	2.50	2.37	2.28	1.93
R ²	0.913		0.929	0.859	0.886	0.805	0.822	0.851	0.820	0.763	0.749	0.737
β	1.95		1.93	1.79	1.98	2.03	1.91	2.07	2.07	2.12	2.19	2.87
Fitting (iii)	m_f (kW·°C ⁻¹)	2.98	2.92	2.65	2.74	2.44	2.41	2.17	2.06	1.72	1.74	1.48
	R ²	0.808	0.825	0.773	0.795	0.729	0.715	0.711	0.693	0.645	0.666	0.644
	β	1.85	1.78	1.79	1.87	1.96	1.81	1.80	1.78	1.74	1.92	2.40
Fitting (iv)	m_f (kW·°C ⁻¹)	3.37	3.32	3.06	3.16	2.82	2.86	2.65	2.58	2.20	2.22	1.75
	R ²	0.481	0.513	0.377	0.386	0.302	0.333	0.752	0.770	-0.0874	0.188	-0.304
	β	2.19	2.13	2.20	2.28	2.41	2.34	2.45	2.48	2.61	2.79	3.15
Fitting (v)	m_f (kW·°C ⁻¹)	3.36	3.44	3.05	3.13	2.90	2.98	2.81	2.75	1.99	2.12	1.71
	R ²	0.169	-0.824	-0.249	0.091	-0.166	0.025	0.591	0.167	0.711	0.663	0.709
	β	2.18	2.23	2.19	2.25	2.50	2.48	2.67	2.71	2.23	2.61	3.04
Fitting (vi)	m_f (kW·°C ⁻¹)	3.38	3.23	2.81	2.72	2.87	2.85	2.63	2.57	2.23	2.23	1.84
	R ²	0.807	0.617	0.271	0.234	0.687	0.397	0.575	0.725	0.438	0.563	0.205
	β	2.20	2.05	1.95	1.85	2.47	2.32	2.42	2.47	2.67	2.81	3.41

Table 8.2: Fitting MQH and VB equations using data by Chow et al. (2003)

Test	MQH equation				VB equation		
	a_m (kW·°C ^{-3/2})	Fitted line		Fitted line (All data)		b_v (kW)	c_v (°C)
		a_f (kW·°C ^{-3/2})	R ²	a_f (kW·°C ^{-3/2})	R ²		
A1a	0.16	0.13	0.967	0.13	0.925	460	414
A1b		0.13	0.9656	0.13	0.9328		
A2a	0.15	0.11	0.9582	0.12	0.9070	407	407
A2b		0.12	0.9589	0.12	0.9214		
A3a	0.14	0.11	0.9234	0.11	0.8640	342	395
A3b		0.11	0.9376	0.11	0.8612		
A4a	0.13	0.10	0.9568	0.097	0.8580	295	383
A4b		0.10	0.9417	0.093	0.8339		
A5a	0.11	0.091	0.8997	0.079	0.7816	222	358
A5b		0.090	0.8923	0.080	0.8056		
A6	0.09	0.083	0.8659	0.073	0.7812	144	314

Table 8.3: Fitting results by Hietaniemi et al. (2004)

Parameters			V1	V2	
Ventilation height h_v (m)			0.6	0.6	
Height of vent bottom above floor h_{vb} (m)			1.3	1.3	
Ventilation factor V_f ($m^{5/2}$)			0.56	0.56	
Ambient air temperature T_0 ($^{\circ}C$)			20	20	
Time for air temperature next to ceiling to reach $600^{\circ}C$ t_T (s)			255	255	
Maximum heat release rate measured \dot{q}_{max} (kW)			2819	2718	
Maximum gas temperature T_{fmax} ($^{\circ}C$)			1137	1194	
BW equation	$m_A / kW^{\circ}C^{-1}$	0.3 \dot{q}_s	m_{AV}	0.18	0.18
			m_A	1.04	1.06
		0.5 \dot{q}_s	m_{AV}	0.29	0.29
			m_{AL}	0.87	0.89
			m_A	1.16	1.18
		0.7 \dot{q}_s	m_{AV}	0.41	0.41
	m_A		1.27	1.30	
	Fitted line	m_f ($kW \cdot ^{\circ}C^{-1}$)		1.83	1.94
		R^2		0.739	0.832
		β		3.29	3.6
	Fitted line (All data)	m_f ($kW \cdot ^{\circ}C^{-1}$)		1.74	2.20
		R^2		0.624	0.707
		β		2.99	4.48
MQH equation	a_m ($kW \cdot K^{-3/2}$)		0.058	0.058	
	Fitted line	a_f ($kW \cdot K^{-3/2}$)	0.063	0.061	
		R^2	0.781	0.871	
	Fitted line (All data)	a_f ($kW \cdot K^{-3/2}$)	0.061	0.074	
		R^2	0.664	0.691	

FIGURES

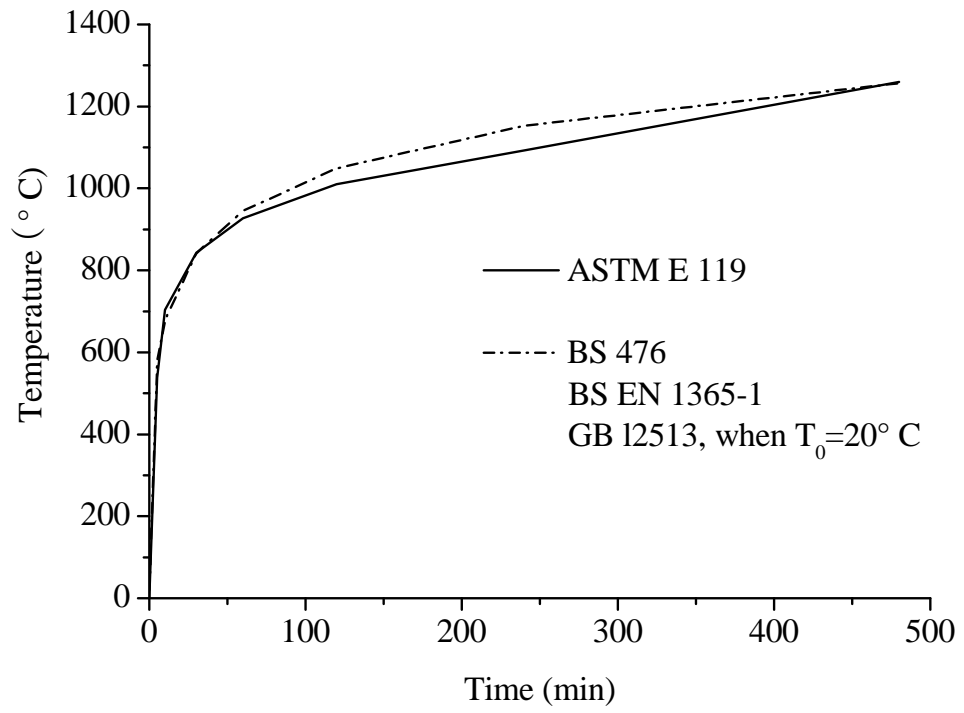


Figure 2.1: Standard temperature-time curves

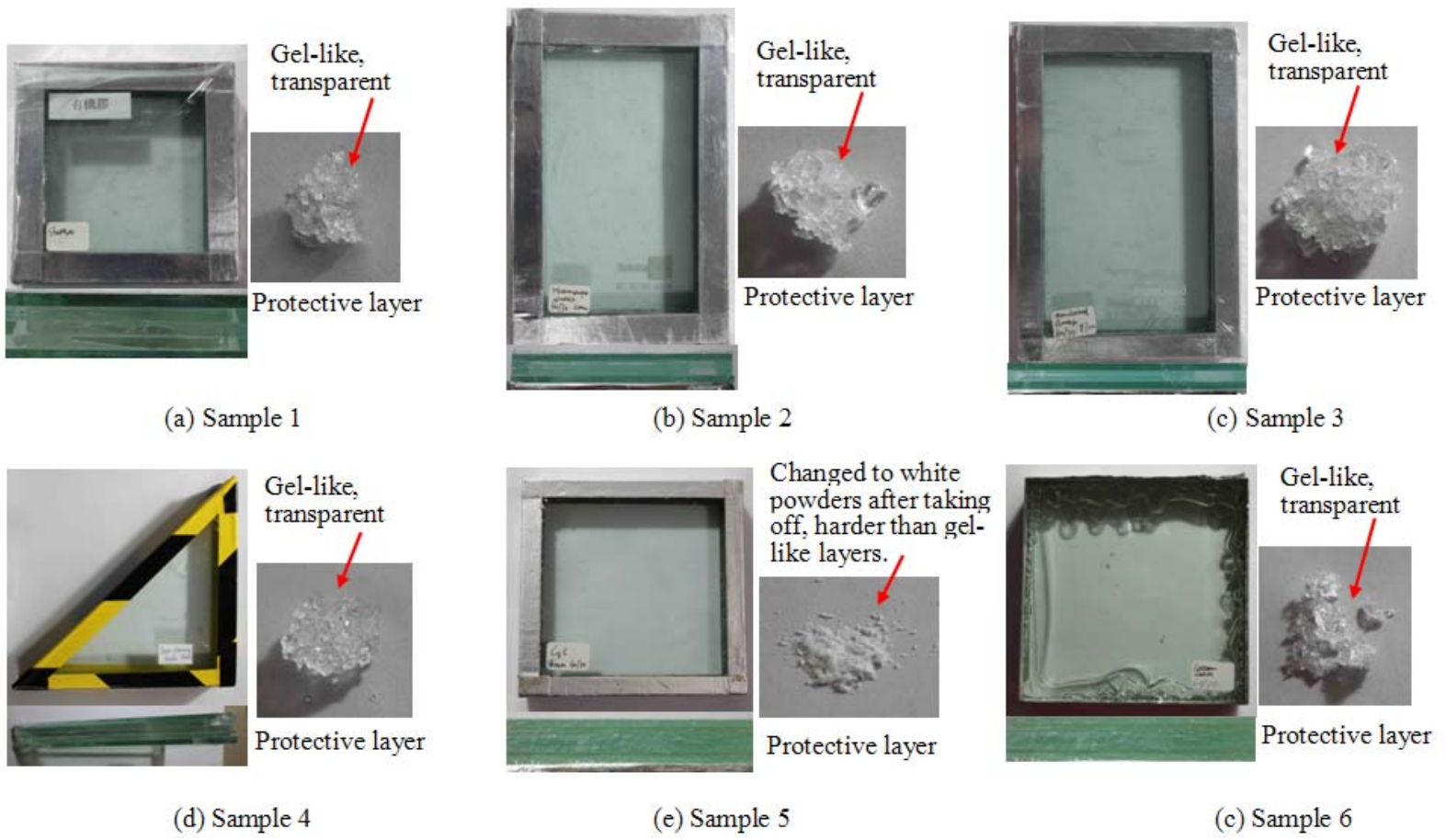
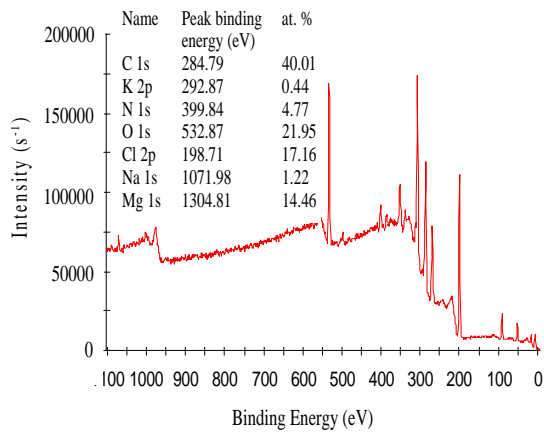
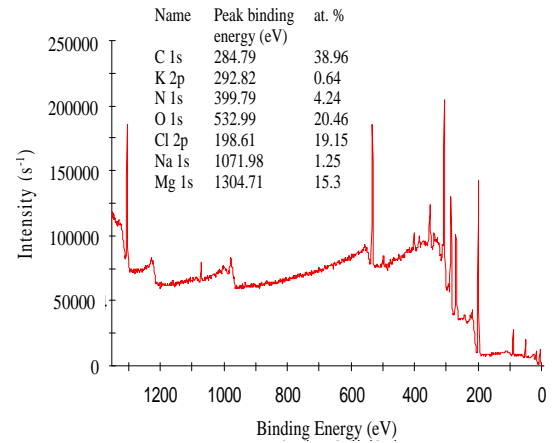


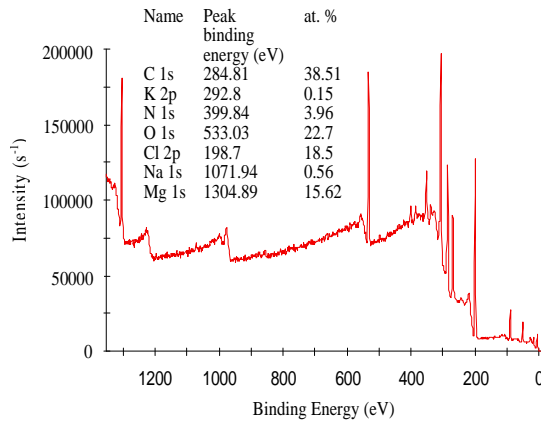
Figure 4.1: Appearance of the tested samples



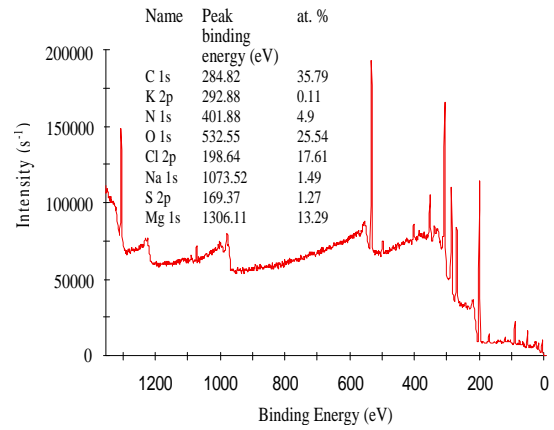
(a) Sample 1



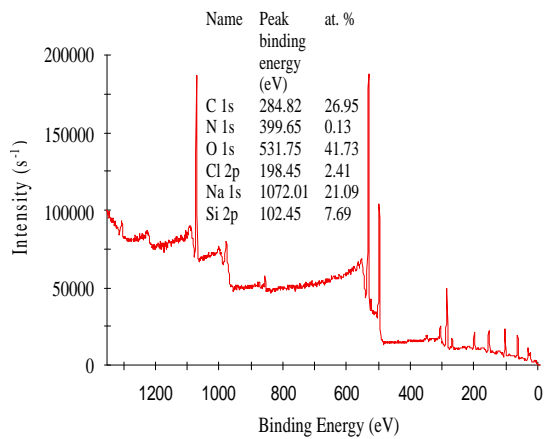
(b) Sample 2



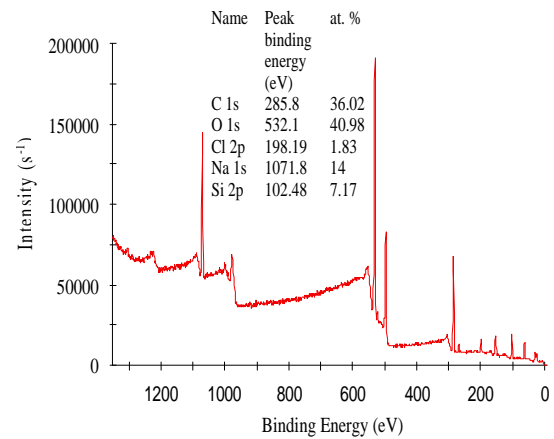
(c) Sample 3



(d) Sample 4



(e) Sample 5



(f) Sample 6

Figure 4.2: XPS spectra of samples

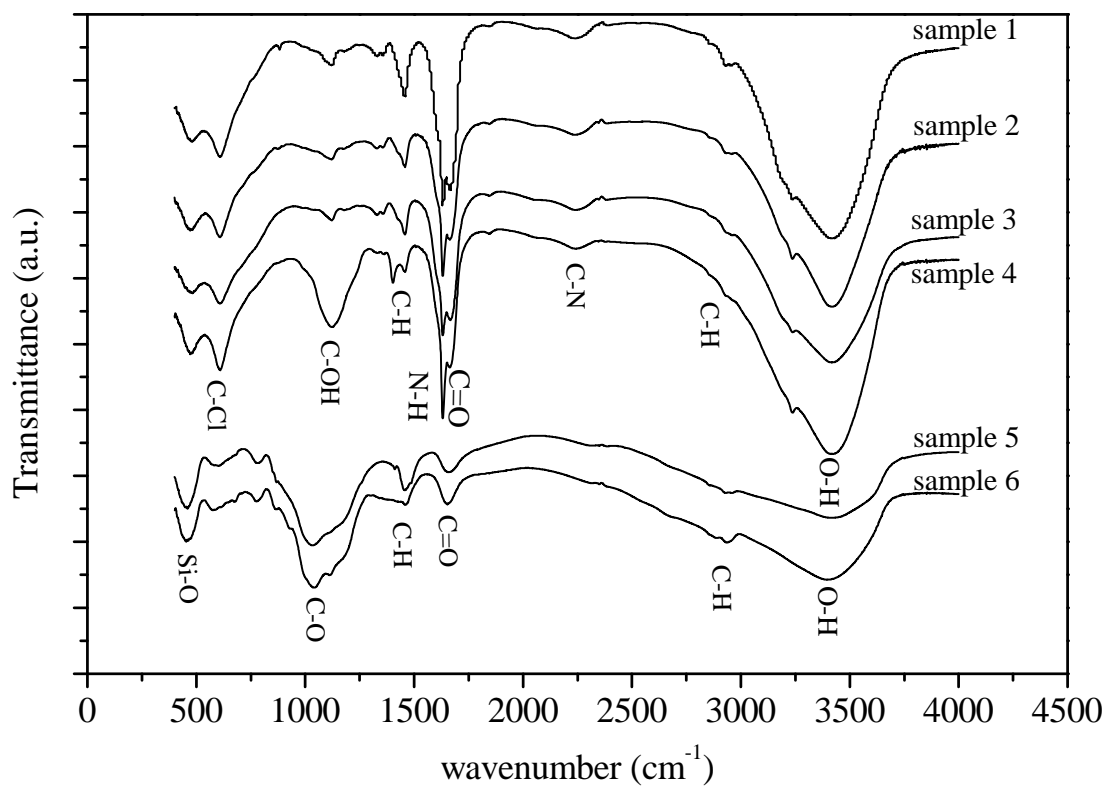
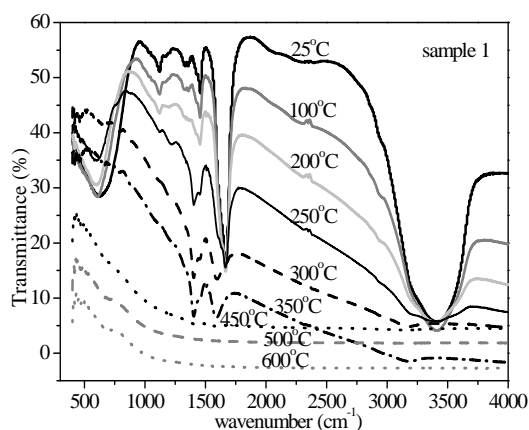
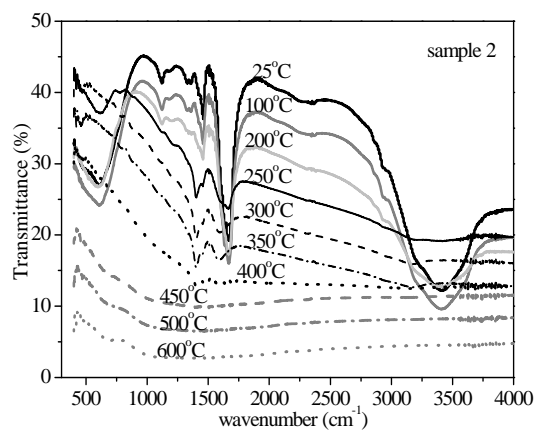


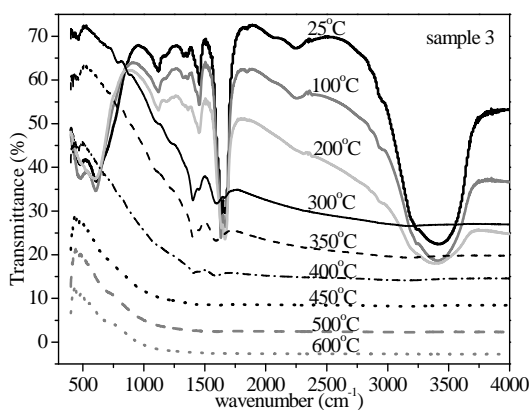
Figure 4.3: FTIR spectra of samples at room temperature



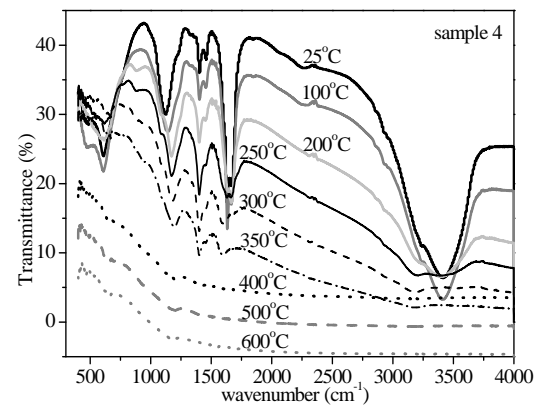
(a) Sample 1



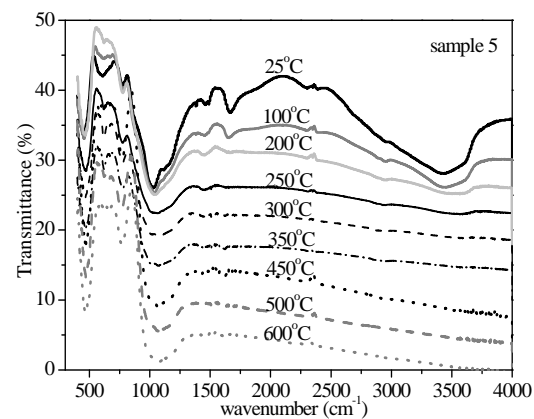
(b) Sample 2



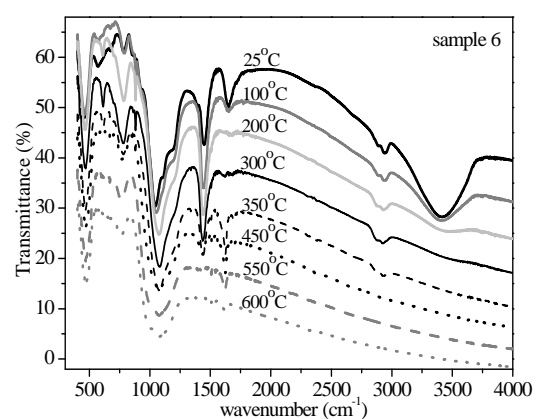
(c) Sample 3



(d) Sample 4

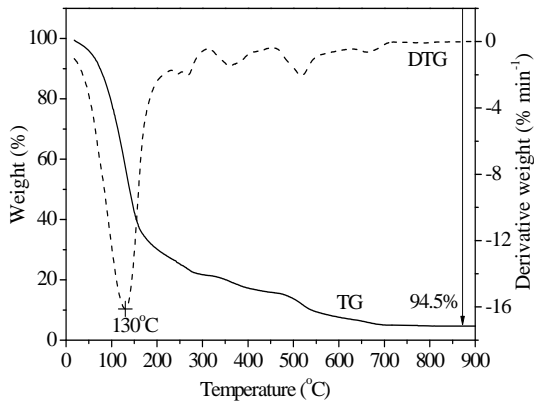


(e) Sample 5

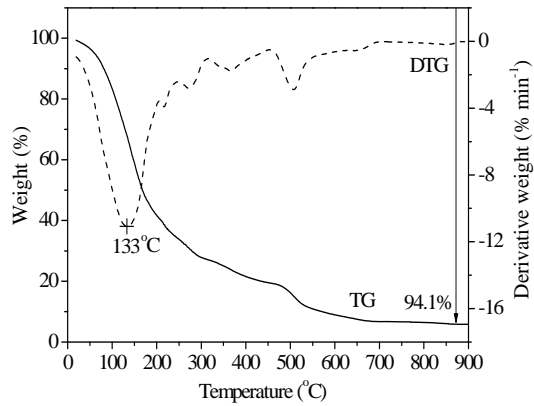


(f) Sample 6

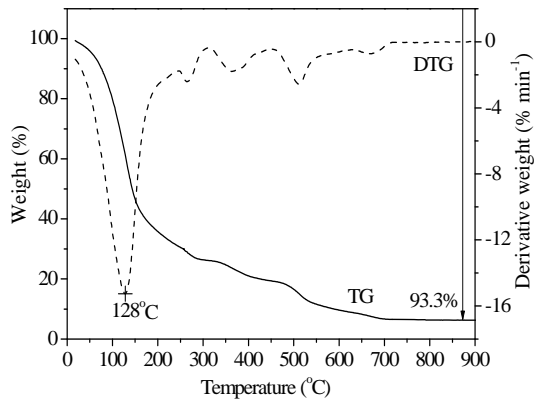
Figure 4.4: FTIR spectra of samples from room temperature to 600 °C at 20 °C·min⁻¹ heating rate



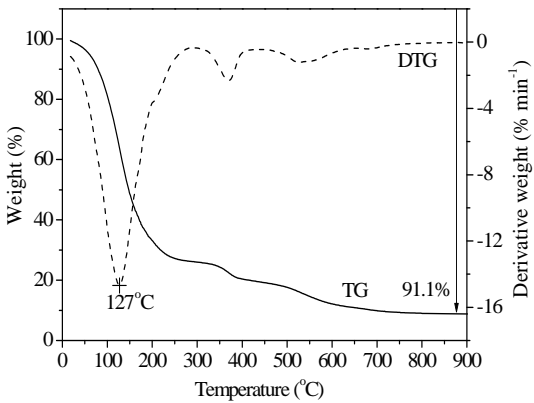
(a) Sample 1



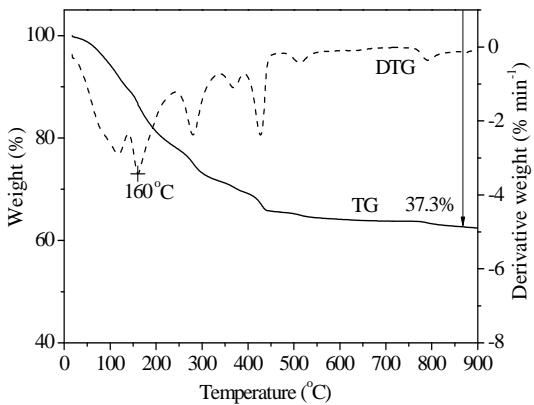
(b) Sample 2



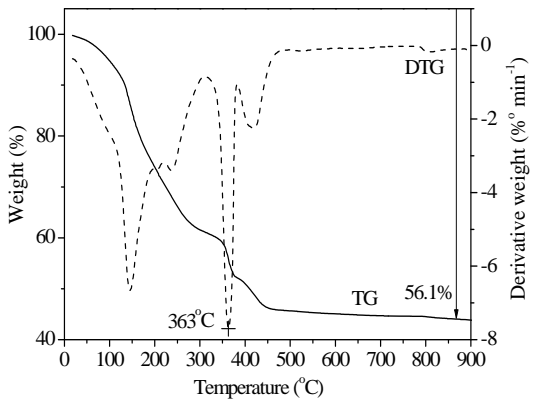
(c) Sample 3



(d) Sample 4

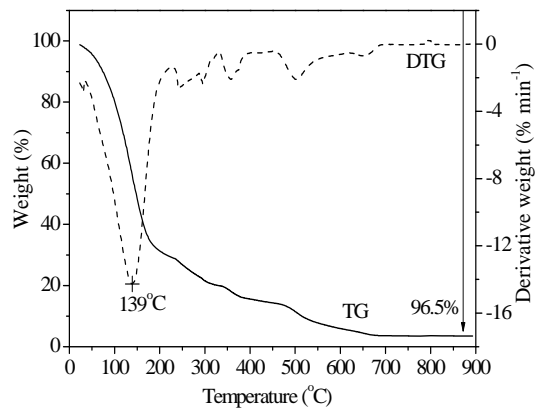


(e) Sample 5

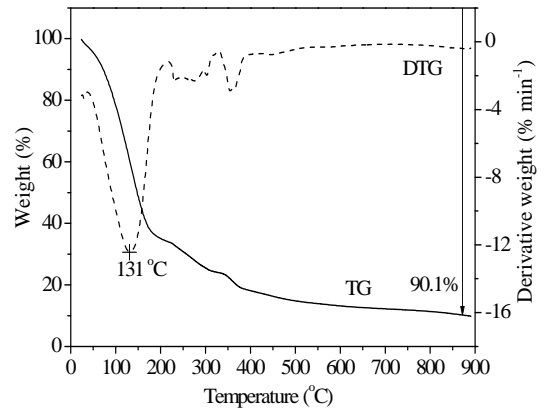


(f) Sample 6

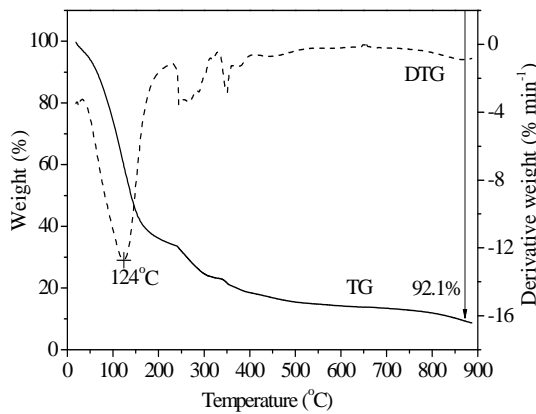
Figure 5.1: TG/DTG profiles of samples in air at $10\text{ }^{\circ}\text{C}\cdot\text{min}^{-1}$ heating rate



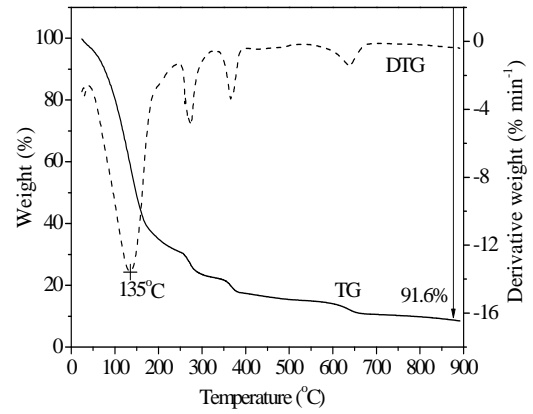
(a) Sample 1



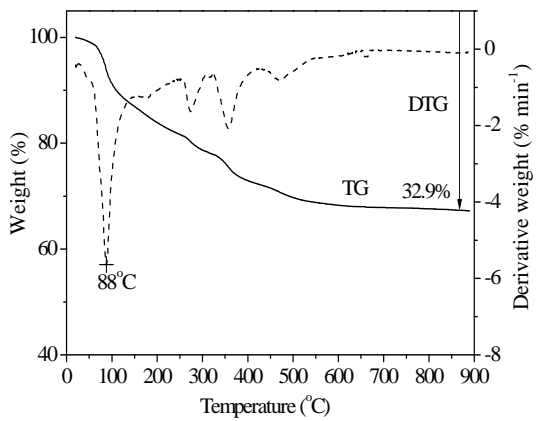
(b) Sample 2



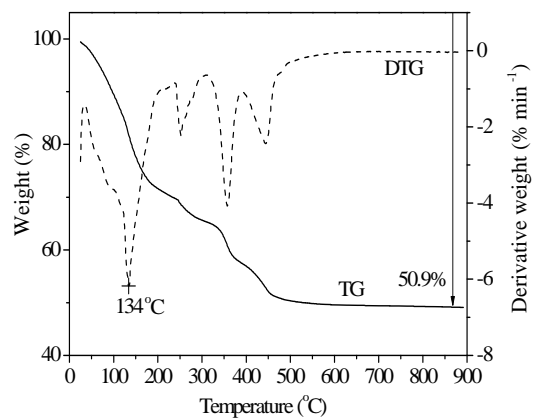
(c) Sample 3



(d) Sample 4



(e) Sample 5



(f) Sample 6

Figure 5.2: TG/DTG profiles of samples in nitrogen at $10\text{ }^{\circ}\text{C}\cdot\text{min}^{-1}$ heating rate

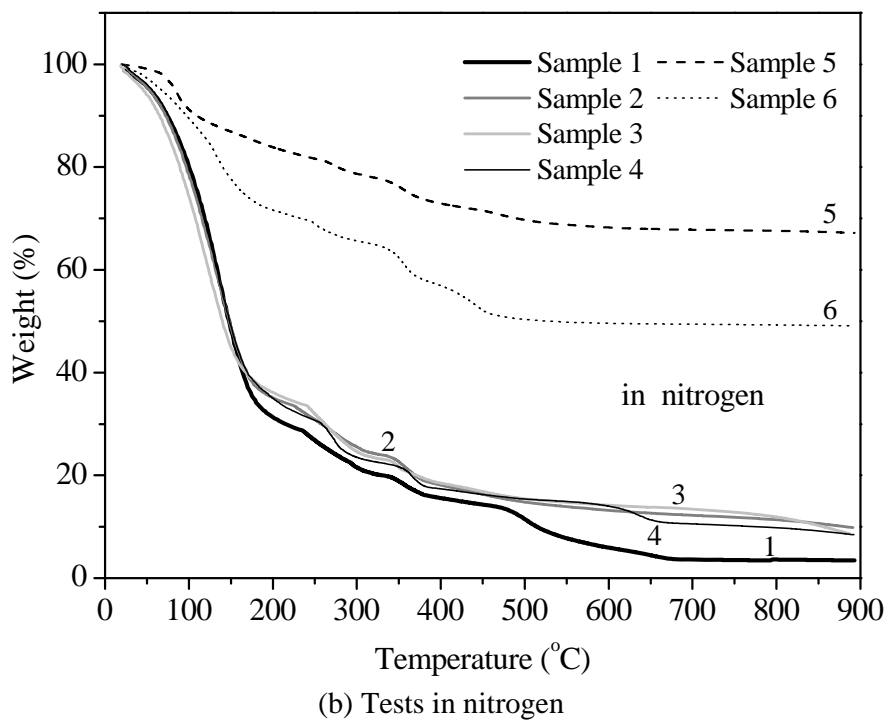
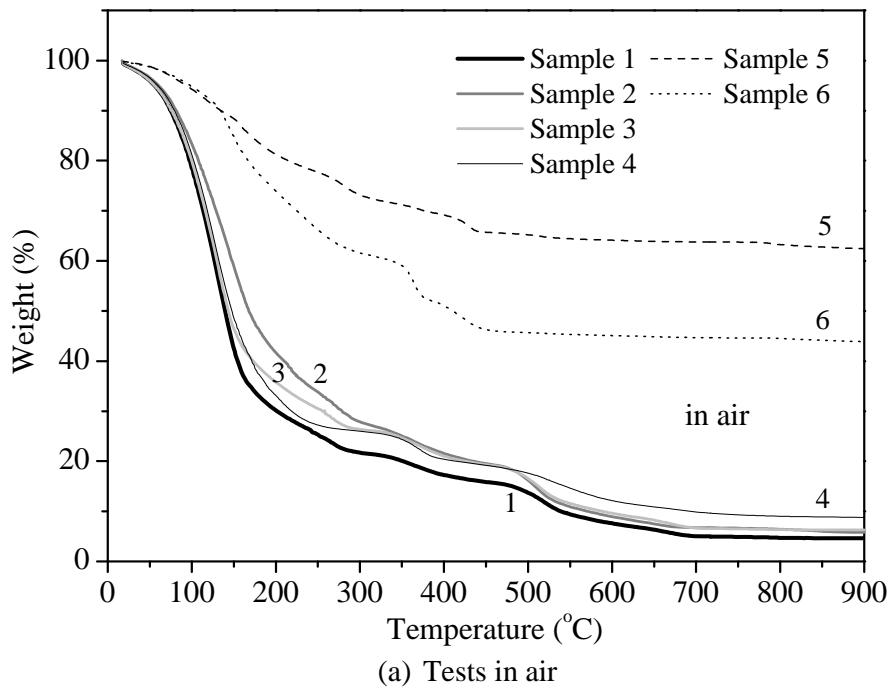


Figure 5.3: Comparison of TG profiles in air and nitrogen at 20 °C·min⁻¹ heating rate

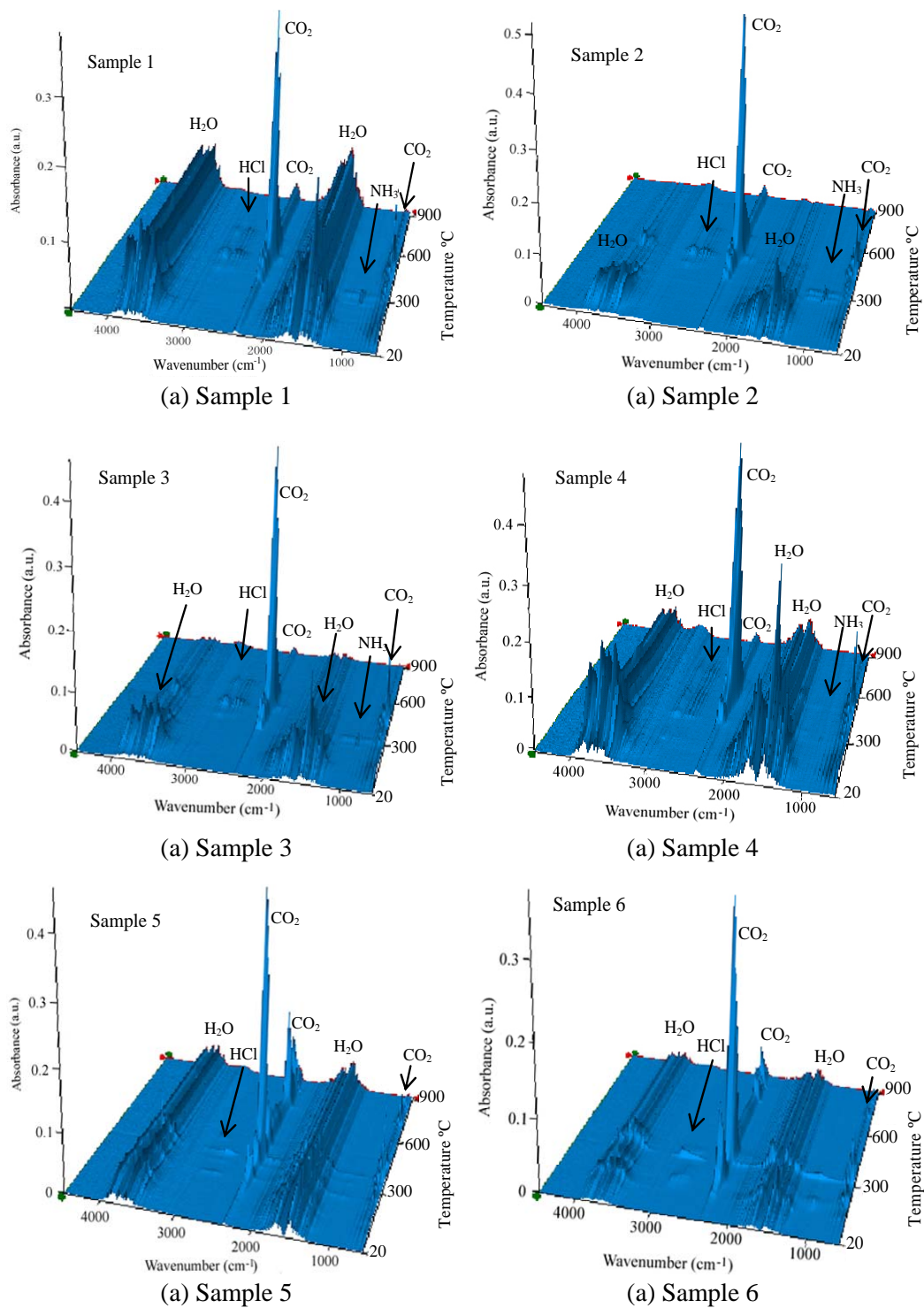


Figure 5.4: FTIR spectra of gases emitted in air at 20 °C·min⁻¹ heating rate from TG-FTIR

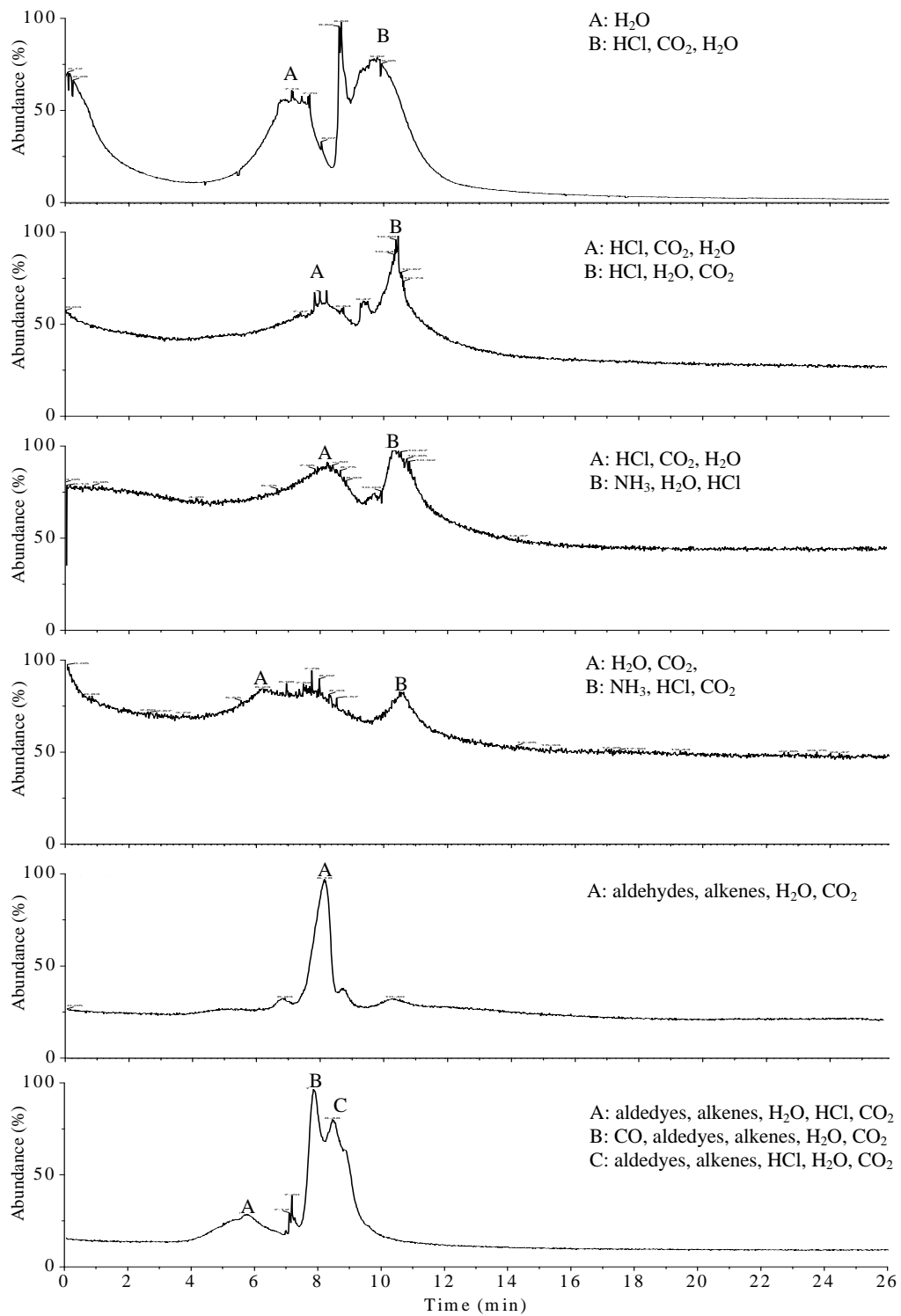


Figure 5.5: GC patterns and gas compositions detected by MS from Py-GC-MS

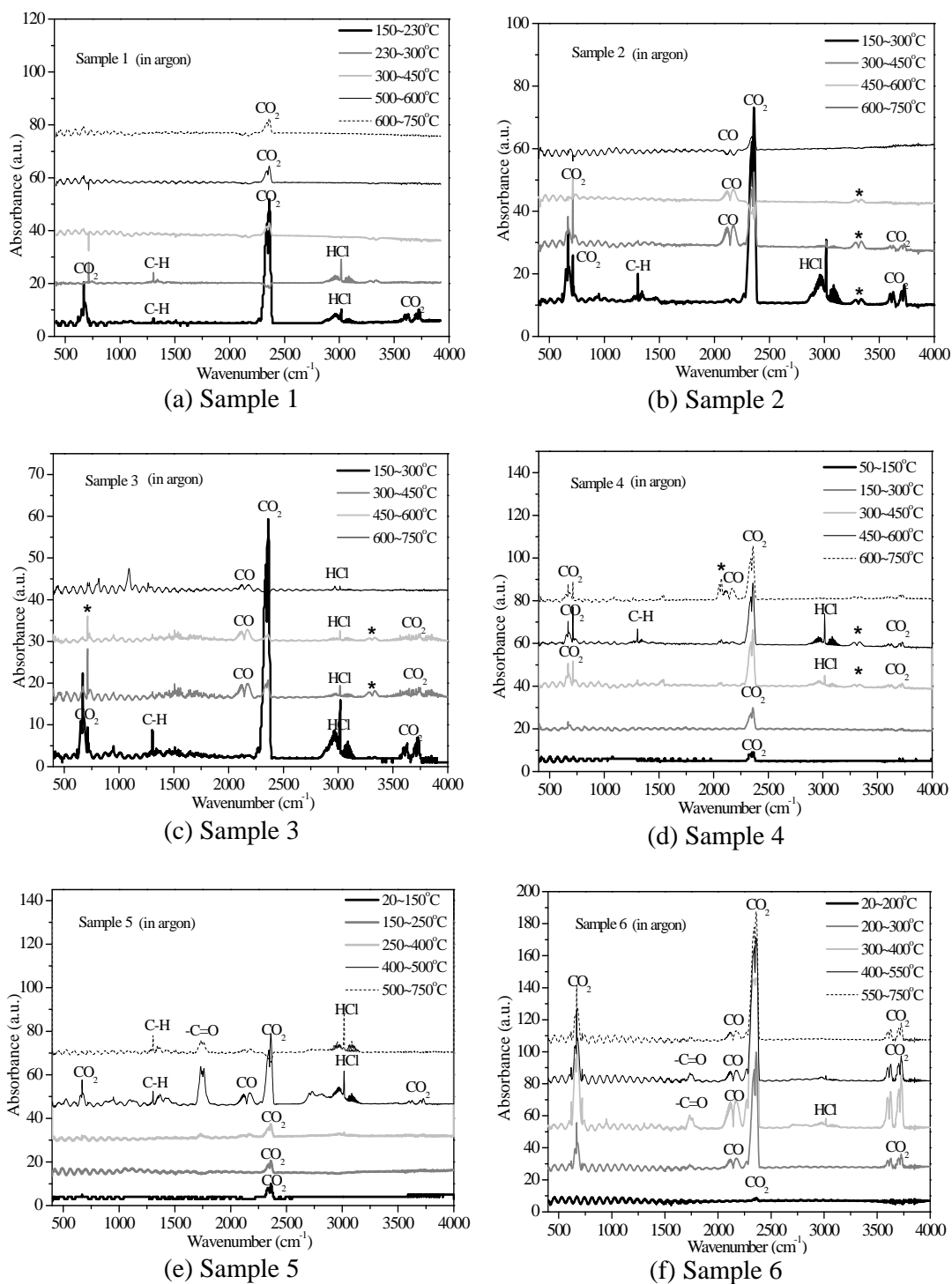


Figure 5.6: FTIR spectra of gases emitted in argon at $10\text{ }^{\circ}\text{C}\cdot\text{min}^{-1}$ heating rate from TF-FTIR

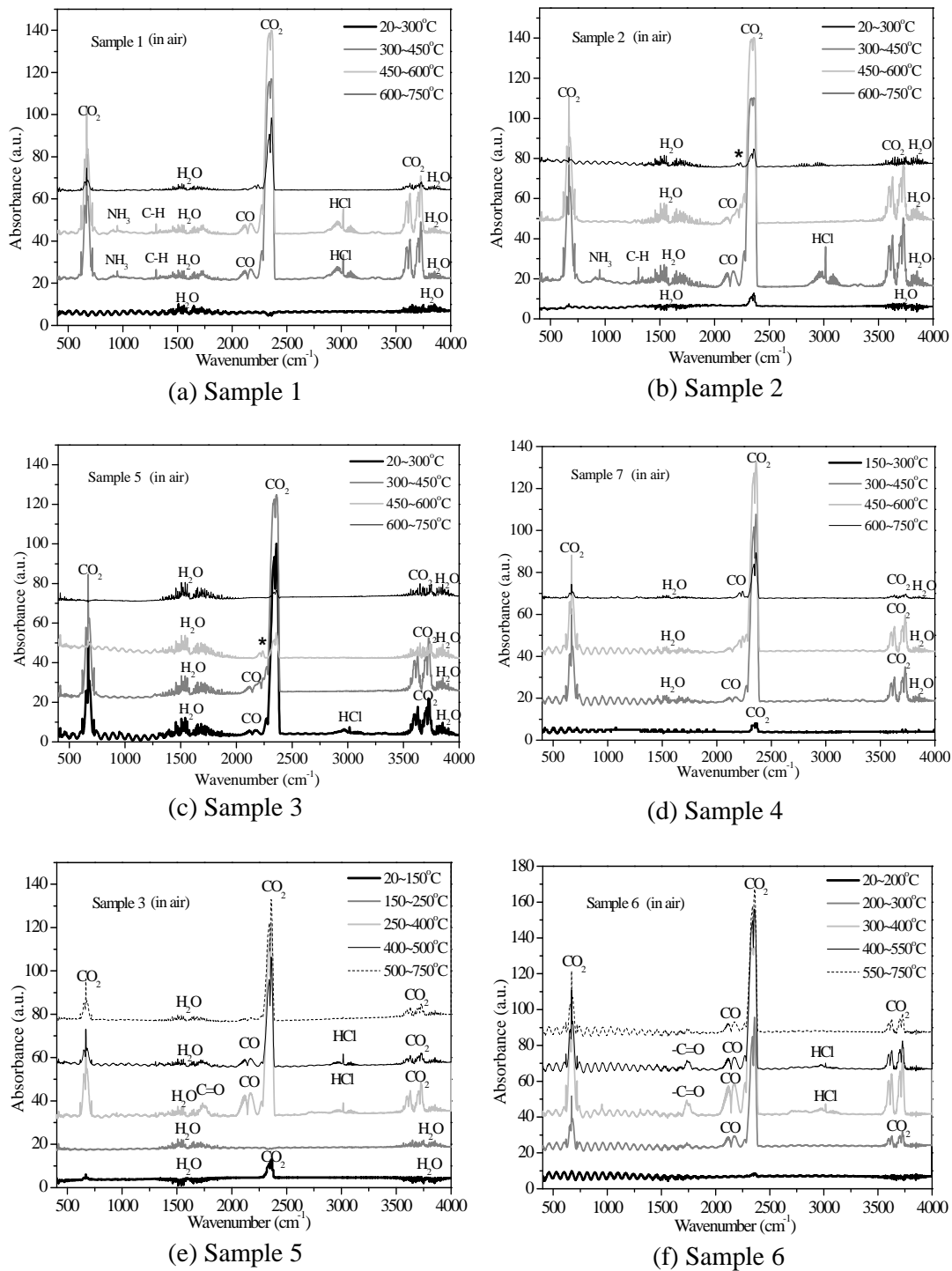
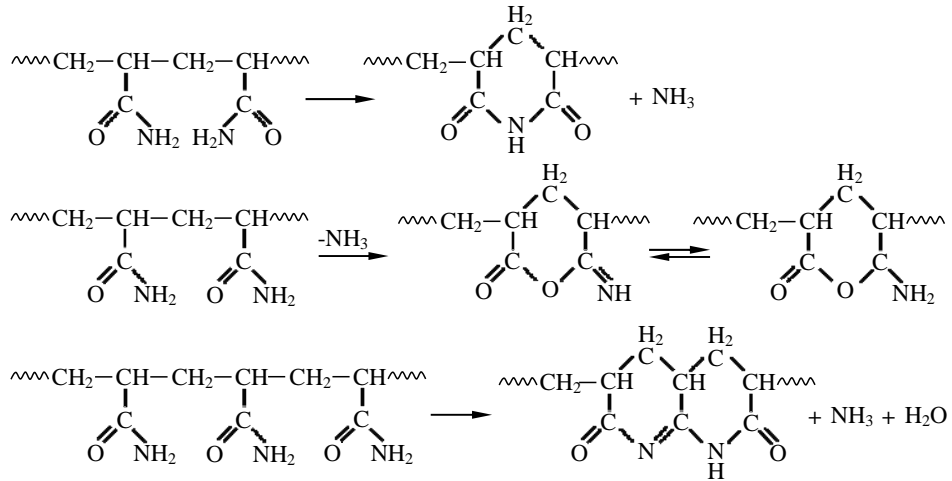


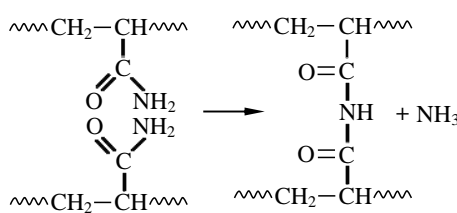
Figure 5.7: FTIR spectra of gases emitted in air at $10\text{ }^{\circ}\text{C}\cdot\text{min}^{-1}$ heating rate from TF-FTIR

Reaction of the amide functional group

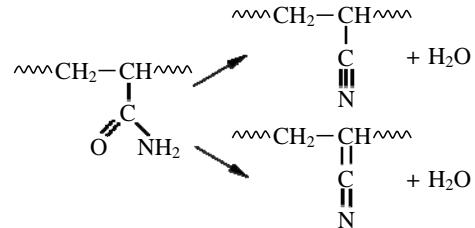
Intramolecular imidization



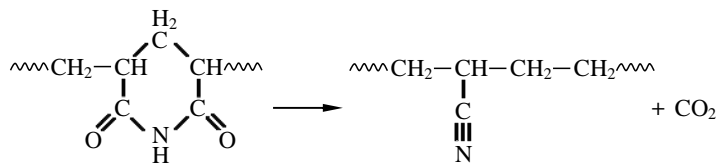
Intermolecular imidization



Dehydration of amide



Breakdown of cyclic imides



Bond homolysis

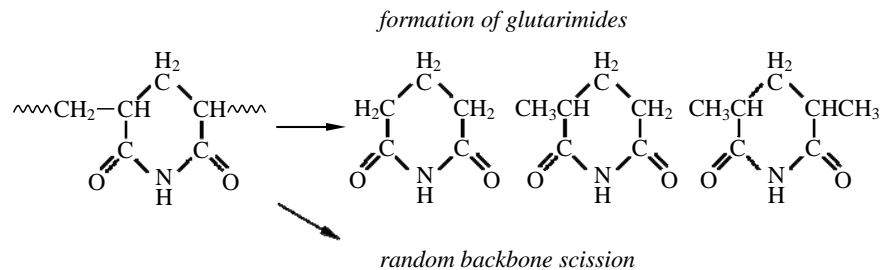


Figure 5.8: Summary of reaction for the thermal decomposition of polyacrylamide

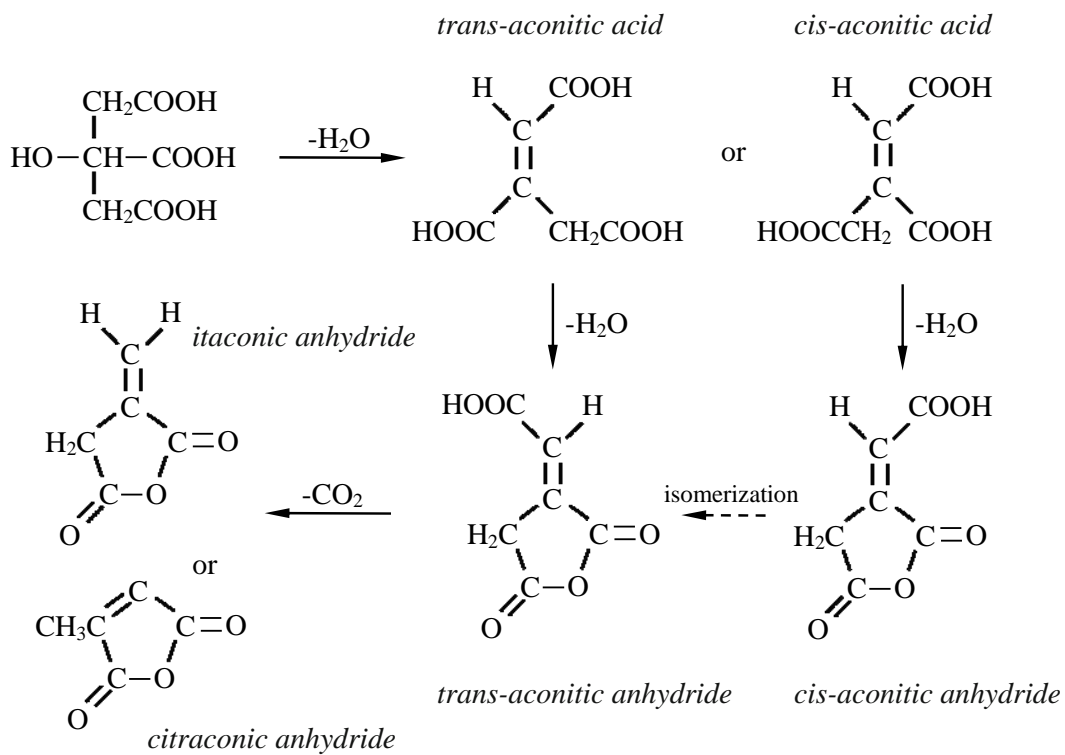
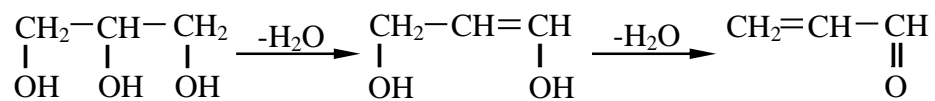


Figure 5.9: Summary of reactions for the thermal decomposition of citric acid

Acrolein formation



Acetaldehyde formation

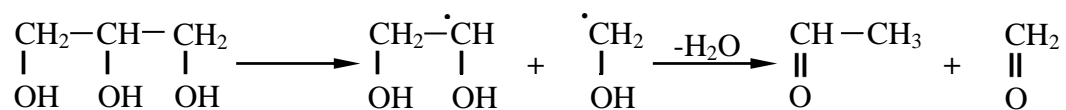


Figure 5.10: Summary of reaction for the thermal decomposition of glycerol

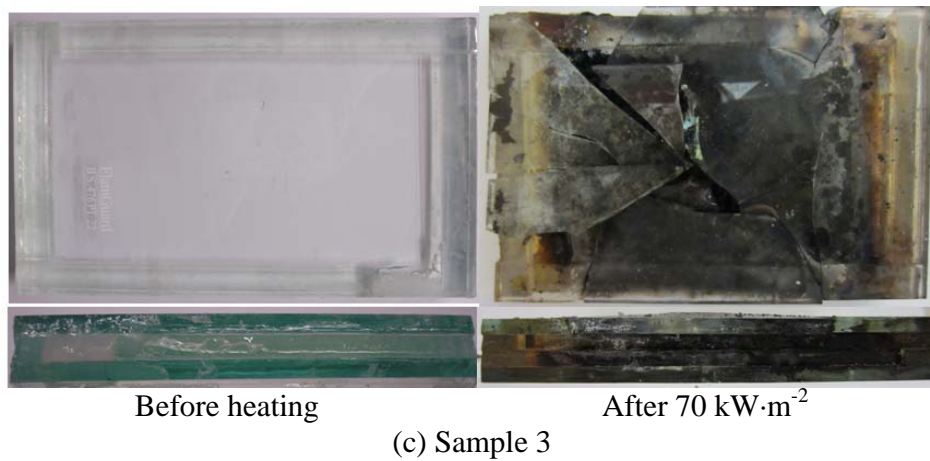
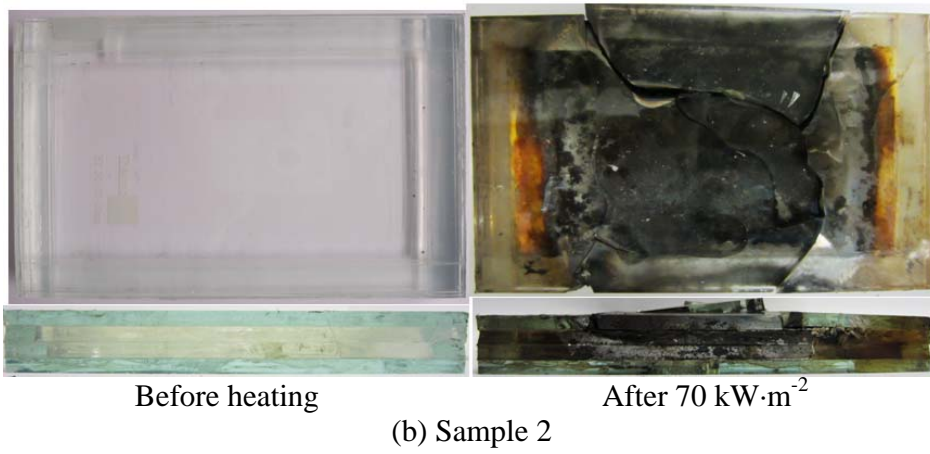
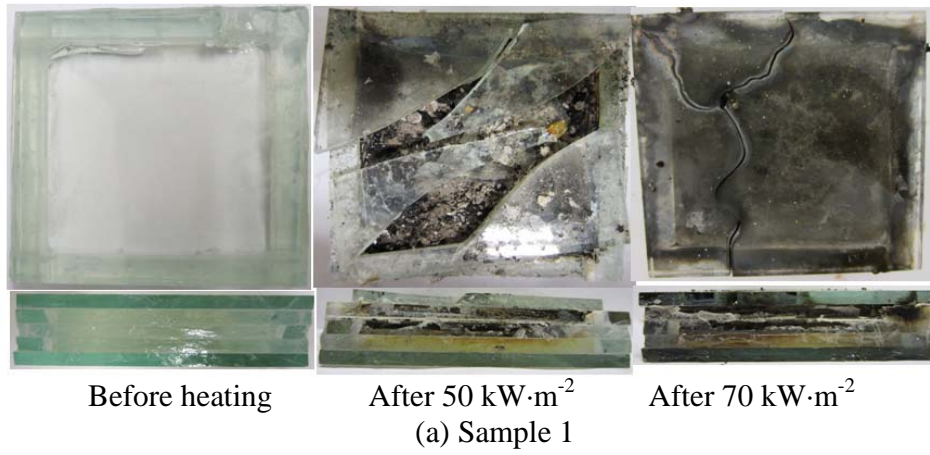
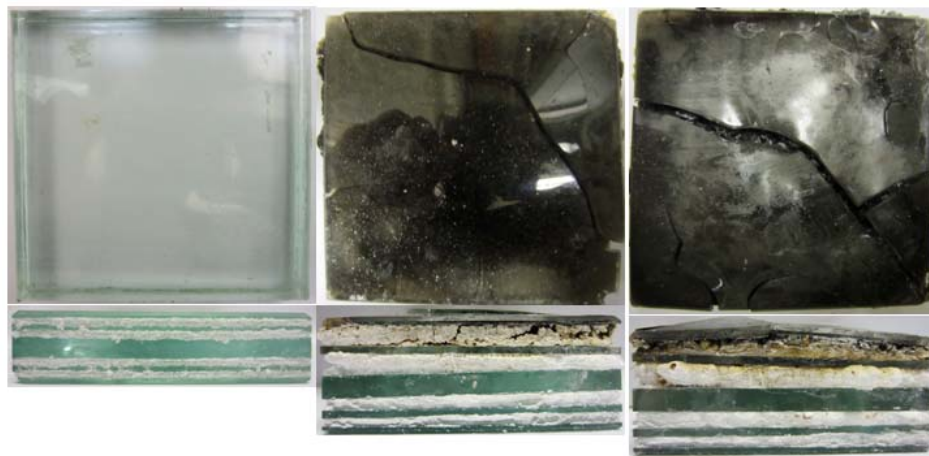


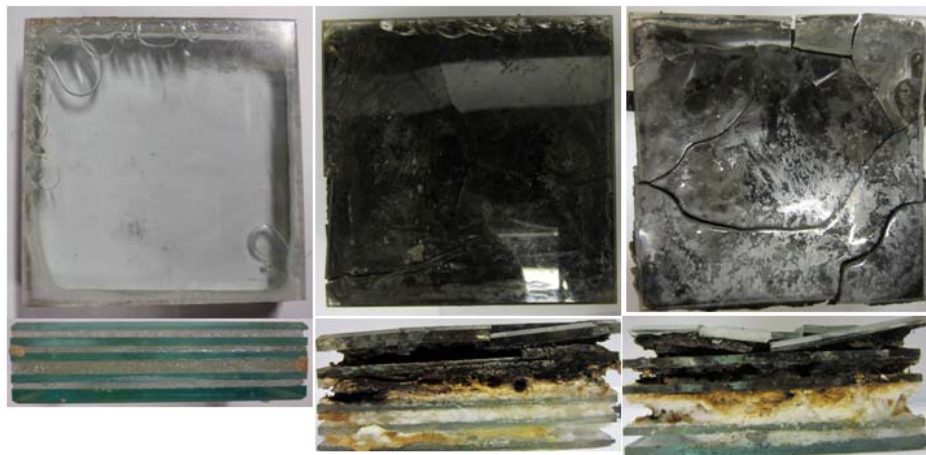
Figure 6.1: Appearance of the tested samples before and after 30 minutes heating in a cone calorimeter



Before heating

After 50 kW·m⁻²
(d) Sample 4

After 70 kW·m⁻²



Before heating

After 50 kW·m⁻²
(e) Sample 5

After 70 kW·m⁻²

Figure 6.1: (Continued) Appearance of the tested samples before and after 30 minutes heating in a cone calorimeter



(a) Sample 5 under $50 \text{ kW}\cdot\text{m}^{-2}$ heat flux



(b) Sample 5 under $70 \text{ kW}\cdot\text{m}^{-2}$ heat flux

Figure 6.2: Cone calorimeter tests

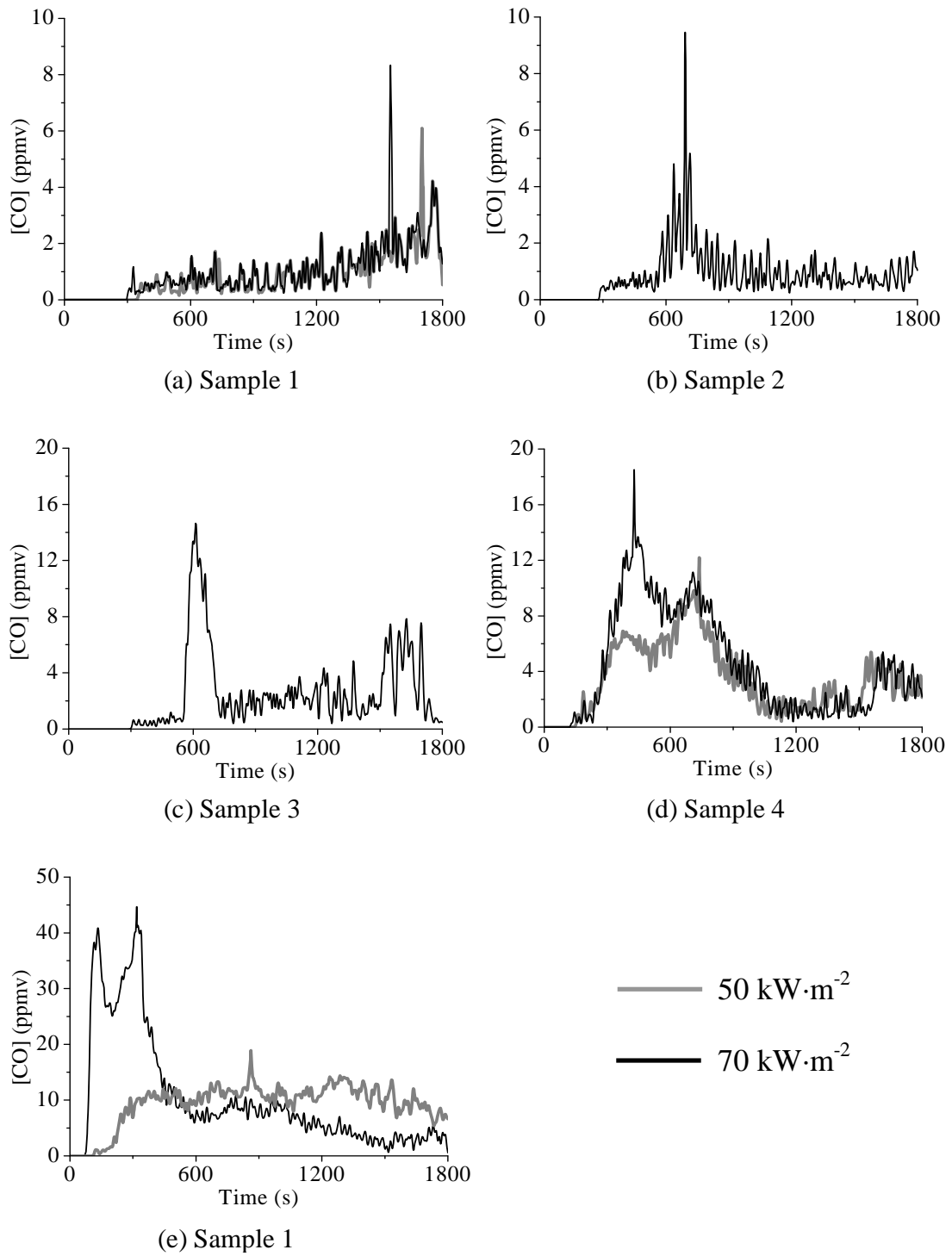
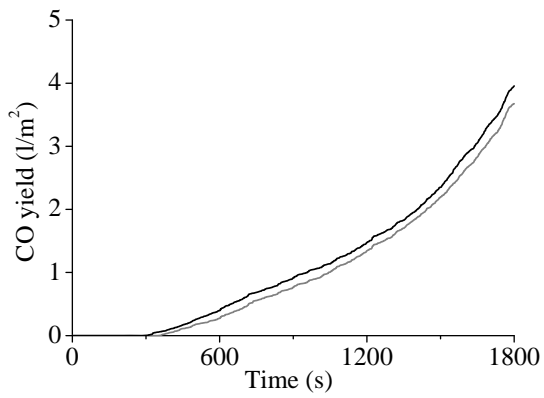
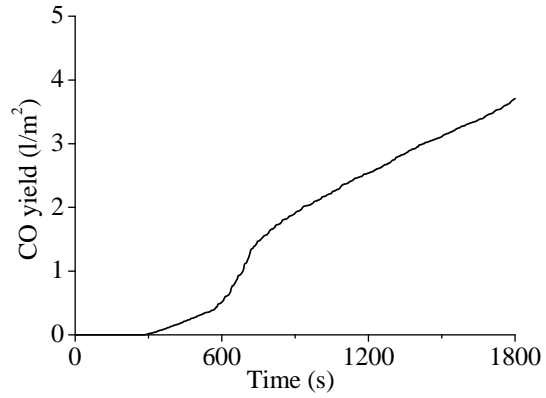


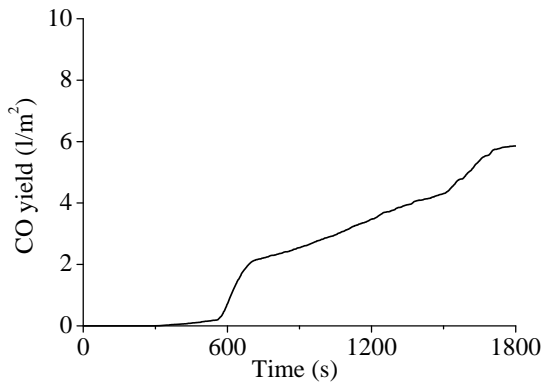
Figure 6.3: Carbon dioxide concentrations recorded



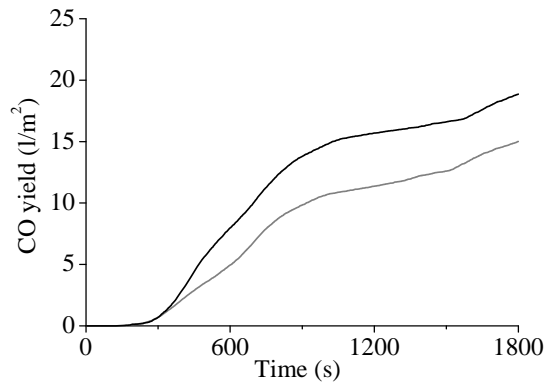
(a) Sample 1



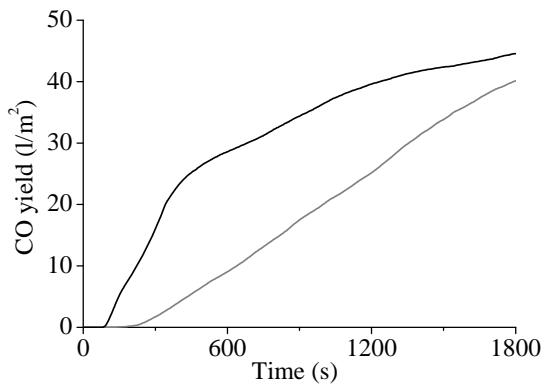
(b) Sample 2



(c) Sample 3



(d) Sample 5



(e) Sample 6

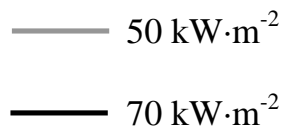


Figure 6.4: Evaluated carbon dioxide yields

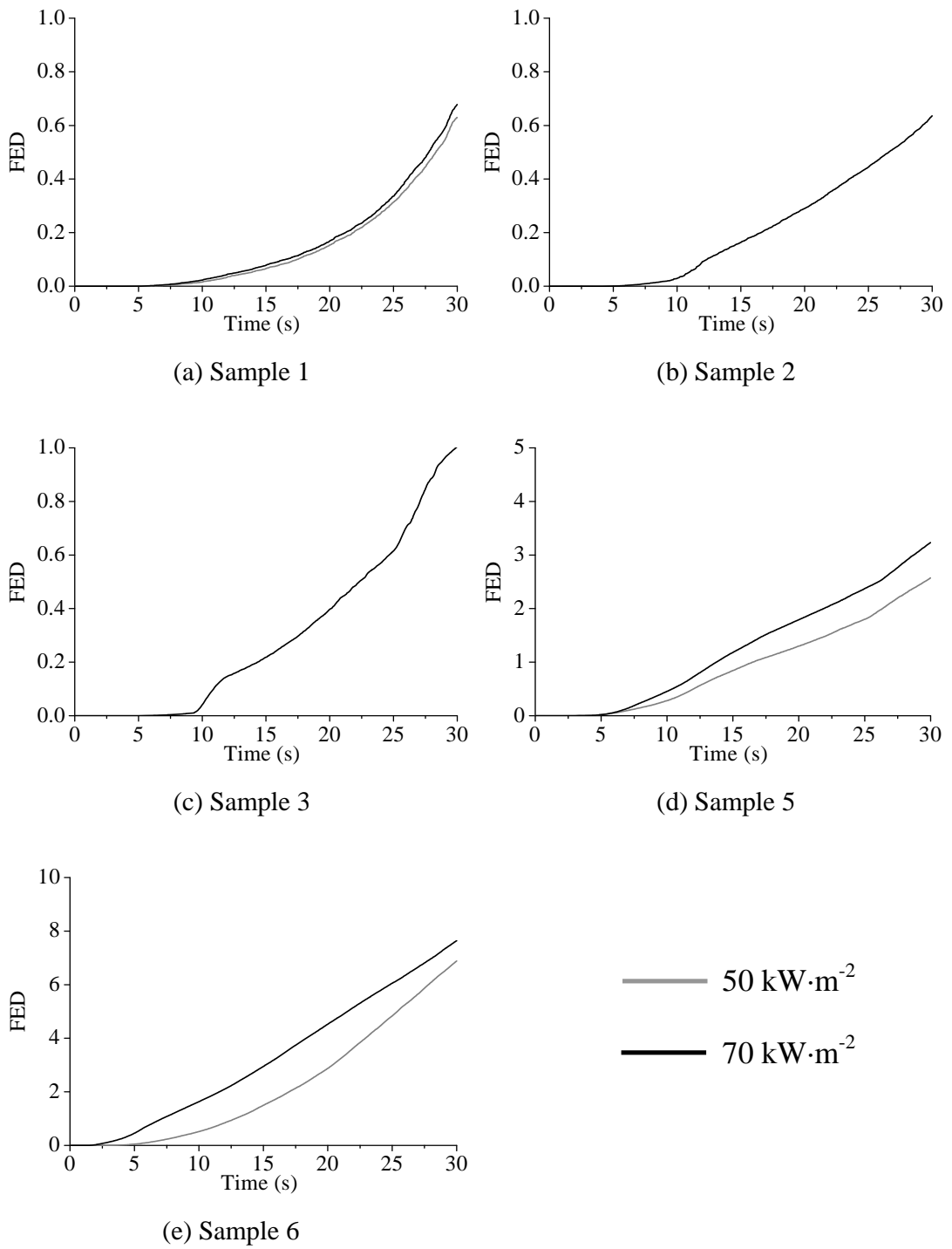


Figure 6.5: Case FED analysis of fire effluents from fire resisting glass panes

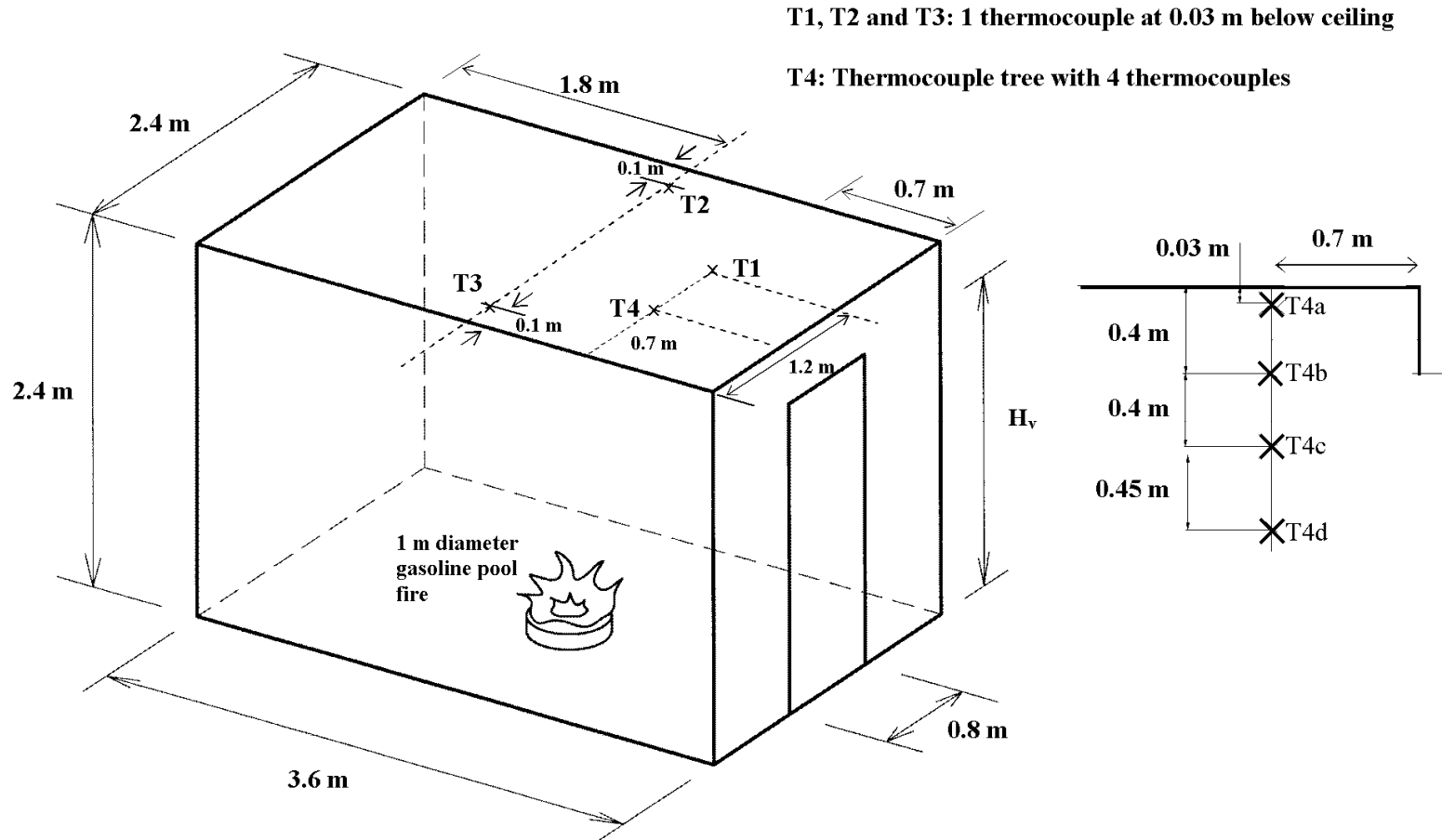


Figure 8.1: The room calorimeter by Chow et al. [2003]

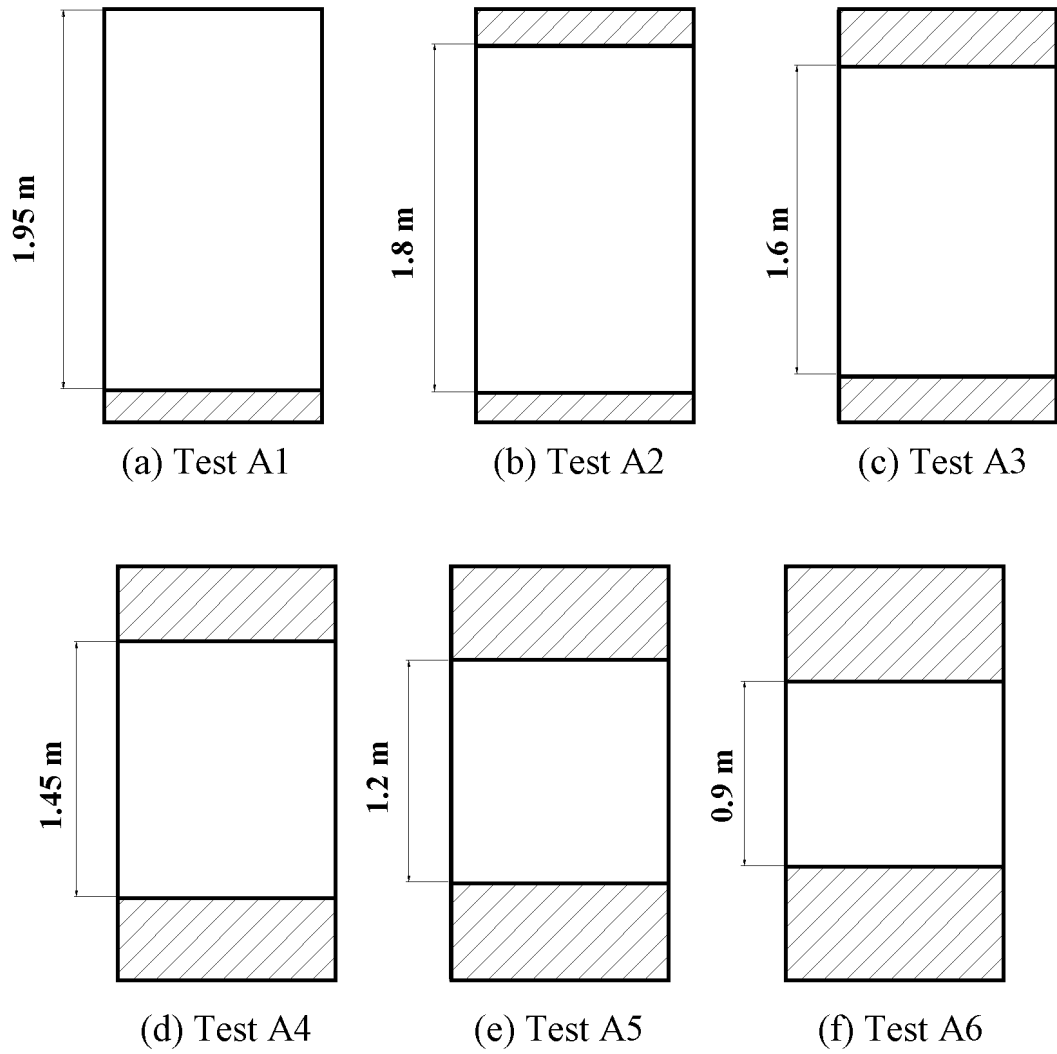


Figure 8.2: Opening arrangement from Chow et al. [2003]

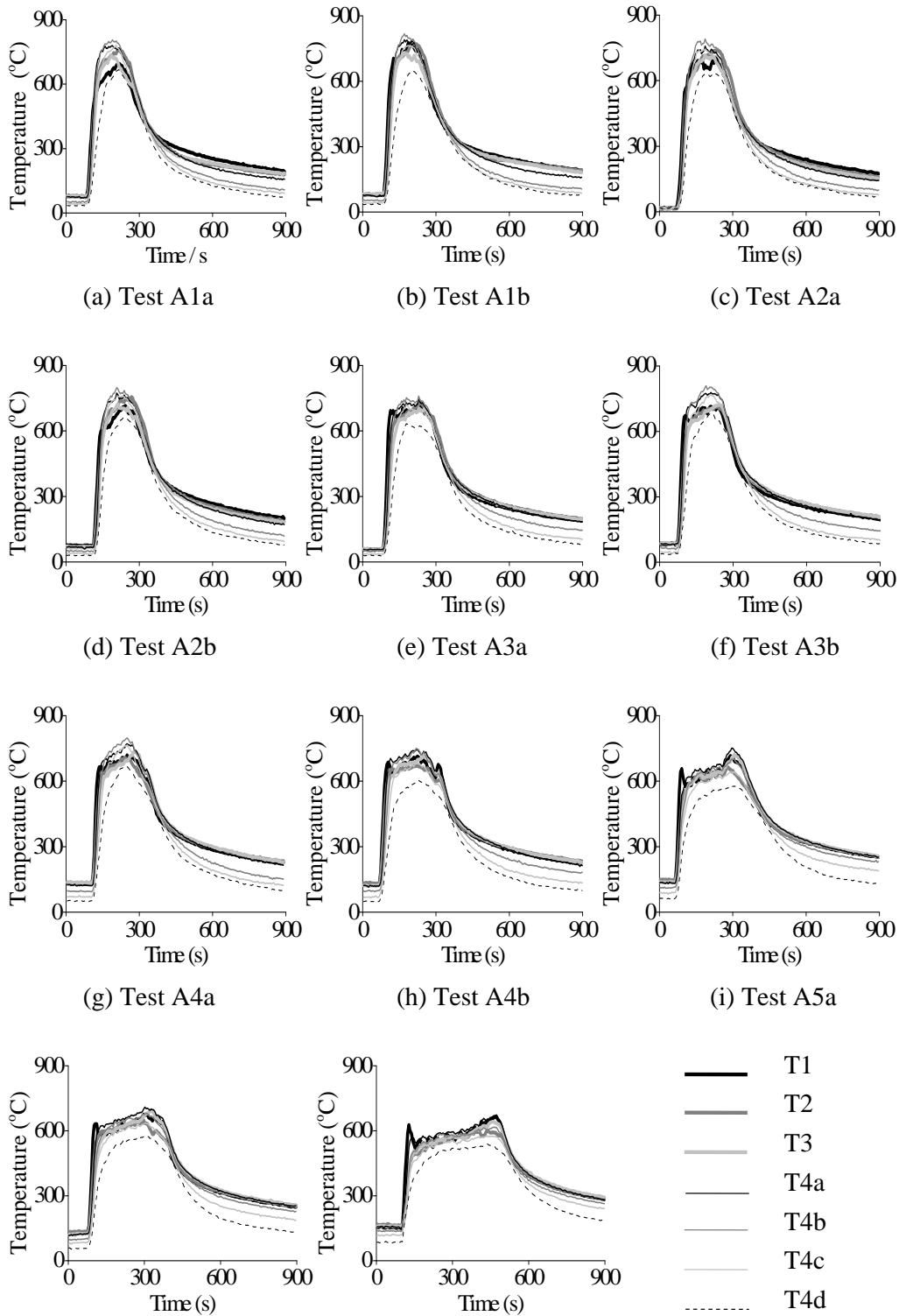


Figure 8.3: Measured gas temperatures reported by Chow et al. [2003]

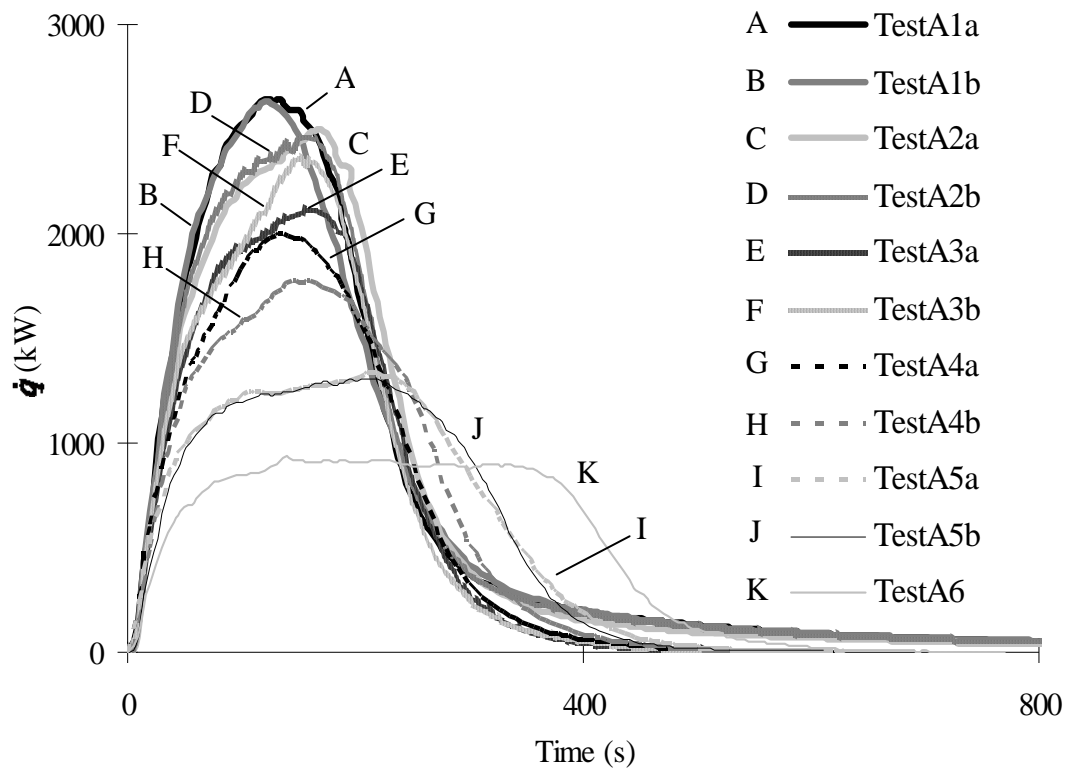


Figure 8.4: Transient heat release rates reported by Chow et al. [2003]

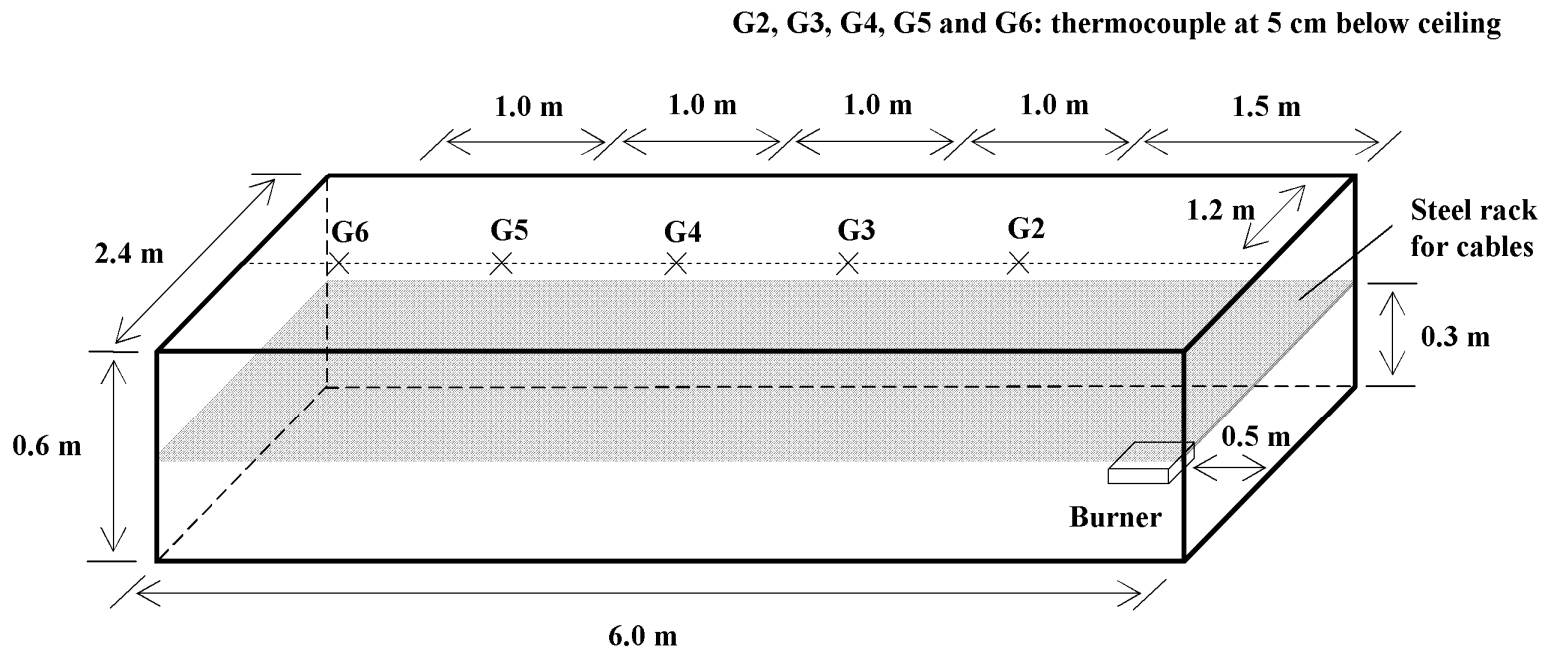


Figure 8.5: The long cavity by Hietaniemi et al. [2004]

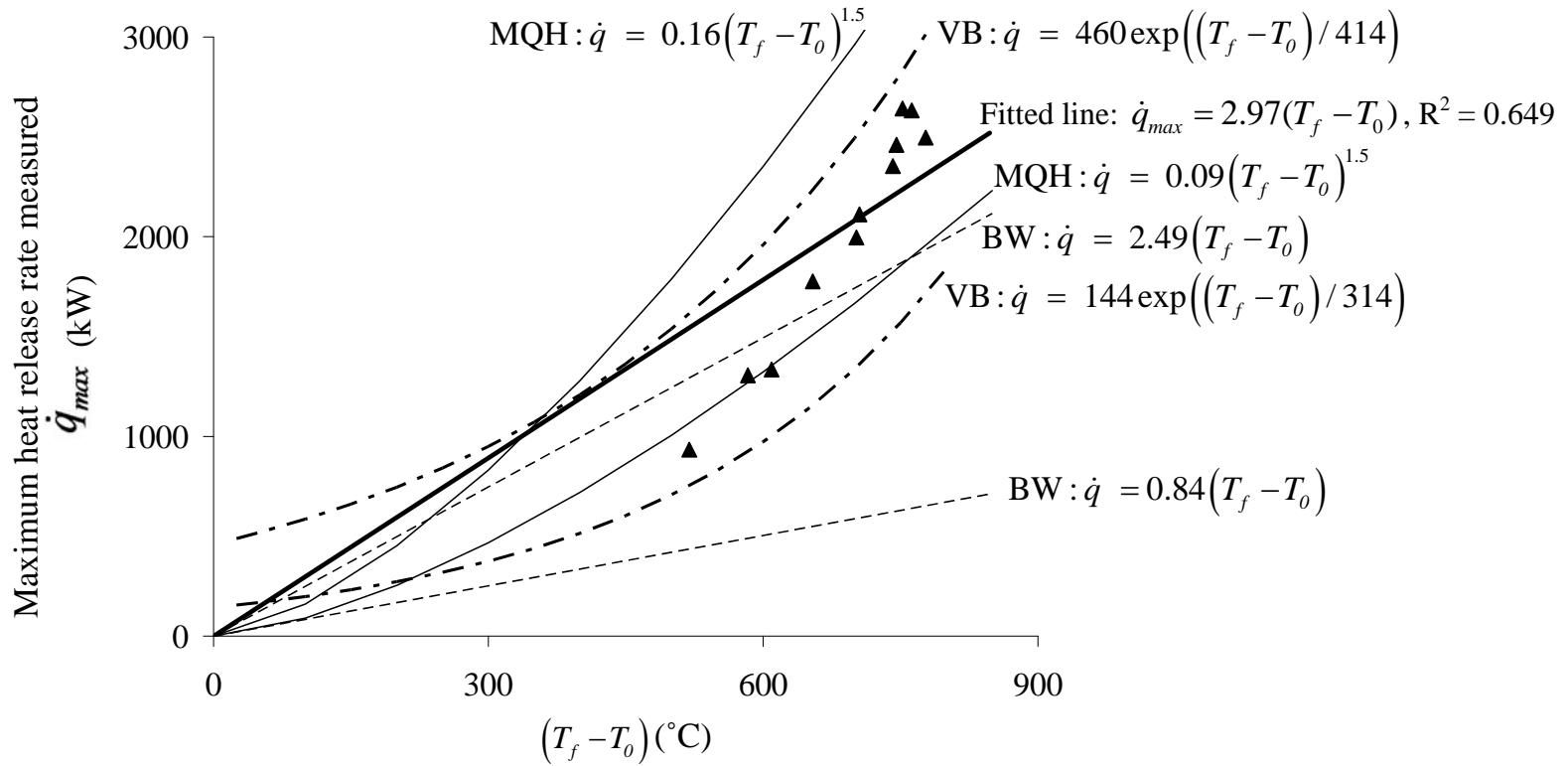


Figure 8.6: Maximum heat release rate against maximum gas temperature reported by Chow et al. [2003]

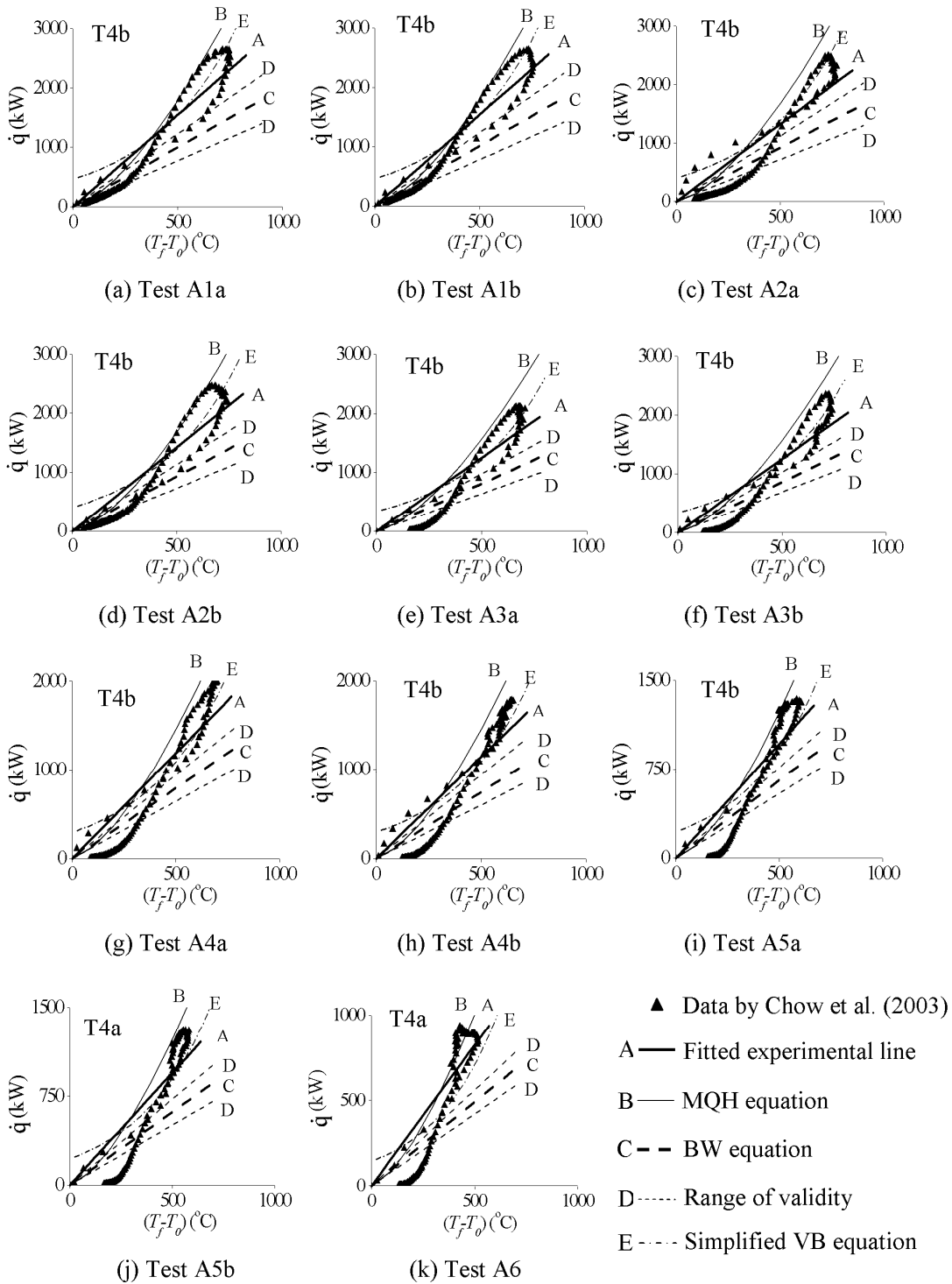


Figure 8.7: Transient results on the set of data with maximum gas temperatures reported by Chow et al. [2003]

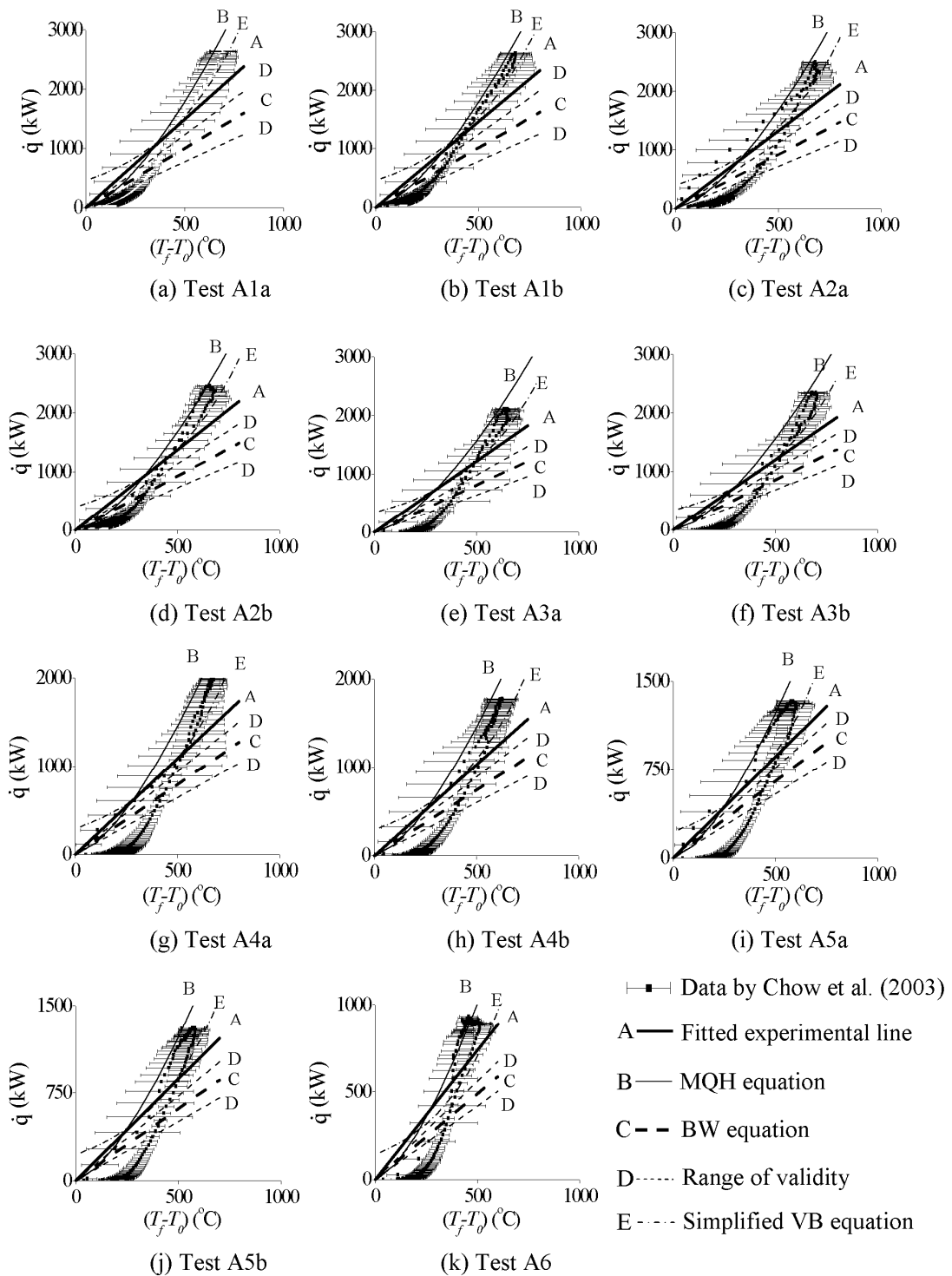


Figure 8.8: Transient heat release rate with all gas temperatures reported by Chow et al. [2003]

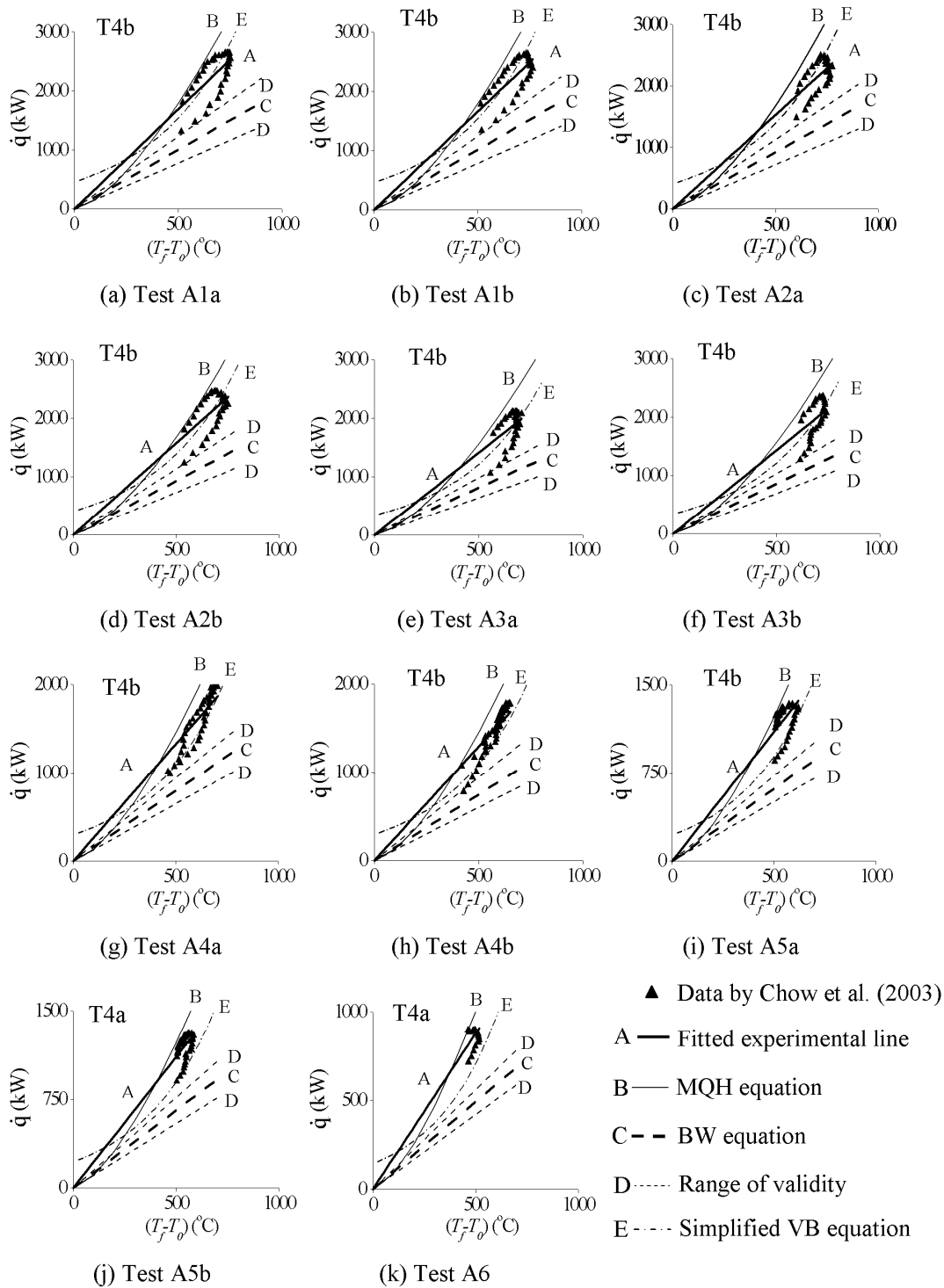


Figure 8.9: Transient results of maximum gas temperatures data set with temperature over 600 °C by Chow et al. [2003]

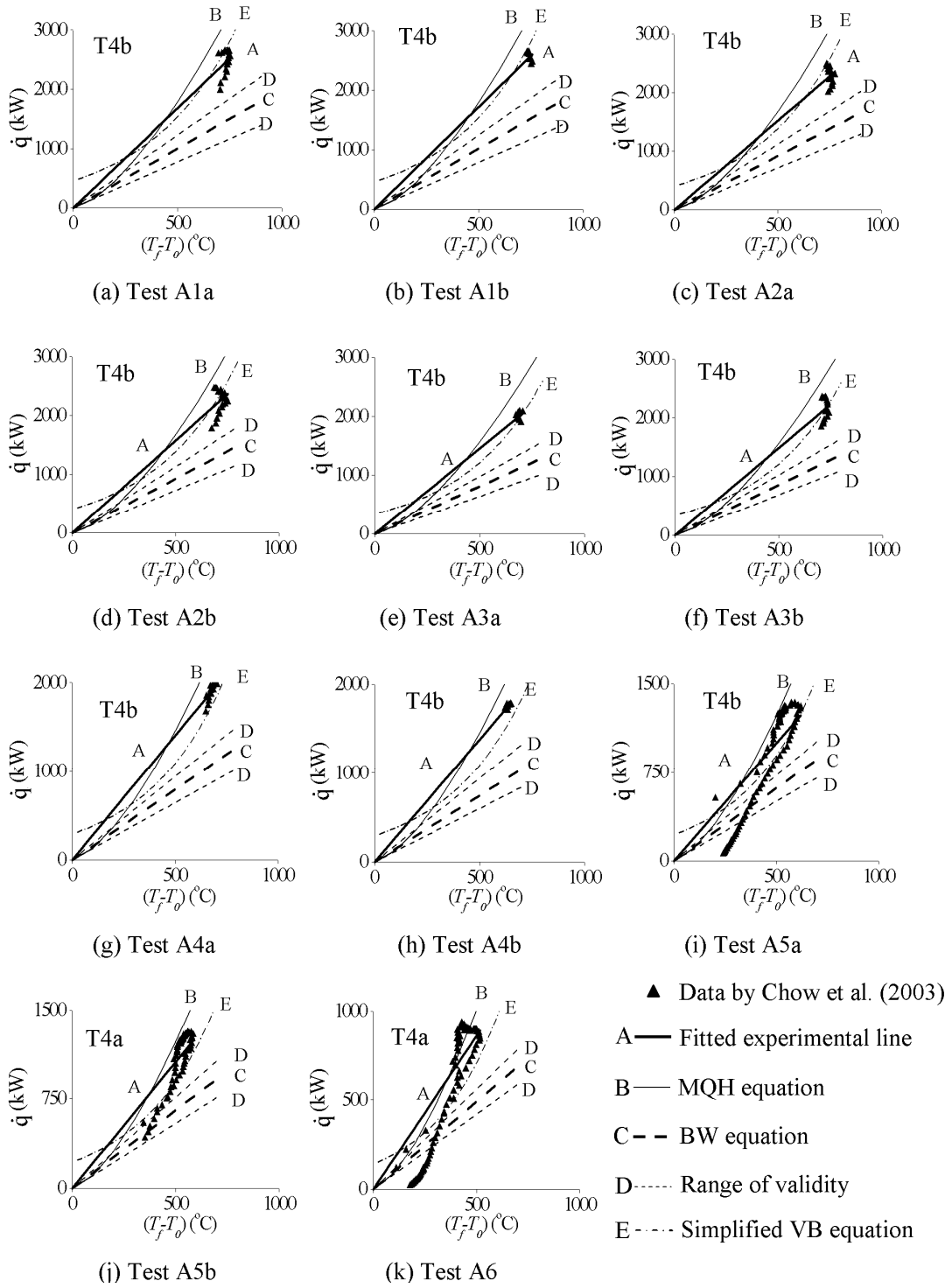


Figure 8.10: Transient results of maximum gas temperatures data set after reaching $20 \text{ kW}\cdot\text{m}^{-2}$ by Chow et al. [2003]

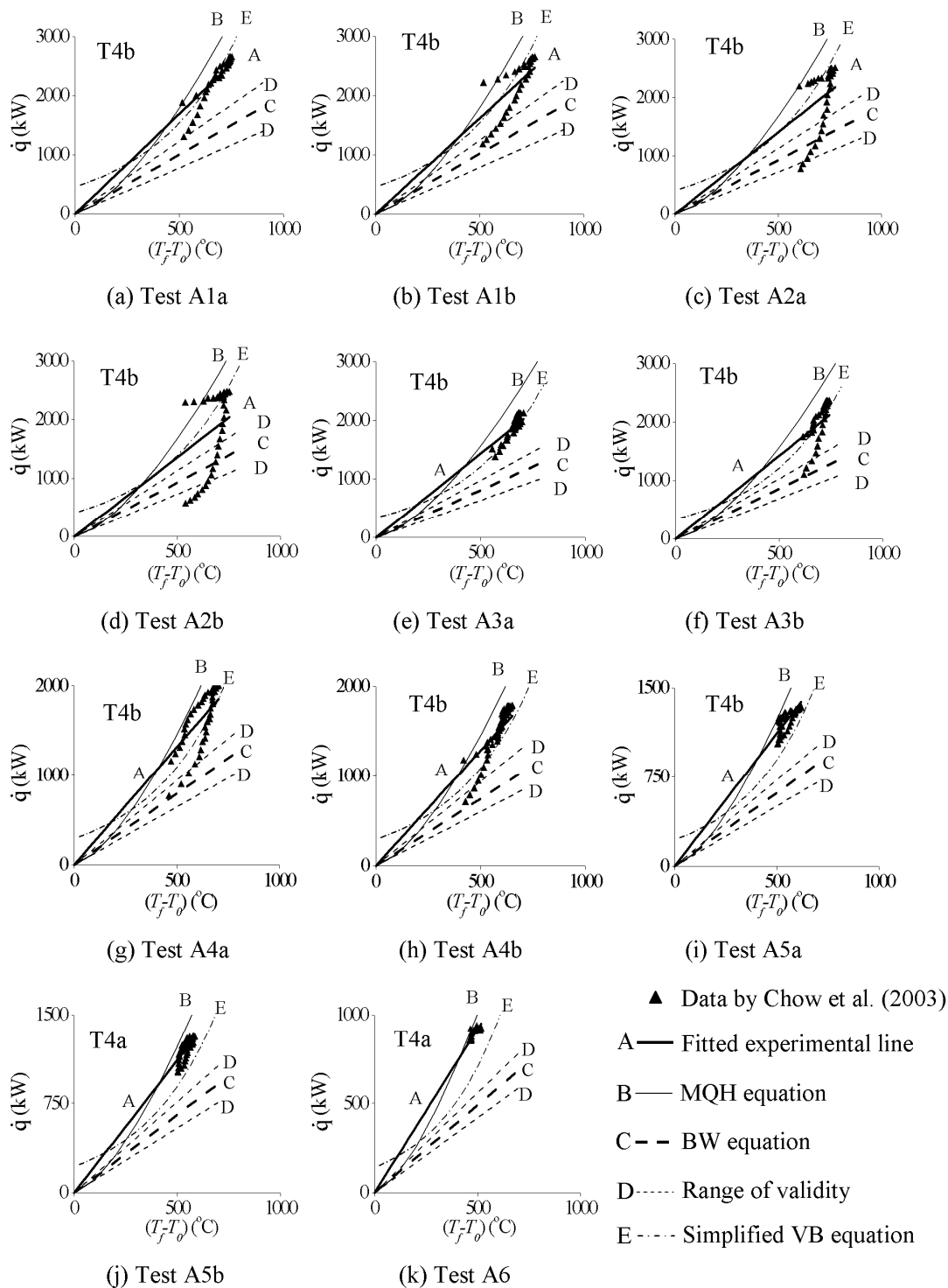
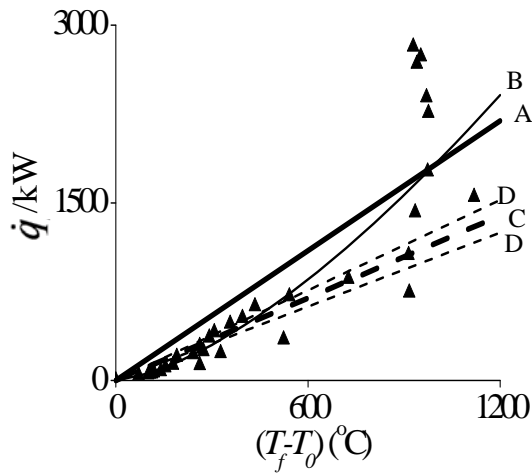
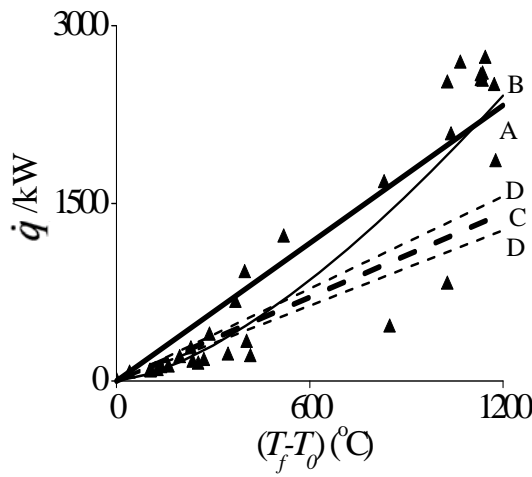


Figure 8.11: Matching maximum heat release rate and temperature above 600 °C on maximum gas temperatures data set by Chow et al. [2003]

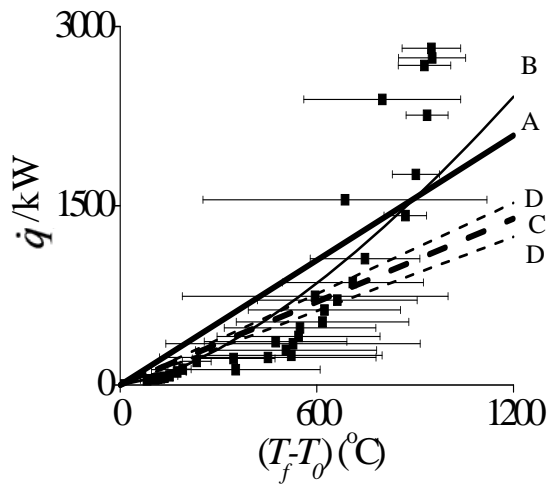


(a) Test V1

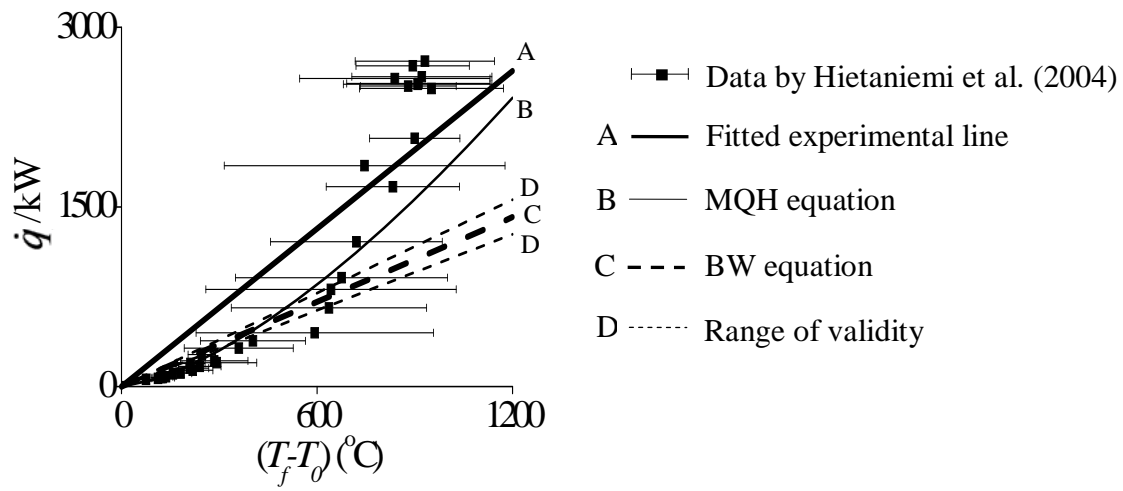


(b) Test V2

Figure 8.12: Transient results on the set of data with maximum gas temperatures reported by Hietaniemi et al. [2004]



(a) Test V1



(b) Test V2

Figure 8.13: Transient heat release rate with all gas temperatures reported by Hietaniemi et al. [2004]

REFERENCES

- Aboulnaga M.M., 2006.
Towards green buildings: Glass as a building element – the use and misuse in the gulf region.
Renewable Energy, 31(5), 631-653.
- ADB, 2006a.
Approved Document B, fire safety, volume 1 – Dwellinghouses.
HMSO, London, UK.
- ADB, 2006b.
Approved Document B, fire safety, volume 2 – buildings other than Dwellinghouses.
HMSO, London, UK.
- Amstock J.S., 1997.
Handbook of glass in construction, p. 101-105.
McGraw-Hill, New York, USA.
- ANSI Z97.1, 2009.
For safety glazing materials used in buildings, safety performance specifications and methods of test.
American National Standards Institute (ANSI), Washington, D.C., USA.
- ASTM E 119, 2011.
Standard test methods for fire tests of building construction and materials.
ASTM International, West Conshohocken, USA.
- ASTM E 1678, 2010.
Standard test method for measuring smoke toxicity for use in fire hazard analysis.
ASTM International, West Conshohocken, USA.
- ASTM E 2226, 2011.
Standard practice for application of hose stream.
ASTM International, West Conshohocken, USA.
- Babrauskas V. and Williamson R.B., 1978.
Post-flashover compartment fires: basis of a theoretical model.
Fire and Materials, 2(1), p. 39-53.

- Babrauskas V., 1980.
Estimating room flashover potential.
Fire Technology, 16(2), p. 94-103.
- Babrauskas V., 1981.
A closed-form approximation for post-flashover compartment fire temperatures.
Fire Safety Journal, 4(1), p. 63-73.
- Babrauskas V., Braun E., Gann R.G., Harris R.H., Levin B.C. and Paabo M., 1991a.
The role of bench-scale test data in assessing real-scale fire toxicity, National Institute of Standards and Technology (NIST) Technical Note 1248.
US Department of Commerce, Washington, D.C., USA.
- Babrauskas V., Levin B.C., Gann R.G., Paabo M. and Harris R.H., 1991b.
Toxic potency measurement for fire hazard analysis, National Institute of Standards and Technology (NIST) Special Publication 827.
US Department of Commerce, Washington, D.C., USA.
- Babrauskas V., 1992a.
Full-scale heat release rate measurements.
Babrauskas V. and Grayson S.J. ed. Heat Release in Fires, cha. 5.
Elsevier Applied Science, London.
- Babrauskas V., 1992b.
The cone calorimeter.
Babrauskas V. and Grayson S.J. ed. Heat Release in Fires, cha. 4.
Elsevier Applied Science, London.
- Babrauskas V., 1997.
Sandwich panel performance in full-scale and bench-scale fire tests.
Fire and Materials, 21(2), p. 53-65.
- Babrauskas V., Gann R.G., Levin B.C., Paabo M., Harris R.H., Peacock R.D. and Yusa S., 1998.
A methodology for obtaining and using toxic potency data for fire hazard analysis.
Fire Safety Journal, 31(4), p. 345-358.
- Babrauskas V., 2000.
Fire safety improvements in the combustion toxicity area: is there a role for LC50 tests.
Fire and Materials, 24(20), p. 113-119.
- Babrauskas V., 2011.
Glass breakage in fires.
[online] Available at: <https://doctorfire.com/GlassBreak.pdf> [Accessed 10 Jan 2013].

Barbooti M.M. and Al-Sammerrai D.A., 1986.
Thermal decomposition of citric acid.
Thermochimica Acta, 98, p. 119-126.

Barrow C.S., Alari Y. and Stock M.F., 1976.
Sensory irritation evoked by the thermal decomposition products of plasticized poly vinyl chloride.
Fire and Materials, 1(4), p. 147-153.

Berhinig R., 2003.
Restructuring confidence in the fire safety of buildings.
Construction Specifier, 55(10), p. 49-51.

Blomqvist P. and Lönnermark A., 2001.
Characterization of the combustion products in large-scale fire tests: comparison of three experimental configurations.
Fire and Materials, 25(2), p. 71–81.

Blomqvist P., Hertzberg T., Dalene M. and Skarping G., 2003.
Isocyanates, aminoisocyanates and amines from fires – a screening of common materials found in buildings.
Fire and Materials, 27(6), p. 275-294.

Blomqvist P. and Simonson-McNamee M., 2010.
Large-scale generation and characterisation of fire effluents.
Stec A.A. and Hull T.R. ed. Fire Toxicity, 1st edition, cha.13.
Woodhead Publishing Ltd, Cambridge, UK.

BS 476-13, 1987.
Fire tests on building materials and structures, part 13 – method of measuring the ignitability of products subjected to thermal irradiance, AMD 5774: January 1988.
British Standards Institution (BSI), London, UK.

BS 476-20, 1987. Fire tests on building materials and construction, part 20 – general requirements.
British Standards Institution (BSI), London, UK.

BS 476-22, 1987.
Fire tests on building materials and constructions, part 22 – methods for the determination of the fire-resistance of non-loadbearing elements of construction.
British Standards Institution (BSI), London, UK.

BS 952-1, 1995.

Glass for glazing, part 1 – classification.

British Standards Institution (BSI), London, UK.

BS EN 1363-2, 1999.

Fire resistance tests, part 2 – alternative and additional procedures.

British Standards Institution (BSI), London, UK.

BS EN 1364-1, 1999.

Fire resistance tests for non-loadbearing elements, part 1 – walls.

British Standards Institution (BSI), London, UK.

BS EN 1365-2, 2000.

Fire Resistance tests for loadbearing elements, part 2 – floors and roofs.

British Standards Institution (BSI), London, UK.

BS EN 12600, 2002.

Glass in building, pendulum test, Impact test method and classification for flat glass,
CORR: April 30, 2010.

British Standards Institution (BSI), London, UK.

BS 7990, 2003.

Tube furnace method for the determination of toxic products yields in for effluents.

British Standards Institution (BSI), London, UK.

BS 6262-4, 2005. Glazing for buildings, part 4 – code of practice for safety related to human impact.

British Standards Institution (BSI), London, UK.

BS EN 13501-2, 2008.

Fire classification of construction products and building elements, part 2 – classification using data from fire resistance tests, excluding ventilation services, AMD: November 30, 2009.

British Standards Institution (BSI), London, UK.

BS EN 1634-1, 2008.

Fire resistance and smoke control tests for door, shutter and openable window assemblies and elements of building hardware, part 1 – fire resistance tests for doors, shutters and openable windows.

British Standards Institution (BSI), London, UK.

BS EN 13823, 2010.

Reaction to fire tests for building products, building products excluding floorings exposed to the thermal attack by a single burning item.

British Standards Institution (BSI), London, UK.

BS EN 60322-3-10, 2010.

Tests on electric and optical fibre cables under fire conditions, part 3-10 – test for vertical flame spread of vertically mounted bunched wires or cables - Apparatus.

British Standards Institution (BSI), London, UK.

BS EN 1363-1, 2012. Fire resistance tests, part 1 – general requirements.

British Standards Institution (BSI), London, UK.

BS EN 1365-1, 2012.

Fire resistance tests for loadbearing elements, part 1 – walls.

British Standards Institution (BSI), London, UK.

Caulfield M.J., Qiao G.G. and Solomon D.H., 2002.

Some aspects of the properties and degradation of polyacrylamides.

Chemical Reviews, 102(9), p. 3067-3084.

Chow C.L., Han S.S. and Chow W.K., 2002.

Smoke toxicity assessment of burning video compact disc boxes by a cone calorimeter.

Journal of Applied Fire Science, 11(4), p. 349-366.

Chow C.L., Chow W.K. and Lu Z.A., 2004.

Assessment of smoke toxicity of building materials.

Proceedings of the 6th Asia-Oceania Symposium on Fire Science & Technology, 17-20 March 2004, Daegu, Korea, p. 132-142.

International Association for Fire Safety Science (IAFSS), London, UK.

Chow C.L., 2009.

Assessment of fire hazard on glass buildings with an emphasis on double-skin façades, PhD Thesis.

Department of Architecture, University of Cambridge, UK.

Chow C.L. and Chow W.K., 2010.

Experimental studies on fire spread over glass façade.

ASME 2010 International Mechanical Engineering Congress & Exposition, IMECE2010, November 12-18, 2010, Vancouver, Canada, Vol.5, p. 415-422.

American Society of Mechanical Engineers (ASME), New York, USA.

Chow C.L. and Chow W.K., 2011.

A point to note in the draft Code of Practice for Fire Safety in Buildings 2011: Smoke toxicity assessment of burning materials.

International Journal on Engineering Performance-Based Fire Codes, 10(40), p. 76-82.

Chow W.K., 1997.

Preliminary studies of a large fire in Hong Kong.

Journal of Applied Fire Science, 6(3), p. 243-268.

Chow W.K., 2002.

Assessment on heat release rate of furniture foam arrangement by a cone calorimeter,

Journal of Fire Science, 20(4), p. 319-328.

Chow W.K., Gao Y., Dong H., Zou G.W., Luo Z. and Meng L., 2003.

Experimental studies on minimum heat release rates for flashover with oxygen consumption calorimetry.

Architectural Science Review, 46(3), p. 291-296.

Chow W.K. and Han S.S., 2004.

Studies on fire behaviour of video compact disc (VCD) materials with a cone calorimeter.

Polymer Testing, 23(6), p. 685-694.

Chow W.K., 2005a.

Building fire safety in the Far East.

Architectural Science Review, 48(4), p. 285-294.

Chow W.K., 2005b.

Evacuation in a supertall residential complex.

Journal of Applied Fire Science, 13(4), p. 291-300.

Chow W.K. and Han S.S., 2006.

Report on a recent fire in a new curtain-walled building in downtown Dalian.

Journal on Engineering Performance-Based Fire, 8(3), p. 84-87.

Chow W.K., Gao Y. and Chow C.L., 2006.

A review on fire safety in buildings with glass facade.

Journal of Applied Fire Science, 16(3), p. 201-223.

Chow W.K. and Gao Y., 2008.

Thermal stresses on window glasses upon heating.

Construction and Building Materials, 22(11), p. 2157-2164.

Chow W.K., 2010.
Several points to note in performance-based design for fire safety provisions in Hong Kong.
Presented at The National Symposium on Fire Safety Science and Engineering, 14-16 October 2010, Beijing, China.

Chow W.K., Chow C.L. and Gao, Y., 2010.
Thermal stresses over glass panel under fire.
Trends in Heat and Mass Transfer, 12, p. 39-48.

Chow W.K. and Chow C.L., 2012.
Possible air pumping action in a room fire.
The International Journal of Ventilation, 11(1), p. 79-89.

Collins B.J., Hinett G.B., Hayden M.W. and Clarges M.E., 1997.
Fire resistant glass.
US patent 5624760.

CPSC 16 CFR 1201, 2008.
Consumer Product Safety Commission, part 1201 – safety standard for architectural glazing materials.
Consumer Product Safety Commission (CPSC), Washington, D.C., USA.

Curkeet R., 2003.
User's guide to fire-rated glazing.
Construction Specifier, 56(1), p. 50-56.

Cuzzillo B.R. and Pagni P.J., 1998.
Thermal breakage of double-pane glazing by fire.
Journal of Fire Protection Engineering, 9(1), p. 1-11.

Davis R.J., 2003.
Building Construction.
Cote, A.E. ed. NFPA Fire Protection Handbook, 19th edition, Sec.12, Cha.2.
National Fire Protection Association (NFPA), Quincy, USA.

De Boel M. and Baudin P., 1980.
Light-transmitting fire screening panel.
US patent 4190698.

De Boel M., 1981.
Fire-screening glazing panels and method of manufacturing same.
US patent 4268581.

De Boel M., 1984.
Fire screening glazing panels.
US patent 4485601.

DEF STAN 02-713, 2012.
Determination of the toxicity index of the products of combustion from small specimens
of materials.
The Ministry of Defense UK (MOD UK), Glasgow, UK.

DIN 53436, 1981-2003.
Producing thermal decomposition products from materials in an air stream and their
toxicological testing, part 1 to 5.
Deutsches Institut Fur Normung E.V. (DIN), Berlin, Germany.

Fawcett M., 1996.
Metallic coating for fire resistant glass.
Glass Technology, 37(3), p. 80.

Emmons H.W., 1986.
The Needed Fire Science.
Fire Safety Science 1, p. 33-53.

FRC Code, 1996.
Code of Practice for Fire Resisting Construction.
Buildings Department, Hong Kong.

Friedman M., Laucirica L. and Visscher G. T., 1999.
Fire-protection and safety composite glass panel.
US patent 5908704.

Frommelt S., Gelderie U. and Plum G., 2002.
Fire-resistant glazing assembly.
US patent 6340508.

FS Code, 2011.
Code of Practice for Fire Safety in Buildings.
Buildings Department, The Hong Kong Special Administrative Region.

Gann R.G., Babrauskas V., Peacock R.D. & Hall J.R., 1994.
Fire conditions for smoke toxicity measurement.
Fire and Materials, 18(3), p. 193-199.

Gann R.G., 2001.
Toxic hazard of building products and furnishings.
Proceedings of International Fire Safety Conference, 11-14 March 2001, San Francisco, USA, p.85-91.
Fire Retardant Chemicals Association (FRCA), Lancaster, USA.

Gann R.G., Averill J.D., Nyden M.R., Johnsson E.L., and Peacock R.D., 2003.
Smoke component yields from room-scale fire tests, National Institute of Standards and Technology (NIST) Technical Note 1453.
US Department of Commerce, Washington, D.C., USA.

Gann R.G., 2004.
On the use of bench-scale smoke toxicity data in fire hazard and risk assessment.
Proceedings of the 10th International Conference on Fire Science and Engineering (INTERFLAM), 5-7 July 2004, Edinburgh, Scotland, p. 1421-1429.
Interscience Communications, London, UK.

Gann R.G., Averill J.D., Marsh N.D. and Nyden M.R., 2007.
Assessing the accuracy of a physical fire model for obtaining smoke toxic potency data.
Proceedings of the 11th International Conference on Fire Science and Engineering (INTERFLAM), 3-5 September 2007, London, England, p. 1021-1032.
Interscience Communications, London, UK.

Gann R.G. and Bryner N.P., 2008.
Combustion products and their effects on life safety.
Cote A.E. ed. NFPA Fire Protection Handbook, 20th edition, Sec. 6, Cha.2.
National Fire Protection Association (NFPA), Quincy, USA.

Gann R.G., Averill J.D., Johnsson E.L., Nyden M.R. and Peacock R.D., 2010.
Fire effluent component yields from room-scale fire tests.
Fire and Materials, 34(6), p. 285-314.

GB 15763.1, 2009.
Safety glazing materials in building, fire-resistant glass.
Standardization Administration of China, Beijing, China.

GB/T 12513, 2006.
Fire resistance tests, elements of building construction – glazed elements.
Standardization Administration of China, Beijing, China.

Gelderie U., Frommelt S, Groteklaes-broring M. and Michels D., 2000.
Fire-resistant glazing panel.
US Patent 6159606.

GGF, 2011.

A guide to best practice in the specification and use of fire-resistant glazed systems.
Glass and Glazing Federation (GGF), London, UK

Goelff P., 2009.

Fire-resistant glazing.
US patent 8057905 B2.

Gomez, L.I., 1987.

Fire-resistant interlayer.
US patent 4681810.

Griffiths J., 2008.

Hose stream or smoke screen.
Doors and Hardware, Feb, p. 32-36.

Haber F, 1924.

Zur geschichte des gaskrieges (On the history of gas warfare).
Fünf Vorträge aus den Jahren 1920–1923 (Five Lectures from the Years 1920–1923), p.
76–92.
Springer, Berlin, Germany.

Hadjisophocleous G.V. and Benichou N., 1999.

Performance criteria used in fire safety design.
Automation in Construction, 8(4), p. 489-501.

Hall, J.R., 2002.

Burns Toxic Gases and Other Hazards Associated with Fires: Deaths and Injuries in Fire
and Non-fire Situations.
National Fire Protection Association (NFPA). Quincy, USA.

Hall J.R. and Twomey E.R., 2008.

Challenges to safety in the built environment.
Cote A.E. ed. NFPA Fire Protection Handbook, 20th edition, Sec.1, Cha.1.
National Fire Protection Association (NFPA), Quincy, USA.

Han S.S. and Chow W.K., 2004.

Cone calorimeter studies on fire behavior of polycarbonate glazing sheets.
Journal of Applied Fire Science, 12(3), p. 245-261.

Han S.S. and Chow W.K., 2005.

Calculating FED and LC50 for testing toxicity of materials in bench-scale tests with a
cone calorimeter.
Polymer Testing, 24(7), p. 920-924.

- Harmathy T.Z., 1993.
Fire safety design and concrete.
Longman Scientific & Technical, Essex, England.
- Hartzell G.E. and Emmons H.W., 1988.
The fractional effective dose model for assessment of toxic hazards in fires.
Journal of Fire Sciences, 6(5), p. 356-362.
- Hartzell G.E., 2001.
Engineering analysis of hazards to life safety in fires: the fire effluent toxicity component.
Safety Science, 38(2), p. 147-155.
- Hartzell G.E., 2003.
Combustion products and their effects on life safety.
Cote A.E. ed. NFPA Fire Protection Handbook, 19th edition, Sec. 8, Cha.2.
National Fire Protection Association (NFPA), Quincy, USA.
- Hemingway A, 2009.
Glass bodyguard for sparky's heroes.
Schott Solutions, 2, p. 36-39.
- Hertzberg T., Blomqvist P., Dalene M. and Skarping G., 2003.
Particles and isocyanates from fires, SP Report 2003:05.
SP Swedish National Testing and Research Institute, Bora, Sweden.
- Hietaniemi J., Hostikka S. and Vaari J., 2004.
FDS simulation of fire spread – comparison of model results with experimental data,
VTT Working Paper 4.
VTT Technical Research Centre of Finland, Finland.
- Holland J.R., Varma K.S. and Holden D.W., 2005.
Fire resistant glazings.
US patent 6929691 B1.
- Holzer G. and Gelderie U., 1991.
Anti-fire glazing.
US patent 4983464.
- Holzer G. and Gelderie U., 1993.
Fire-resistant glazing and method of making same.
US patent 5223313.

Hull T.R., Quinn R.E., Areri I.G. and Purser D.A., 2002.
Combustion toxicity of fire retarded EVA.
Polymer Degradation and Stability, 77(2), p. 235-242.

Hull T.R., Wills C.L., Artingstall T., Price D. and Milnes G.J., 2005.
Mechanisms of smoke and CO suppression from EVA composites.
Le Bras M., Wilkie C.A. and Bourbigot S. ed. Fire Retardancy of Polymers, Cha.28.
Royal Society of Chemistry, London, UK.

Hull T.R. and Paul K.T., 2007.
Bench-scale assessment of combustion toxicity – a critical analysis of current protocols.
Fire Safety Journal, 42(5), p. 340-365.

Hull T.R., Stec A.A., Lebek K. and Price D., 2007.
Factors affecting the combustion toxicity of polymeric materials.
Polymer Degradation and Stability, 92(12), p. 2239-2246.

Hull T.R., Lebek K., Pezzani M. and Messa S., 2008.
Comparison of toxic product yields of burning cables in bench and large-scale experiments.
Fire Safety Journal, 43(2), p. 140-150.

Hull T.R., Stec A.A. and Nazare S., 2009.
Fire retardant effects of polymer nanocomposites.
Journal of Nanoscience and Nanotechnology, 9(7), p. 4478-4486.

Hull T.R., 2010.
Bench-scale generation of fire effluents.
Stec A.A. and Hull T.R. ed. Fire toxicity, 1st edition, cha.12.
Woodhead Publishing Ltd, Cambridge, UK.

Hull T.R. and Stec A.A., 2010.
Introduction to fire toxicity.
Stec A.A. and Hull T.R. ed. Fire toxicity, 1st edition, cha.1.
Woodhead Publishing Ltd, Cambridge, UK.

Hung W.Y. and Chow W.K., 2002.
Review on the Requirements on Fire Resisting Construction.
International Journal on Engineering Performance-Based Fire Codes, 4(3), p. 68-83.

IEC TS 60695-7-50, 2002.
Fire hazard testing, part 7-50 – toxicity of fire effluent – estimation of toxic potency – apparatus and test method.
International Electrotechnical Commission (IEC), Geneva, Switzerland.

Ihm P., Nemri A. and Krarti M., 2009.
Estimation of lighting energy savings from daylighting.
Building and Environment, 44(3), p. 509-514.

ISO 9705, 1993.
Fire tests, full-scale room test for surface products.
International Organization for Standardization (ISO), Geneva, Switzerland.

ISO TR 9122-4, 1993.
Toxicity testing of fire effluents, part 4 – the fire model (furnaces and combustion apparatus used in small-scale testing).
International Organization for Standardization (ISO), Geneva, Switzerland.

ISO 5657, 1997.
Reaction to fire tests - Ignitability of building products using a radiant heat source - Second Edition.
International Organization for Standardization (ISO), Geneva, Switzerland.

ISO 5660-1, 2002.
Reaction-to-fire tests, heat release, smoke production and mass loss rate, part 1 – heat release rate (cone calorimeter method).
International Organization for Standardization (ISO), Geneva, Switzerland.

ISO 5660-2, 2002.
Reaction-to-fire tests, heat release, smoke production and mass loss rate, part 2 – Smoke production rate (dynamic measurement).
International Organization for Standardization (ISO), Geneva, Switzerland.

ISO 13344, 2004.
Estimation of the lethal toxic potency of fire effluents.
International Organization for Standardization (ISO), Geneva, Switzerland.

ISO TR 16312-2 , 2007.
Guidance for assessing the validity of physical fire models for obtaining fire effluent toxicity data for fire hazard and risk assessment, part 2 – evaluation of individual physical fire models.
International Organization for Standardization (ISO), Geneva, Switzerland.

ISO TS 19700, 2007.
Controlled equivalence ratio method for the determination of hazardous components of fire effluents.
International Organization for Standardization (ISO), Geneva, Switzerland.

ISO 24473, 2008.

Fire tests, open calorimetry, measurement of the rate of production of heat and combustion products for fires of up to 40 MW.

International Organization for Standardization (ISO), Geneva, Switzerland.

ISO 16312-1, 2010.

Guidance for assessing the validity of physical fire models for obtaining fire effluent toxicity data for fire hazard and risk assessment, part 1 – criteria.

International Organization for Standardization (ISO), Geneva, Switzerland.

ISO 19706, 2011.

Guidelines for assessing the fire threat to people.

International Organization for Standardization (ISO), Geneva, Switzerland.

ISO 13571, 2012.

Life-threatening components of fire, guidelines for the estimation of time to compromised tenability in fires.

International Organization for Standardization (ISO), Geneva, Switzerland.

ISO 5659-2, 2012.

Plastics, smoke generation, part 2 – determination of optical density by a single-chamber test.

International Organization for Standardization (ISO), Geneva, Switzerland.

Kawagoe K., 1958.

Fire behaviour in rooms, Report No. 27.

Building Research Institute, Tokyo, Japan.

Klassen M.S., Sutula J.A., Holton M.M., Roby R.J. and Izbicki T., 2006.

Transmission through and breakage of multi-pane glazing due to radiant exposure.

Fire technology, 42(2), p. 79-107.

Klein W., 1993.

Glazing against fire.

Glass Science and Technology, 66(6-7), p. 185-190.

Knegt A. M., 2008.

At the sharp end of fire resistant glazing.

Industrial Fire Journal, 2008 Apr.

Krarti M., Erickson P.M. and Hillman T.C., 2005.

A simplified method to estimate energy savings of artificial lighting use from daylighting.

Building and Environment, 40(6), p. 747-754.

- Lawson, J.R., 2009.
A history of fire testing: past, present, and future.
ASTM International, 6(4), p. 1-39.
- Leung W.M., Axelson D.E. and Van Dyke J.D., 1987.
Thermal degradation of polyacrylamide and poly (acrylamide-co-acrylate).
Journal of Polymer Science Part A: Polymer Chemistry, 25(7), p. 1825-1846.
- Levin B.C, Paabo M., Gurman J.L., Clark H.M. and Yoklavich M.F., 1988.
Further studies of the toxicological effects of different time exposures to the individual and combined fire gases: carbon monoxide, hydrogen cyanide, carbon dioxide, and reduced oxygen.
Polyurethane'88, Proceedings of the 315th Society of Plastics Meeting, p. 249-252.
Technomic Publishing, Lancaster, USA.
- Levin B.C., Braun E., Navarro M. and Paabo, M.,1995.
Further development of the N-gas mathematical model: an approach for predicting the toxic potency of complex combustion mixtures.
ACS Symposium Series No. 599, p. 293-311.
American Chemical Society, Washington D.C., USA.
- Levin B.C., Fowell A.J., Birby M.M., Paabo M., Stolte A. and Malek D., 1982.
Further development of a test method for the assessment of the acute inhalation toxicity of combustion products, NBSIR 82-2532.
US Department of Commerce, Washington, D.C., USA.
- Levin B.C., Paabo M., Bailey C., Harris S.E., Gurman J.L.,1985.
Toxicological effects of the interactions of fire gases and their use in a toxic hazard assessment computer model.
The Toxicologist, 5(1), p. 127.
- Li D.H. and Tsang E.K., 2008.
An analysis of daylighting performance for office buildings in Hong Kong.
Building and Environment, 43(9), p. 1446-1458.
- Lyons A., 2007.
Materials for Architects and Builders, 3rd edition, p. 221-222.
Butterworth-Heinemann, Oxford, UK.
- Manzello S.L., Gann R.G., Kukuck S.R., Prasad K.R. and Jones W.W., 2007.
An experimental determination of a real fire performance of a non-load bearing glass wall assembly.
Fire Technology, 43(1), p. 77-89.
- McCaffrey B.J., Quintiere J.G. and Harkleroad M.F., 1981.

Estimating room temperatures and the likelihood of flashover using fire data correlations.
Fire Technology, 17(2), p. 98-119.

Morgan H.P., 1989.

The influence of window flows in the onset of flashover.

SFSE/FRS Symposium on Flow Through Openings, 13 June 1989, Borehamwood, UK,
p. 1-21.

Building Research Establishment (BRE), Watford, UK.

National Institute for Occupational Safety and Health (NIOSH), 1994.

Documentation for Immediately Dangerous to Life or Health Concentrations (IDLHs),
NTIS Publication No, PB-94-195047.

National Technical Information Service (NTIS), Springfield, USA.

NFPA 251, 2006.

Standard methods of tests of fire resistance of building construction and materials.

National Fire Protection Association (NFPA), Quincy, USA.

NFPA 252, 2012.

Standard methods of fire tests of door assemblies.

National Fire Protection Association (NFPA), Quincy, USA.

NFPA 257, 2012.

Standard on fire test for window and glass block assemblies.

National Fire Protection Association (NFPA), Quincy, USA.

NFPA 269, 2012.

Standard test method for developing toxic potency data for use in fire hazard modeling.

National Fire Protection Association (NFPA), Quincy, USA.

NFPA 270, 2013.

Standard test method for measurement of smoke obscuration using a conical radiant
source in a single closed chamber.

National Fire Protection Association (NFPA), Quincy, USA.

NFX 70-100, 2006.

Fire tests, analysis of gaseous effluents, part 1 – methods for analyzing gases stemming
from thermal degradation; part 2 tubular furnace thermal degradation method.

Association Française de Normalisation (AFNOR), Paris, France.

Nolte H., 1984.

Method of forming a laminated fire screening panel.

US patent 4451312.

Nolte H., Grunzel H. and Harbecke B., 1998.

Fire resistant glass structure.
US patent 5766770.

Ortmans G. and Hassiepen, M., 1989.
Fire-resistant glazing and method of making same.
US patent 4830913.

Petrella R.V., 1994.
The assessment of full-scale fire hazards from cone calorimeter data.
Journal of Fire Sciences, 12(1), p. 14-43.

Purser D.A., 2000a.
Interactions among carbon monoxide, hydrogen cyanide, low oxygen hypoxia, carbon dioxide and inhaled irritant gases.
Penney D.G. ed. Carbon Monoxide Toxicity, cha.7.
CRC Press, Boca Raton, USA.

Purser D.A., 2000b.
Toxic product yields and hazard assessment for fully enclosed design fires.
Polymer International 2000. 49(10), p. 1232–1255.

Purser D.A., 2008.
Assessment of hazards to occupants from smoke, toxic gases and heat.
DiNenno P.J. ed. The SFPE Handbook of Fire Protection Engineering, 4th edition, Sec.2,
Cha.6.
National Fire Protection Association (NFPE), Quincy, USA.

Purser D.A., 2010a.
Asphyxiant components of fire effluents.
Stec A.A. and Hull T.R. ed. Fire Toxicity, 1st edition, cha.4.
Woodhead Publishing Ltd, Cambridge, UK.

Purser D.A., 2010b.
Hazards from smoke and irritants.
Stec A.A. and Hull T.R. ed. Fire Toxicity, 1st edition, cha.3.
Woodhead Publishing Ltd, Cambridge, UK.

Q'Keeffe W., 2007.
Specifying fire-rated glazing choices codes, and clarifications.
Construction Specifier, 60(3), p. 58-66.

- Quintiere J.G., 1976.
Growth of fire in building compartments.
Robertson ed. Fire Standards and Safety, ASTM STP 614, p. 131-167.
ASTM International, West Conshohocken, USA.
- Quintiere J.G. and McCaffrey B.J., 1980.
The burning of wood and plastic cribs in an enclosure, Vol. 1 and 2, NBSIR 80-2054.
US Department of Commerce, Washington, D.C., USA.
- Razwick J., 2006.
An introduction to fire-rated glass, technical glass products.
[online] Available at: http://www.fireglass.com/press_room/articles/intro.asp [Accessed 22 Oct 2009].
- Rockett J.A., 1976.
Fire induced gas flow in an enclosure.
Combustion Science and Technology, 12, p. 165-175.
- Rutledge S.A., 2006.
Heat transfer and fire-rated glazing: why you should care?
Glass Magazine, Feb.
- SAFTI FIRST, 2010.
The hose stream test, safety test or sales strategy?
[online] Available at: http://www.saftifirst.com/articles/hose_stream_safetyorsales.html
[Accessed 22 Feb 2010].
- Sakamoto A., Katagi K. and Shibuya T., 1993.
Fire-protection and safety composite glass panel.
US patent 5230954.
- Sato H., Tsuruda T., Ogawa Y., Noguchi T., Tamura M., Liu K.Y., Ishii S., Hashibe Y.,
Sawada M. and Tsujimoto H., 2006.
Behavior of fireproof glasses under condition of real fire.
Report of National Research Institute of Fire and Disaster No. 100, p. 44-53. National
Research Institute of Fire and Disaster, Tokyo, Japan.
- Schueller F., Nieven J., Linden R. and Geith A., 1997.
Fire-resistant glazing.
US patent 5698277.
- Stec A.A., Hull T.R., Purser J.A. and Purser D.A., 2009.
Comparison of toxic product yields from bench-scale to ISO room.
Fire Safety Journal, 44(1), p. 62-70.

- Stec A.A. and Hull T.R., 2011.
Assessment of the fire toxicity of building insulation materials.
Energy and Buildings, 43(2-3), p. 498-506.
- Stec A.A., Hull T.R. and Lebek K., 2008.
Characterisation of the steady state tube furnace (ISO TS 19700) for fire toxicity assessment.
Polymer Degradation and Stability, 93(11), p. 2058–2065.
- Stec A.A., Hull T.R., Lebek K., Purser J.A. and Purser D.A., 2008.
The effect of temperature and ventilation condition on the toxic product yields from burning polymers.
Fire and Materials, 32(1), p. 49-60.
- CIBSE Guide E, 2010.
Fire safety engineering.
The Chartered Institution of Building Services Engineers (CIBSE), London, UK.
- Stein Y.S., Antal M. J. and Jones M., 1983.
A study of the gas-phase pyrolysis of glycerol.
Journal of Analytical and Applied Pyrolysis, 4(4), p. 283-296.
- Thomas P.H., 1981.
Testing products and materials for their contribution to flashover in rooms.
Fire and Materials, 5(3), p. 103-111.
- Thomas P.H., Bullen M.L., Quintiere J.G. and McCaffrey B.J., 1980.
Flashover and instabilities in fire behavior.
Combustion and Flame, 38, p. 159-171.
- UL 10B, 2008.
UL Standard for safety fire tests of door assemblies – 10th edition.
Underwriters Laboratories Inc. (UL), Northbrook, USA.
- UL 10C, 2009.
UL Standard for safety positive pressure fire tests of door assemblies – 2nd edition.
Underwriters Laboratories Inc. (UL), Northbrook, USA.
- UL 263, 2011.
UL Standard for safety fire tests of building construction and materials – 4th edition.
Underwriters Laboratories Inc. (UL), Northbrook, USA.

UL 9, 2009.

UL Standard for safety fire tests of window assemblies – 8th edition.
Underwriters Laboratories Inc. (UL), Northbrook, USA.

Utiskul Y.P. and Quintiere J.G., 2008.

An application of mass loss rate model with fuel response effects in fully-developed compartment fires.

Fire Safety Science, 9, p. 827-838.

Vanderstukken R., 1993.

Fire screening, light-transmitting panels with intumescent material and exposed connection surfaces.

US patent 5244709.

Van Dyke J.D. and Kasperski K.L., 1993.

Thermogravimetric study of polyacrylamide with evolved gas analysis.

Journal of Polymer Science Part A: Polymer Chemistry, 31(7), p. 1807-1823.

Vondrasek R.J., 2003.

Confining fires.

Cote, A. E. ed. NFPA Fire Protection Handbook, 19th edition, Sec.12, Cha.4.

National Fire Protection Association (NFPA), Quincy, USA.

Walton W.D. and Thomas P.H., 2003.

Estimating temperatures in compartment fires.

DiNenno P.J. ed. The SFPE handbook of fire protection engineering, 4th edition, Sec.3, Cha.6.

National Fire Protection Association (NFPE), Quincy, USA.

Wong N.H., Wang L.P., Noplie A.N., Pandey A.R. and Wei X.L., 2005.

Effect of double glazed facade on energy consumption, thermal comfort and condensation for a typical office building in Singapore.

Energy and Buildings, 37(6), p. 563-572.

Wood M., 2007.

Clear designs.

Fire Prevention and Fire Engineers Journals, Nov.

Wu M. and Chow W.K. 2011.

Thermal Empirical Equations for Post-flashover Compartment Fires.

Fire Safety Science, 10, p. 1489-1497.

Wu M. and Chow W.K., 2012.
A review on fire resistant glass with high rating.
18th National Symposium of Higher Education Institutes on Engineering Thermal
Physics, 17-19 May 2012, Guangzhou, China.

Wu M. and Chow W.K., 2013.
A review on fire-resistant glass with high rating.
Journal of Applied Fire Science, 23(1), p. 59-76.